INHIBITING PROTEIN CLEARANCE TO INDUCE CELL DEATH IN TUBEROUS SCLEROSIS AND PANCREATIC CANCER

Jeremiah William Hendricks

Submitted to the faculty of the University Graduate School
in partial fulfillment of the requirements
for the degree
Master of Science
in the Department of Biochemistry and Molecular Biology,
Indiana University

April 2014

Accepted by the Graduate Faculty, Indiana University, in partial fulfillment of the requirements for the degree of Master of Science.

Master's Thesis Committee

Lawrence A. Quilliam, Ph.D., Chair

Simon J. Atkinson, Ph.D.

Ronald C. Wek, Ph.D.

Jian-Ting Zhang, Ph.D.

DEDICATION

I would like to dedicate this thesis to my parents George and Janice Hendricks. Without their love and support I would never have been able to reach this point.

ACKNOWLEDGMENTS

I would like to thank my mentor and advisor Dr. Lawrence Quilliam for his guidance, support, and input in my thesis work. He has been provided much influence in my scientific understanding and professional goals. I would also like to thank the many members of the Quilliam lab who I have worked with and have given me support especially Dr. Hoa Nguyen and Dr. Justin Babcock.

I would like to thank my committee members Dr. Simon Atkinson, Dr. Ronald Wek, and Dr. Jian-Ting Zhang for their valuable input and guidance during my thesis work. I also owe my sincere appreciation to Seth Winfree of the Indiana Center for Biological Microscopy for performing the confocal microscopy experiments and for providing advice on image quantitation. I am indebted to Dr. Clark Wells and the members of his lab including Brandon Lane, Lauren Bringman, Dr. William Ranahan, and Dr. Jacob Adler for their assistance and for microscope usage. I owe many thanks to Tom Baird of the Wek lab and Dr. Derek Woods of the Turchi lab for assistance and advice. I would also like to thank the faculty and staff of the Department of Biochemistry and Molecular Biology, including Sandy McClain, Sheila Reynolds, Melissa Pearcy, Jack Arthur, Patty Dilworth, Jamie Schroeder, and Darlene Lambert.

I would also like to thank my parents, sibling, and friends for their continued love and support.

Jeremiah William Hendricks

INHIBITING PROTEIN CLEARANCE TO INDUCE CELL DEATH IN TUBEROUS SCLEROSIS AND PANCREATIC CANCER

Sequestration at the aggresome and degradation through autophagy are two approaches by which a cell can counteract the toxic effect of misfolded proteins. Tuberous sclerosis (TS) and cancer cells can become dependent on autophagy for survival due to the high demand for protein synthesis, thus making protein clearance a potential therapeutic target. Because of its histone deacetylase (HDAC) inhibitory activity, we hypothesized that 4-phenylbutyrate (4-PBA) inhibits HDAC6 and aggresome formation to induce TS cell death. We found that 4-PBA treatment increases cell death and reduces bortezomib-induced aggresome formation. To link these results with HDAC inhibition we used two other HDAC inhibitors, trichostatin A (TSA) and tubastatin, and found that they also reduce bortezomib-induced protein aggregation. Because tubulin is a target of HDAC6, we next measured the effect of the HDAC inhibitors and 4-PBA treatment on tubulin acetylation. As expected, tubastatin increased tubulin acetylation but surprisingly TSA and 4-PBA did not. Because 4-PBA did not significantly inhibit HDAC6, we next hypothesized that 4-PBA was alternatively inducing autophagy and increasing aggresome clearance. Surprisingly, autophagy inhibition did not prevent the 4-PBA-induced reduction in protein aggregation. In conclusion, we found 4-PBA to induce cell death and reduce aggresome levels in TS cells, but we found no link between these phenomena. We next hypothesized that loss of the Ral guanine nucleotide exchange factor Rgl2 induces cell death via autophagy inhibition in pancreatic adenocarcinoma (PDAC) cells. KRas is mutationally activated in over 90% of PDACs and directly activates Rgl2. Rgl2 activates RalB, a known regulator of autophagy, and Rgl2 has been shown to promote PDAC cell survival. We first confirmed that loss of Rgl2 does increase cell death in PDAC cells. Initial experiments using doubly tagged fluorescent p62 and LC3 (autophagy markers) suggested that loss of Rgl2 inhibited autophagosome accumulation, but after developing a more sophisticated quantitation method we found loss of Rgl2 to have no effect. We also measured endogenous LC3 levels, and these experiments confirmed loss of Rgl2 to have no effect on autophagy levels. Therefore, loss of Rgl2 increases cell death in PDAC cells, but does not have a significant effect on autophagy.

Lawrence A. Quilliam, PhD, Chair

TABLE OF CONTENTS

LIST OF FIGURES ix

LIST OF ABBREVIATIONS x

CHAPTER 1. INTRODUCTION 1

1.1 Introduction to cancer signaling 2
1.2 Small GTPase signaling 3
1.3 Ras family proteins 4
1.4 KRas effectors 5
1.5 Ral signaling 8
1.6 mTOR signaling 10
1.7 Introduction to pancreatic cancer 13
1.8 PDAC biology and common mutations 14
1.9 TSC and LAM 15
1.10 Therapeutic attempts at targeting KRas signaling 16
1.11 Introduction to autophagy 17
1.12 The aggresome 18
1.13 Molecular components of autophagosome formation 21
1.14 Signaling inputs to autophagy 22
1.15 Autophagy and cancer 25
1.16 4-Phenylbutryic acid 26

CHAPTER 2. MATERIALS AND METHODS 28

2.1 General cell culture and drug treatments 29
2.2 Lentiviral production 30
2.3 Western blotting and antibodies 30
2.4 Immunofluorescent microscopy 33
2.5 Soluble/insoluble fractionation 33
2.6 Live imaging 34
2.7 Colony formation assay 34
2.8 Trypan blue assay 35
2.9 Statistical analysis 36

CHAPTER 3. TREATMENT WITH 4-PBA INHIBITS CELL SURVIVAL AND STRESS INDUCED AGGRESOME FORMATION IN ELT3 CELLS 38

3.1 Introduction 39
3.2 Results 40
  3.2.1 Treatment with 4-PBA increases cell death 40

3.2.2 Treatment with 4-PBA decreases protein aggregation 43
3.2.3 Treatment with HDAC inhibitors decrease protein aggregation 47
3.2.4 4-PBA treatment does not increase tubulin acetylation 50
3.2.5 Autophagy inhibition does not restore protein aggregation decreased by 4-PBA 52
3.3 Discussion 55
3.3.1 4-PBA treatment does not protect against cell death 55
3.3.2 The inhibition of aggresome formation by 4-PBA treatment does not correlate with HDAC6 inhibition 56
3.4 Future directions 57

CHAPTER 4. RGL2 LOSS INHIBITS CELL SURVIVAL BUT NOT AUTOPHAGY IN MIA-PACA-2 PANCREATIC CANCER CELLS 59

4.1 Introduction 60
4.2 Results 62
4.2.1 Rgl2 but not RalGDS loss inhibits autophagosome maturation in PANC1 cells 62
4.2.2 Loss of Rgl2 inhibits anchorage-dependent colony formation in PDAC cells 65
4.2.3 Loss of Rgl2 increases cell death in MIA-PACA-2 cells 67
4.2.4 Loss of Rgl2 decreases total p62-positive puncta in PANC1 cells during glucose starvation 71
4.2.5 Loss of Rgl2 has no effect on autophagosome maturation in MIA-PACA-2 cells 74
4.2.6 PDAC cells accumulate LC3-II during glucose starvation 78
4.2.7 Loss of Rgl2 and RalB do not significantly inhibit LC3-II accumulation during glucose starvation in PDAC cells 81
4.2.8 Loss of Rgl2 and RalB do not significantly impact LC3 flux during glucose starvation in PDAC cells 86
4.3 Discussion 90
4.4 Future directions 92

APPENDIX – NUCLEOTIDE SEQUENCES 94

REFERENCES 95

CURRICULUM VITAE

LIST OF FIGURES

Figure 1-1 KRas signals to effectors PI3K, Raf, and RalGEFs triggering a number of cellular responses 7
Figure 1-2 mTOR is regulated by a number of upstream signaling events to regulate protein synthesis and autophagy 12
Figure 1-3 Aggregated proteins are delivered to a perinuclear region to form the aggresome 20
Figure 1-4 A number of protein complexes regulate autophagosome formation 24
Figure 3-1 Treatment with 4-PBA increases ELT3 cell death 42
Figure 3-2 Treatment with 4-PBA decreases ubiquitinated protein aggregation 45
Figure 3-3 Treatment with HDAC inhibitors decreases ubiquitinated protein aggregation 48
Figure 3-4 4-PBA treatment does not increase tubulin acetylation 51
Figure 3-5 3-MA treatment does not restore protein aggregation decreased by 4-PBA 53
Figure 4-1 Rgl2 but not RalGDS loss inhibits autophagosome maturation in PANC1 cells 64
Figure 4-2 Loss of Rgl2 inhibits anchorage-dependent colony formation in PDAC cells 66
Figure 4-3 Loss of Rgl2 increases MIA-PACA-2 cell death 68
Figure 4-4 Loss of Rgl2 decreases total p62-positive puncta in PANC1 cells during glucose starvation 72
Figure 4-5 Loss of Rgl2 has no effect on autophagosome maturation in MIA-PACA-2 cells 76
Figure 4-6 PDAC cell lines accumulate LC3-II during glucose starvation 79
Figure 4-7 Loss of Rgl2 and RalB do not significantly inhibit LC3-II accumulation during glucose starvation in PDAC cell lines 82
Figure 4-8 Loss of Rgl2 and RalB do not significantly impact LC3 flux during glucose starvation in PDAC cell lines 87

LIST OF ABBREVIATIONS

3-MA	3-Methlyadenine
4EBP1	4E binding protein 1
4-PBA	4-Phenylbutyric Acid
ADM	Acinar-to-ductal metaplasia
AMPK	Adenosine monophosphate-activated protein kinase
ARF	Alternate reading frame
Atg1	Autophagy related 1
Atg10	Autophagy related 10
Atg12	Autophagy related 12
Atg13	Autophagy related 13
Atg14	Autophagy related 14
Atg16L1	Autophagy related 14-like 1
Atg3	Autophagy related 3
Atg35	Autophagy related 35
Atg5	Autophagy related 5
Atg7	Autophagy related 7
Bcl-2	B-cell lymphoma 2
BRCA1	Breast cancer 1
CFTR	Cystic fibrosis transmembrane conductance regulator
CQ	Chloroquine
Ctrl	Control
DAPI	4',6-diamidino-2-phenylindole
DMEM	Dulbecco's modified Eagle's medium
EDTA	Ethlyenediaminetetraacetic acid
EGFR	Epidermal growth factor receptor
ER	Endoplasmic reticulum
ERK	Extracellular signal-regulated kinase
Exo84	Exocyst complex 84 kDa subunit
FBS	Fetal bovine serum
FIP200	FAK family-interacting protein of 200 kDa
FTI	Farnesyl transferase inhibitor
GβL	G protein beta subunit-like
GAP	GTPase activating protein
GDP	Guanosine diphosphate
GEF	Guanine nucleotide exchange factor
GFP	Green fluorescent protein
GSK3β	Glycogen synthase kinase 3 beta
GTP	Guanosine triphosphate
HDAC	Histone deacetylase
HDAC6	Histone deacetylase 6
IKKβ	IκB kinase β

JNK1	c-Jun N-terminal kinase 1
LAM	Lymphangioleiomyomatosis
LAMP-2	Lysosome-associated membrane glycoprotein 2
LC3	Microtubule-associated protein 1 light chain 3
MAPK	Mitogen-activated protein kinase
MEK	Mitogen-activated protein kinase kinase
MTOC	Microtubule organizing center
mTOR	Mammalian target of rapamycin
mTORC1	Mammalian target of rapamycin complex 1
mTORC2	Mammalian target of rapamycin complex 2
NBR1	Neighbor of BRCA1 gene 1 protein
Nf1	Neurofibromin 1
PanIN	Pancreatic intraepithelial neoplasia
PBS	Phosphate buffer saline
PDAC	Pancreatic ductal adenocarcinoma
PDK1	Phosphoinositide-dependent kinase-1
PEI	Polyethylenimine
PI3K	Phosphatidylinositol 3-kinase
PI_3P	Phosphatidylinositol 3-phosphate
PKA	Protein kinase A
PRAS40	40 KDa proline-rich Akt substrate
Rab7	Ras-like in rat brain 7
Raf	Rapidly accelerated fibrosarcoma
RalA	Ras-like A
RalB	Ras-like B
RalGDS	Ral guanine nucleotide dissociation stimulator
RalGPS1a	Ral GEF with PH domain and SH3-binding motif 1a
RalGPS1b	Ral GEF with PH domain and SH3-binding motif 1b
RalGPS2	Ral GEF with PH domain and SH3-binding motif 2
Rap	Ras proximate
Ras	Rat sarcoma viral oncogene homolog
RBD	Ras binding domain
RFP	Red fluorescent protein
Rgl	RalGDS-like
Rgl2	RalGDS-like 2
Rgl3	RalGDS-like 3
Rheb	Ras homolog enriched in brain
S6K1	Ribosomal S6 kinase 1
SDS	Sodium dodecyle sulfate
shRNA	Small hairpin RNA
siRNA	Small interfering RNA
SMAD4	Mothers against decapentaplegic homolog 4
SNARE	Soluble N-ethylmaleimide-sensive factor attachment protein

	receptor
SOS1	Son of sevenless 1
TFEB	Transcription factor EB
TGFβ	Transforming growth factor beta
TSA	Trichostatin A
TSC	Tuberous sclerosis
Ulk1	Unc-51-like kinase 1
Ulk2	Unc-51-like kinase 2
Vps15	Vacuolar protein sorting 15
Vps34	Vacuolar protein sorting 34

CHAPTER 1. INTRODUCTION

1.1 Introduction to cancer signaling

Signal transduction pathways communicate external stimuli via a series of proteins to elicit a response from the cell. These external stimuli can be other protein ligands, changes in ion concentration, or even physical stress [1-3]. The external stimulus is recognized by a membrane receptor and communicated to the interior of the cell by a series of second messengers [4]. Responses of cells can include changes in protein expression, cell growth, or alternatively initiation of apoptosis [5-7]. A number of gene mutations that transition a normal cell to a cancer cell often interrupt a normal signaling pathway [8]. The two main types of mutated genes in cancer are tumor suppressors that inactivate otherwise protective genes and oncogenes that will drive the growth of a tumor. The mutationally activated *KRAS* is considered an oncogene because it drives PDAC tumorigenesis and progression [9]. Mutant KRas drives Ras signaling even in the absence of stimulus. TSC1 and TSC2, on the other hand, normally signal to mTOR to slow protein production [10]. TSC is therefore considered a tumor suppressor syndrome because mutated TSC1 and TSC2 cannot inhibit unrestrained cell growth. Tumor cells take advantage of mutations in signaling proteins to always maintain a pro-growth signal and ignore anti-growth and pro-death stimuli.

1.2 Small GTPase signaling

Small GTPases are a type of guanine nucleotide-binding proteins which bind to guanosine triphosphate (GTP) and hydrolyze it into guanosine diphosphate (GDP) via their intrinsic GTPase activity. While approximately 150 small GTPases exist in the human body, the prototype and best characterized example of a small GTPase is Ras [11]. The activity of a small GTPase is dictated by being bound to GTP, “on” state, or GDP, “off” state. When bound to GTP, small GTPases typically undergo a conformation change that creates a binding surface otherwise not present when the GTPase is bound to GDP. For example, when Ras is bound to GTP it can interact with a number of effectors, such as Raf, and localize them to the plasma membrane [12]. The intrinsic hydrolysis of GTP to GDP by a small GTPase is catalyzed by a GTPase activating protein (GAP) [13]. When a GAP is bound to a small GTPase, the catalytic machinery of the GTPase is stabilized and allows for quicker hydrolysis. One example of a GAP is neurofibromin (encoded by the Nf1 tumor suppressor locus), which catalyzes hydrolysis of RasGTP to RasGDP, thus turning Ras-directed signaling “off” [14].

The counterparts to GAPs are guanine nucleotide exchange factors (GEFs). When GEFs bind to GDP bound small GTPases, the binding conformation causes a quick release of GDP [15]. Because GTP is found at a higher concentration in the cytosol relative to GDP, a GTP will rapidly bind and take the GDP’s place, displacing the GEF in the process. Therefore, GEF’s have the capability to turn a small GTPase “on”. One GEF of Ras is Son of Sevenless-1(SOS1) which is first recruited to the plasma membrane by EGFR where it can then activate Ras [16]. Small GTPase signaling is a unique molecular mechanism for transmitting a signal and many different small GTPase pathways are important in tumor cell signaling.

1.3 Ras family proteins

The Ras family of proteins play an important role in cancer signaling, about 20% of all human cancers have an activating mutation in a *Ras* gene [17]. The Ras proteins get their name from rat sarcoma viruses, a reflection of their discovery that when the cellular activated Ras was encoded in retroviruses it elicited tumors in infected rodents [18]. HRas, NRas, and KRas, the three primary Ras proteins, have about 85% sequence identity and are all found with activating mutations in tumors [17]. All three of these proteins are widely expressed with KRas being almost ubiquitous. Ras proteins are first farnesylated at a C-terminal CaaX box, the aaX residues are cleaved off and then the COO^- group of the terminal cystein is methylated to allow attachment into the plasma membrane. Membrane attachment is also facilitated in NRas and HRas via subsequent palmitoylation of adjacent Cys residues, or in the case of KRas via a polybasic sequence adjacent to the prenylation site that binds negative phospholipids [19]. Localization to the inner surface of the plasma membrane is required for normal function of the Ras proteins. This has been shown by mutagenesis or inhibition of the above post-translational events. Once properly localized and activated, Ras proteins signal to a number of downstream signaling pathways to promote cellular proliferation.

A number of other proteins also belong to the Ras family. Rap proteins, originally named Ras proximate, regulate cell-cell and cell-matrix adhesion [20]. The Rap proteins include Rap1A, Rap1B, Rap2A, Ralp2B, and Rap2C. Mutationals that activate Rap proteins do not typically cause transformation and can actually inhibit Ras transformation via competition for effectors or by promoting growth inhibitory cellular changes [21]. Other members of the Ras family are the Ras-like proteins, RalA and RalB. Ral proteins are directly downstream of Ras and play a dominant role in Ras-mediated transformation in human cell lines [22]. The Ral proteins will be a topic of further discussion in Section 1.8. Another notable Ras family protein is Ras homolog enriched in brain (Rheb) that regulates growth and cell cycle regulation by activating mTOR. Despite its name, Rheb is ubiquitously expressed and is the protein that TSC1/2 directly inhibit to suppress mTOR signaling (TSC is the Rheb GAP). Ras family proteins play a number of direct roles in tumorigenesis by regulating cell growth and proliferation.

1.4 KRas effectors

KRas signals to three main downstream pathways: Raf/MEK/ERK, PI3K/Akt/mTOR, and RalGDS/Ral (Figure 1-1). The best characterized of these is the Raf/MEK/ERK pathway. The Raf (rapidly accelerated fibrosarcoma)/MEK (mitogen-activated protein kinase/ERK kinase)/ERK (extracellular-signal-regulated kinase) pathway is also known as a mitogen-activated protein kinase (MAPK) cascade and controls such fundamental processes as proliferation, differentiation, survival, and apoptosis [23]. Raf binds to Ras-GTP, which localizes it to the membrane where it can then be phosphorylated [24]. This activation then permits Raf to phosphorylate MEK which in turn phosphorylates ERK [25]. Activated ERK is localized to the membrane and especially the nucleus where it can convert the MAPK signal into biological effect by enhancing gene expression via increasing DNA availability and phosphorylating transcription factors [26]. The role of the MAPK cascade in cancer is enhanced by aberrant upstream activation, such as mutated KRas, and can include inhibition of cell death [27].

Another well characterized pathway downstream of KRas is PI3K/Akt/mTOR. Ras-GTP binds to phospoinositide 3-kinase (PI3K) and increases its kinase activity [28]. PI3K is a lipid kinase that phosphorylates the 3’-hydroxyl group of phosphoinositides. One product of this reaction is phosphatidylinositol-3,4,5-triphosphate, (PIP_3) which then recruits Akt to membranes for phosphorylation by phosphoinositide-dependent kinase 1 (PDK1) [29, 30]. Phosphorylation of Akt stimulates its own catalytic activity, resulting in the phosphorylation of a number of targets including TSC2. Phosphorylation of TSC2 prevents its inhibition of Rheb and consequently mTOR which then permits proliferation and cell cycle progression [31]. This pathway plays important roles in many cancers. It has been shown that PI3K is necessary and sufficient to maintain RAS-transformed xenograft tumors after the loss of Ras [32]. Also, *AKT2* is amplified in 20% of PDAC tumors [33]. Activated KRas stimulates tumor growth through both the MAPK cascade and the PI3K/Akt/mTOR pathway.

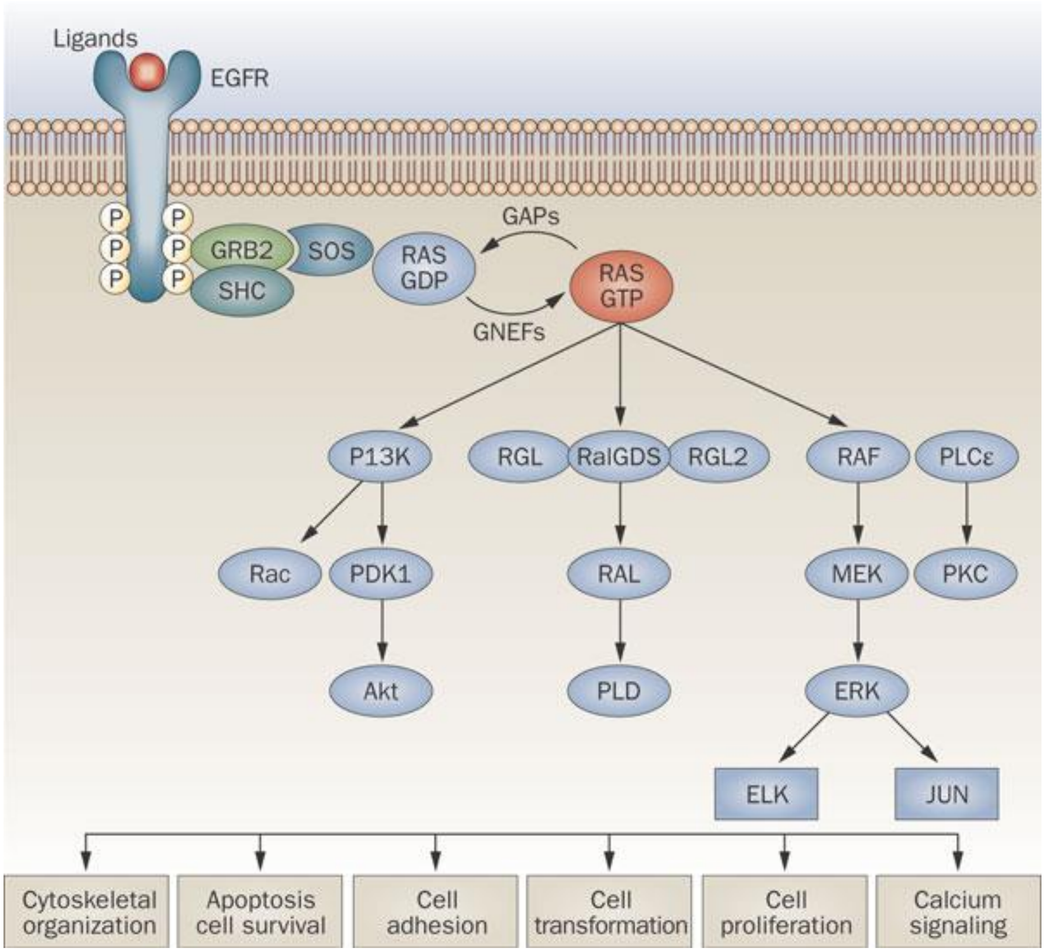
Ligands
EGFR
P
P
P
P
P
P
GRB2
SOS
SHC
RAS GDP
GAPs
GNEFs
RAS GTP
P13K
RGL
RalGDS
RGL2
RAF
PLCε
Rac
PDK1
RAL
MEK
PKC
Akt
PLD
ERK
ELK
JUN
Cytoskeletal organization
Apoptosis cell survival
Cell adhesion
Cell transformation
Cell proliferation
Calcium signaling

Figure 1-1. KRas signals to effectors PI3K, Raf, and RalGEFs triggering a number of cellular responses

Ras-GDP is converted to Ras-GTP by RasGEFs such as SOS, which is localized to the plasma membrane via ligand activation of receptors such as EGFR. Activated Ras-GTP binds to various effectors including PI3K, RalGDS proteins, and Raf. These signaling pathways activate multiple cellular responses including survival, transformation, and proliferation.

Image reproduced from: Normanno, Tejpar [34]

1.5 Ral signaling

A third, less characterized pathway downstream of KRas is the RalGEF/Ral pathway. The two Ral proteins, RalA and RalB, are small GTPases activated by RalGEFs and deactivated by RalGAPs. The Ral guanine nucleotide dissociation stimulator (RalGDS) family is a group of RalGEFs that bind to Ras-GTP via their Ras binding domain (RBD) and then exchange Ral-GDP for Ral-GTP [35]. The RalGDS family consists of RalGDS, RalGDS-like (Rgl), Rgl2, and Rgl3. RalGPS1a, GPS1b, and RalGPS2 are also RalGEFs but do not interact with Ras. However, these RalGEFs do contain pleckstrin homology (PH) domains and SRC homology 3 (SH3) binding motifs which may substitute for Ras-mediated membrane recruitment/GEF activation [36]. Ral-GTP then activates an effector such as Ral binding protein 1 (RalBP1) which regulates actin dynamics and endocytic pathways [37, 38]. Activated Ral also targets Sec5 and Exo84, two components of the exocyst [39, 40]. The exocyst is a multiprotein complex that regulates vesicle targeting, from the Golgi to the basal-lateral membrane for example [41]. RalGAP1 and RalGAP2 deactivate Ral by catalyzing the hydrolysis of GTP to GDP [42].

Despite sharing 85% amino acid sequence identity, recent work has suggested that RalA and RalB have distinct functions [43]. Loss of RalA but not RalB has been shown to reduce transformed and tumorigenic growth in pancreatic cancer cells [44]. This study also showed that RalB but not RalA is crucial for tumor cell invasion and metastases in mice [44]. These results were recently echoed in another research artice that showed loss of RalA but not RalB decreased anchorage-independent growth in colorectal cells [45]. Surprising, this same study found that RalA and RalB have antagonistic effects; overexpression of RalB also inhibited anchorage-independent growth [45].

Another study has shown that RalA and RalB both regulate the exocyst at different stages of cytokinesis during mitosis. It was suggested that these distinct functions are dictated by divergent localization [46]. This hypothesis is strengthened by an earlier report that RalA is found at the plasma membrane and RalB on endosomes [47]. It has been suggested that RalA and RalB achieve divergent localization via post-translational modifications [48]. Even in light of these hypotheses, it is still not completely clear how RalA and RalB achieve distinct functions.

There has been some discussion over whether the many different RalGEFs are redundant or if they have unique functions. Protein kinase A (PKA) phosphorylates Rgl2 at Ser737, reducing its ability to bind HRas. This phosphorylation site is not conserved among RalGDS, Rgl, or Rgl3 [49], and therefore this modification scheme could be one mechanism of imparting unique functions to Rgl2. Another possible means of delineating functions among the RalGEFs could be different cell localizations. During cytokinesis, it was found that RalGDS specifically colocalizes with RalA whereas Rgl colocalizes with RalB [46]. Furthermore, Rgl2 has been found to colocalize with RalB at the leading edge of PDAC cells and be required for RalB to be situated there [50]. Differential expression is a third mechanism that could instill different functions for RalGEFs. In the PDAC cell lines SW-1990, MIA-PACA-2, CFPAC-I, AsPC-1, BxPC-3, and

Capan-1, it was found that RalGDS and Rgl2 are more highly expressed than Rgl and Rgl3 [50]. Rgl2 was also shown to be required for anchorage-independent growth in these cells. There is not sufficient evidence yet to determine if the six RalGEFs are redundant or have unique function.

1.6 mTOR signaling

TOR was originally discovered in yeast as the target of rapamycin, an anti-mycotic compound discovered in bacteria isolated from the soil of the island Rapa Nui [51]. Its mammalian homologue, mTOR, is the catalytic subunit of the rapamycin sensitive mTOR complex 1 (mTORC1) and the rapamycin insensitive mTORC2 [52] (Figure 1-2). The other elements of mTORC1 and mTORC2 include PRAS40, GβL, and debtor. mTORC1 also includes a phosphorylation-dependent regulator protein named raptor, while mTORC2 has a similar substrate-binding protein named rictor [53]. mTORC1 is primarily responsible for activating protein synthesis by phosphorylating ribosomal S6 kinase 1 (S6K1) and eukaryotic translation initiation factor 4E-binding protein 1 (4EBP1). When S6K1 is phosphorylates it activates the ribosomal protein S6 that stimulates mRNA translation [54]. 4EBP1 phosphorylation, on the other hand, facilitates the activity of eIF4F complex, a key component of mRNA translation [55]. The small GTPase Rheb drives mTOR activity by recruiting it to the cytoplasmic surface of lysosomes [56]. TSC2 inhibits the activity of Rheb by acting as a RhebGAP, catalyzing the hydrolysis of GTP to GDP [57]. TSC2 acts as a signaling hub in regulation of mTOR. In addition to being negatively regulated by Akt, TSC2 and TSC1 are also inhibited by ERK and IKKβ respectively, while TSC2 is activated by AMPK and GSK3β [58]. In both TSC2-null diseases and PDAC, mTOR signaling is increased and protein expression is amplified.

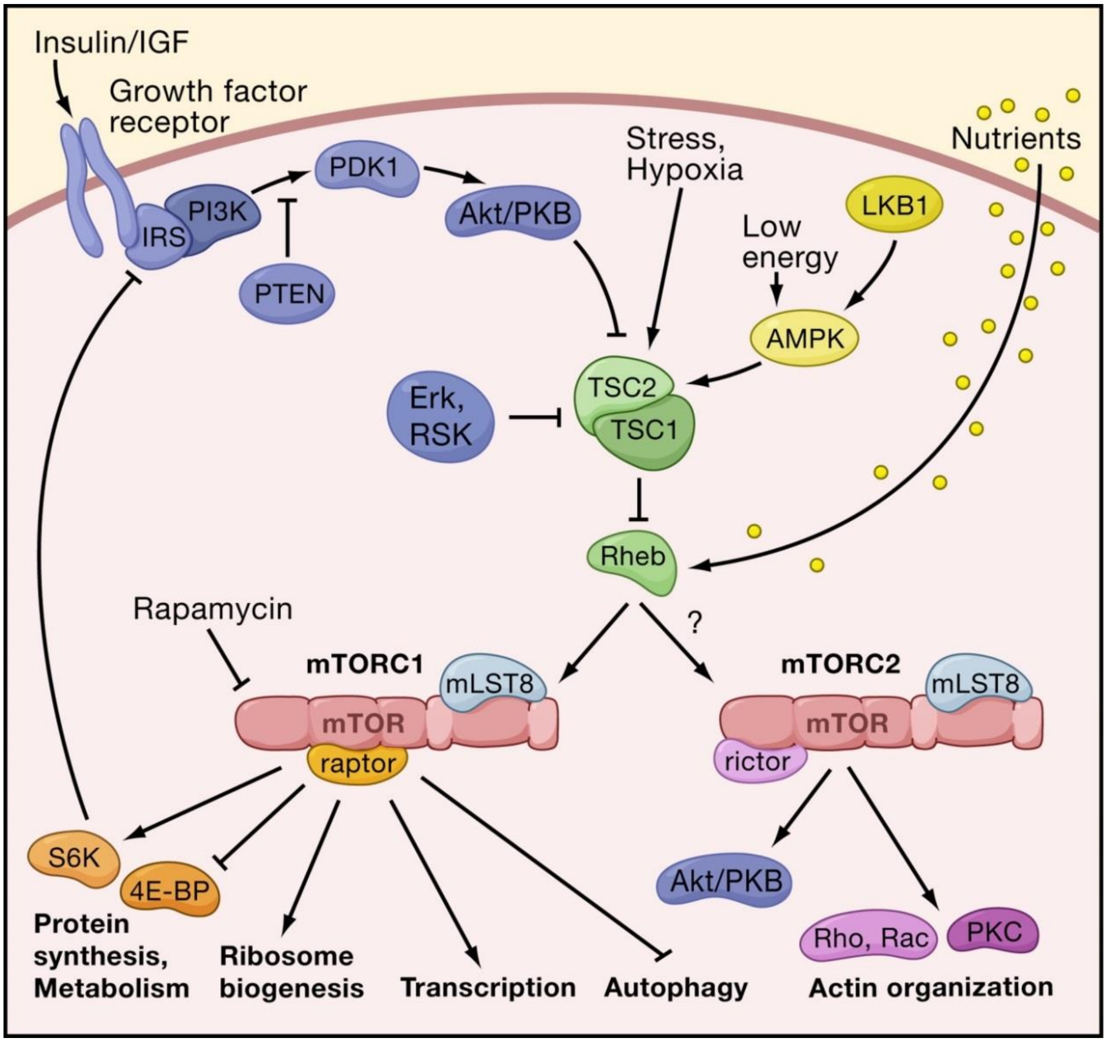
Insulin/IGF
Growth factor receptor
IRS
PI3K
PDK1
PTEN
Akt/PKB
Stress, Hypoxia
Nutrients
LKB1
Low energy
AMPK
Erk, RSK
TSC2
TSC1
Rheb
?
Rapamycin
mTORC1
mLST8
mTOR
raptor
mTORC2
mLST8
mTOR
rictor
S6K
4E-BP
Protein synthesis, Metabolism
Ribosome biogenesis
Transcription
Autophagy
Akt/PKB
Rho, Rac
PKC
Actin organization

Figure 1-2. mTOR is regulated by a number of upstream signaling events to regulate protein synthesis and autophagy

The TSC1 and TSC2 complex is a RhebGAP that deactivates Rheb activity by catalyzing the hydrolysis of bound GTP to GDP. Various signaling proteins including ERK and Akt deactivate TSC1/2 via phosphorylation facilitating Rheb activity. Meanwhile phosphorylation of TSC2 by AMPK stimulates its GAP activity. Once active, Rheb can bind and activate mTOR which drives mRNA translation via phosphorylation of S6K and 4E-BP. mTOR also inhibits autophagy by phosphorylating Ulk, inhibiting autophagosome assembly.

Image reproduced from: Wullschleger, Loewith [59]

1.7 Introduction to pancreatic cancer

Pancreatic cancer is one of the most difficult cancers to effectively treat, with only 6% of afflicted patients surviving five years after diagnosis[60]. Unfortunately, little progress has been made in pancreatic cancer treatment since 1975; the five year survival rate has only increased from 2% to 6% since that time, compared with an increase from 49% to 68% survival among all cancers combined [60]. The incidence of pancreatic cancer is low to moderate, with 45,220 estimated new cases in 2013, but has a high mortality rate with 38,460 estimated deaths [61]. Some non-genetic risk factors for pancreatic cancer include cigarette smoking, obesity, and chronic pancreatitis [60]. Pancreatic ductal adenocarcinoma (PDAC) is the most common type of pancreatic cancer and is the fourth leading cause of cancer death in the United States [62]. PDACs, which get their name from a histological resemblance to ductal cells, are believed to be preceded by pancreatic intraepithelial neoplasias (PanINs) which are common in older adults and have been found in as many as 30% of patients [62]. Currently the standard treatments for pancreatic cancer are the DNA damaging agent, gemcitabine, and the EGFR inhibitor, erlotinib. Early clinical trials using a combination of gemcitabine and erlotinib increased the median survival by a fraction of a month and were considered a success [63]. However, due to the high mortality rate and low success of this therapy, much more research is required to develop effective therapies for pancreatic cancer.

1.8 PDAC biology and common mutations

The histological progression of a normal pancreas cell to a PDAC cell has been well studied and defined. The origin of this disease is two cell types in the pancreas including exocrine acinar cells, that produce digestive enzymes, and ductal cells, which form the ducts that transport the enzymes. Recent studies have found that the initial stage of pancreatic tumor formation is transdifferentiation of cells from an acinar phenotype to a ductal one, a process known as acinar-to-ductal metaplasia (ADM) [64]. These transdifferentiated cells can then develop into PanINs which exhibit dysplastic growth and are graded from stages I to III, III being the stage of most extreme architectural disorganization [62]. Late stage PanINs then progress to PDAC, which is characterized by a dense stroma of fibroblasts and inflammatory cells and exhibit a glandular pattern with duct-like structures and some degree of cellular atypia [62]. PDAC cells have a great potential for metastasis due, at least in part, to the hypoxic microenvironment of the tumor, and there is even evidence for metastasis of early stage PanINs [65]. Such early metastatic events make PDAC a difficult disease for both early diagnosis and treatment.

There are a number of common genes that are mutated and as a consequence activated or repressed in pancreatic tumors. *SMAD4*, *TP53*, *p16*, and *KRAS* are altered in at least 55% of PDACs [60]. For example, SMAD4 binds to the Smad binding elements (Sme) within the responsive elements of TGFβ responsive genes, repressing transcriptional expression. The resulting increased TGFβ signaling inhibits cell growth and promotes differentiation; therefore, defective mutations in *SMAD4* promote tumor growth [66]. Mutations in *SMAD4* occur in 55% of patient samples. Mutations in *TP53* appear to arise in later stage PanINs and occur in more than 50% of patient samples [62]. Loss of functional p53 promotes the growth and survival of tumor cells with DNA damage. *p16,* another gene commonly inactivated in PDAC, encodes the protein ARF which stabilizes p53. *p16* is altered in many different cancers and is inactivated in 95% of PDAC patients. The most commonly mutated gene in PDAC is *KRAS*, with more than 90% of patients having mutations. Unlike the other commonly mutated or inactivated genes, the common mutations in *KRAS* create a constitutively activated gene product. Activated KRas is an initiating step in PDAC and promotes tumor cell growth and survival [62]. Having a number of commonly altered genes creates a potential for therapeutically targeting PDAC that unfortunately has not yet been realized.

1.9 TSC and LAM

Tuberous sclerosis complex (TSC) and lymphangioleiomyomatosis (LAM) are both diseases characterized by inactivating mutations in *TSC1* or *TSC2*. These mutations cause constitutive activity in mammalian target of rapamycin (mTOR), which will induce excessive protein synthesis. TSC is characterized by the formation of harmartomas, benign malformations, in multiples tissues and the rate of birth incidence is about 1 in 6000 [67]. About 90% of patients with TSC will develop dermatological abnormalities and 50-80% will develop renal lesions [67]. Patients with TSC can also develop neurological abnormalities such as epilepsy or neurocognitive dysfunction. LAM is a cystic lung disease that primarily affects women. Patients with TSC can develop LAM, however LAM predominantly develops sporadically. Most noteworthy, malignant renal tumors develop in 63% of patients with sporadic LAM [68]. Recent clinical trials studied the use of sirolimus, an inhibitor of mTOR, to treat patients with TSC and LAM [69].

1.10 Therapeutic attempts at targeting KRas signaling

Due to its abnormally high activity, many attempts have been made at therapeutically targeting KRas and its effectors in cancer. For KRas to function it must be modified by a farnesyltransferase in order to attach to the plasma membrane. Some of the most promising KRas-targeting work has been using farnesyltransferase inhibitors (FTI). Tipifarnib, an FTI, was tested in clinical trials in combination with gemcitabine but ultimately failed to provide promising results [70]. A suspected reason for the failure of FTIs is that KRas can be alternatively lipid modified by type I geranylgeranyltransferase. Inhibitors of this geranylgeranyltransferase are currently being studied in combination with FTIs [71]. There have also been promising studies focused on decreasing KRas expression in PDAC cells with small interfering RNAs (siRNAs), but these studies have not entered clinical trials [72].

Much research has also targeted KRas effectors. Sorafenib is a Raf inhibitor approved for treatment of hepatocellular carcinoma and renal cell carcinoma. A recent Phase II trial of sorafenib in combination with gemcitabine did not show significant activity in PDAC, however. CI-1040, a MEK inhibitor, also made it to Phase II trials in patients with lung, breast, colon, and pancreatic cancer but did not demonstrate enough antitumor activity to justify further study [73]. Temsirolimus, an mTOR inhibitor, is approved for use in renal cell carcinoma but also shows little activity in pancreatic cancer [74]. Much less research has been done with inhibiting Ral signaling compared to the Raf/MEK/ERK and PI3K/Akt/mTOR pathways [75]. Due to the lack of success at inhibiting the other components in KRas signaling, further research could reveal the potential of inhibiting Ral signaling in PDAC.

1.11 Introduction to autophagy

The word autophagy is derived from Greek meaning “self-eating”, and describes a process by which the cell generates metabolic substrates by degrading its own organelles and protein [76]. Autophagy can be triggered by a number of conditions including nutrient deprivation, hypoxia, protein aggregation, and ER stress [77]. As opposed to protein degradation through the proteasome, cytosolic components are degraded in the lysosome in autophagy. These components are delivered to the lysosome by double-membrane vesicles called autophagosomes. When an autophagosome binds with a lysosome, the drop in pH and contact with hydrolases results in degradation of the autophagosome’s contents [78].

Many different selective types of autophagy have been discovered that target such specific organelles, such as the ER, mitochondria, and peroxisome [79]. The inflammasome, a multiprotein complex activated after cellular infection or stress, and the aggresome, a complex of unfolded aggregated proteins, are both protein structures degraded via the autophagosome [80, 81]. These structures are degraded by basal nonspecific autophagy. The best characterized proteins responsible for targeting such structures to the autophagosome are p62 (sequestosome-1) and neighbor of BRCA1 gene (NBR1). NBR1 and p62 both bind ubiquitinated cargo proteins and are selectively degraded by autophagy [82]. Autophagy is a vital process shown to be important in such physiological processes as adaptation to starvation, cell differentiation, and immunity [78].

1.12 The aggresome

A newly synthesized protein must first be correctly folded in order to be functional. If a protein fails to fold or is misfolded it can aggregate and excessive protein aggregation is toxic to a cell [83]. Misfolded proteins are handled by a cell in one of three ways: refolding by a protein chaperone, degraded by the proteasome, or sequestered with other aggregates in a structure called the aggresome [84] (Figure 1-3). The aggresome is a pericentriolar structure composed of aggregated ubiquitinated proteins located at the microtubule organizing center (MTOC) [83]. Individual aggregated particles are generated throughout the cytosol and are then transported on microtubules to the aggresome via the motor protein dynein [85]. Aggregate cargo is recruited to the dynein motors by histone deacetylase 6 (HDAC6), due to its ability to bind both polyubiquitinated misfolded protein and dynein [86]. HDAC6 is a part of the class II HDAC family and has been shown to both deacetylate tubulin and regulate microtubule-dependent cell motility [87]. Aggresome formation has also been found to be dependent on p62 [88]. Although chaperones and proteasomes are both recruited to the aggresome, it is believed that aggresomes are ultimately degraded through autophagy [89]. The degradation of aggresomes via autophagy is dependent on the interaction between p62 and microtubule-associated protein 1 light chain 3 (LC3) [88]. The aggresome permits cells to degrade large protein aggregates while under stressed conditions.

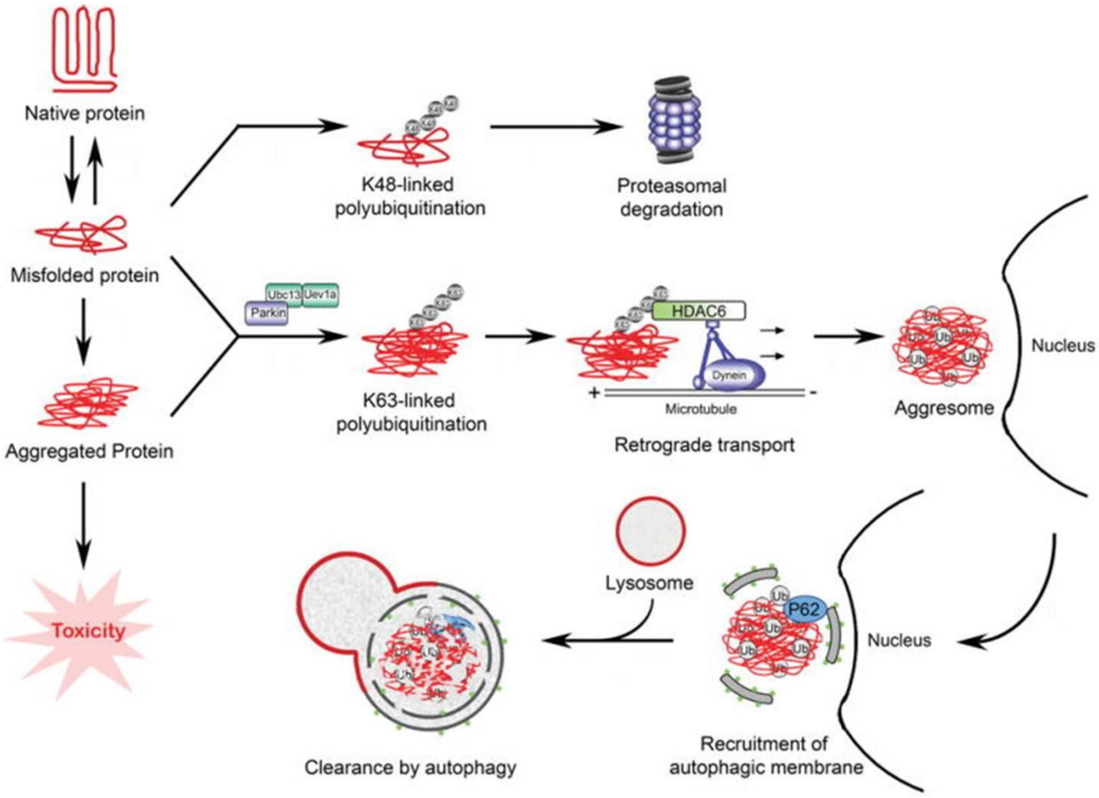
Native protein
Misfolded protein
Aggregated Protein
Toxicity
K48-linked polyubiquitination
Proteasomal degradation
Ubc13
Uev1a
Parkin
K63-linked polyubiquitination
HDAC6
Dynein
Microtubule
+
-
Retrograde transport
Ub
Aggregesome
Nucleus
Lysosome
P62
Nucleus
Clearance by autophagy
Recruitment of autophagic membrane

Figure 1-3. Aggregated proteins are delivered to a perinuclear region to form the aggresome

Misfolded proteins can aggregate in the cytoplasm and become toxic to the cell. To prevent toxicity, misfolded proteins can be ubiquitinated and degraded via proteasomes. Toxicity can also be prevented by the sequestration of protein aggregates at the aggresome. The aggregates are ubiquitinated and delivered to the mitochondrial organizing center (MTOC) by HDAC6. The aggresome is an accumulation of aggregated proteins and can be ultimately degraded via autophagy.

Altered image reproduced from: Chin, Olzmann [90]

1.13 Molecular components of autophagosome formation

There are three main stages that take place over the course of autophagosome maturation: a cup-shaped double membrane structure called the phagophore forms in the cytosol, the membrane elongates and closes to form a double membrane vesicle called the autophagosome, and finally the outer membrane fuses with the lysosome to enable degradation of the autophagosome's contents [91]. Genetic analyses in yeast have revealed that over 30 genes are required for these processes, and these proteins were designated Atg1 to Atg35 [92]. The proposed initiating site for autophagosome assembly is the phagophore assembly site (PAS), a hybrid of the forming membrane and a subset of proteins required in all types of autophagy (called the core autophagy machinery) [93]. The generation of the phagophore requires Vps34 in complex with Beclin1, Atg14, and Vps15 to form PI_3P; a complex whose activity is dependent on Ulk1/2, Atg13, and FIP200 [94] (Figure 1-4). The elongation of the phagophore then is regulated by two ubiquitination-like reactions. In the first reaction, Atg12 (a ubiquitin-like protein) is conjugated to Atg5 by Atg7 and Atg10. This Atg5-Atg12 complex then interacts with Atg16L1 to form a complex which associates with phagophores but dissociates from the completed autophagosomes [95]. In the second ubiquitination-like reaction, LC3 is conjugated to phosphatidylethanolamine by Atg7 and Atg3 generating LC3-II [96]. LC3-II remains associated with the autophagosome until fusing with the lysosome, at which point LC3-II inside the autolysosome is degraded and LC3-II on the surface remains. The exact mechanism of autophagosome maturation and lysosome fusion is unclear, but it is generally accepted that endosomal protein Rab7 and lysosomal LAMP-2 are required [97, 98]. Recent studies have also discovered other necessary components for fusion, including rubicon and syntaxin-5 SNARE complex [99, 100]. Therefore, autophagosome formation and maturation is a complex process with many individual parts, making it prime for regulation and manipulation.

1.14 Signaling inputs to autophagy

Autophagy is regulated by a number of different signaling events. One of the primary regulators of autophagy is mTOR. When mTOR is activated, it phosphorylates Ulk1 preventing binding to Atg13 and FIP200 and so blocking initiation of phagophore generation [101] (Figure 1-4). mTOR also phosphorylates TFEB which causes TFEB to be retained in the cytoplasm. TFEB is a transcription factor that normally drives transcriptional expression of genes necessary for all stages of autophagy, but must be in the nucleus to do so [102]. mTOR is such a potent regulator of autophagy that inhibition of mTOR, such as with rapamycin, is a standard method of inducing autophagy [103]. JUN N-terminal kinase 1 (JNK1) also regulates autophagy by phosphorylating Bcl-2. When Bcl-2 is phosphorylated it dissociates from Beclin-1, freeing Beclin-1 to initiate phagophore generation [104]. Another protein recently discovered to regulate autophagy is RalB. RalB, but not RalA, directly binds to Exo84 which induces the assembly of Ulk1 and Vps34 complexes on the exocyst, facilitating the initiation of autophagy [105]. All of these signaling pathways represent ways the cell regulates autophagy and possible means to manipulate normal autophagy function.

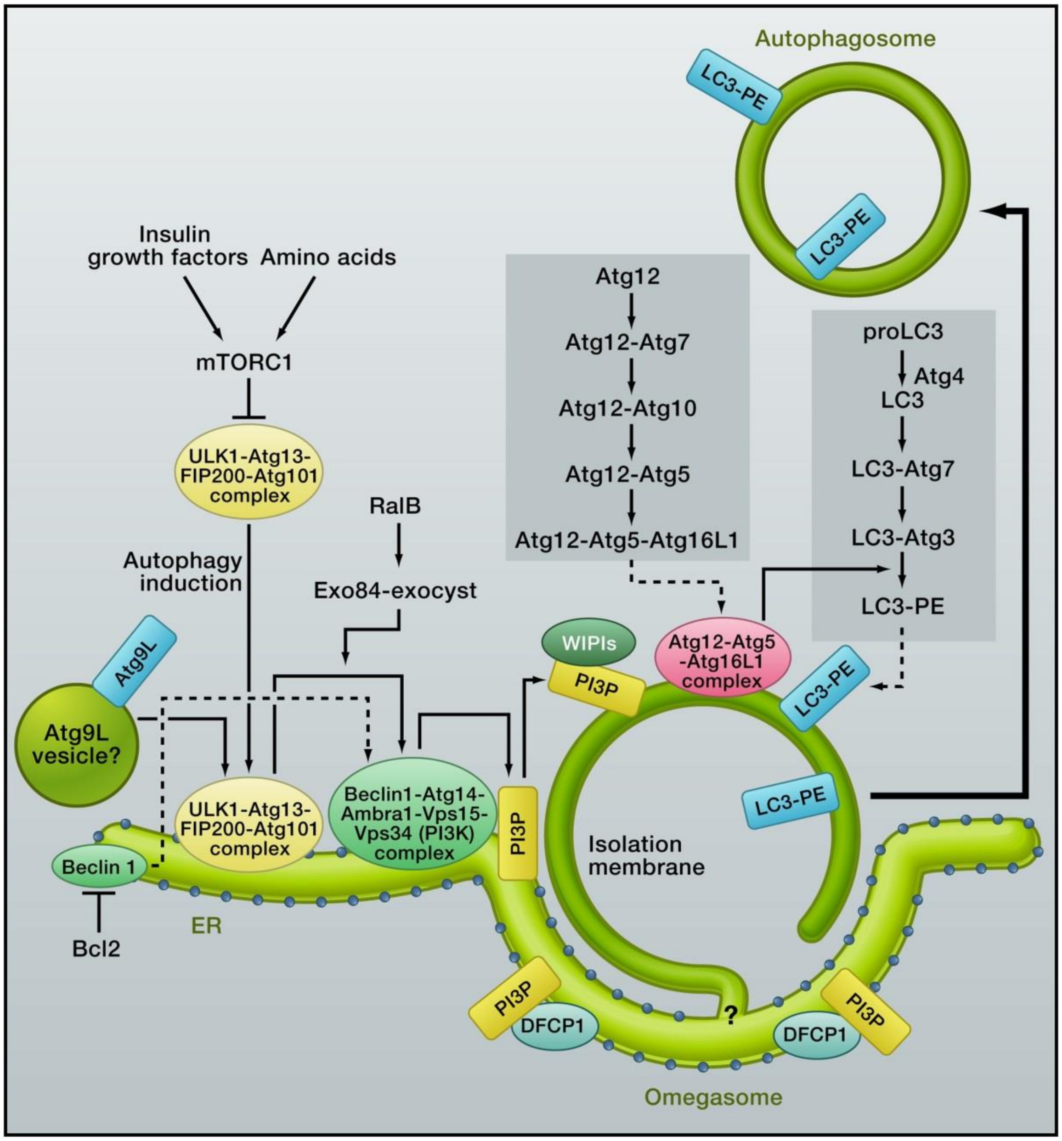
Autophagosome
LC3-PE
LC3-PE
Insulin
growth factors
Amino acids
mTORC1
ULK1-Atg13-FIP200-Atg101 complex
RalB
Autophagy induction
Exo84-exocyst
Atg12
Atg12-Atg7
Atg12-Atg10
Atg12-Atg5
Atg12-Atg5-Atg16L1
proLC3
Atg4
LC3
LC3-Atg7
LC3-Atg3
LC3-PE
WIPIs
PI3P
Atg12-Atg5 -Atg16L1 complex
LC3-PE
Atg9L
Atg9L vesicle?
ULK1-Atg13-FIP200-Atg101 complex
Beclin1-Atg14-Ambra1-Vps15-Vps34 (PI3K) complex
PI3P
Isolation membrane
LC3-PE
Beclin 1
Bcl2
ER
PI3P
DFCP1
?
DFCP1
PI3P
Omegasome

Figure 1-4. A number of protein complexes regulate autophagosome formation

The Ulk and Vps34 complexes initiate autophagosome assembly via membrane nucleation. The elongation of the membrane is then facilitated by the Atg5-Atg12-Atg16L1 complex and the lipidation of LC3-I into LC3-II. LC3-II remains bound to the autophagosome after maturation and is a common autophagy marker. Signaling inputs to autophagosome assembly include mTOR, Bcl2, and RalB. mTOR inhibits formation of the Ulk1 complex, Bcl2 inhibits Beclin1 and formation of the Vps34 complex, and RalB facilitates exocyst assembly which drives Vps35 complex assembly.

Image reproduced from: Mizushima and Komatsu [106]

1.15 Autophagy and cancer

The relationship between cancer and autophagy is complex. Autophagy can both suppress tumor initiation and help tumor cells endure metabolic stress [107, 108]. Deletion of Beclin1 has been shown to increase spontaneous malignancies in mice and is associated with increased susceptibility to breast cancer, demonstrating that autophagy inhibits tumorigenesis [109, 110]. Oncogenic *KRas* signaling, on the other hand, can both suppresses autophagy through PI3K/Akt/mTOR signaling, and potentially activate autophagy through Raf/Erk and RalB signaling [111]. Studies supporting the requirement of autophagy in tumors have shown that autophagy is essential for KRas-induced transformation and that silencing of Beclin1 reduces KRas driven clonogenic survival [112, 113]. One proposed reason for the discrepancy of KRas signaling inhibiting autophagy and KRas-driven tumors requiring autophagy is that mutant KRas alters metabolism in such a way to require autophagy, possibly by mitophagy (autophagy-mediated degradation of the mitochondria) to overcome glucose deficiency [114]. This hypothesis is supported by the fact that increased expression of autophagy proteins correlates with poor clinical outcome in patients with PDAC [115]. The dependency of some tumors on autophagy has created interest in the potential for anti-autophagy therapeutics for cancers. Chloroquine (CQ), a compound that inhibits the acidification of the autophagosome, in combination with the Src family kinase inhibitor saracatinib, was shown to decrease prostate tumor growth in mice by 64% compared to 26% with saracatinib alone [116]. On the basis of such clinical studies, several Phase I/II trials are currently being performed with hydroxychloroquine (a modified, more soluble, version of CQ) in a variety of tumor types, including pancreatic cancer [108]. 3-methyladenine (3-MA) inhibits autophagosome generation by blocking the production of PI_3P [117]. In mice, combination of 3-MA and the chemotherapeutic 5-fluorouracil inhibited xenograft tumor growth more significantly than 5-fluorouracil alone [118]. In spite of the complex relationship between cancer and autophagy, autophagy inhibitors have emerged as promising anti-cancer therapeutics.

1.16 4-Phenylbutric acid

4-Phenylbutric acid (4-PBA) is a low molecular weight fatty acid with a variety of potential clinical applications. Primarily, 4-PBA is approved for clinical use in patients with urea cycle disorders due to its activity as an ammonia scavenger [119]. Also, 4-PBA has the ability to induce β-globin expression in precursor red blood cells and is used to treat sickle cell disease and thalassemia [120]. Other 4-PBA applications include neuroprotective effects in mouse models of Alzheimer’s and Parkinson’s disease and restoration of glucose homeostasis in mouse models of type II diabetes [121-123].

The variety of physiological effects of 4-PBA can be accredited to two reported functions, as an HDAC inhibitor and a chemical chaperone. The HDAC inhibitor activity of 4-PBA induces differentiation in tumor cells and has led to 4-PBA being used as basis in HDAC inhibitor design and synthesis [124]. Because of its potential anti-tumor activity, 4-PBA has also been tested in Phase I trials in patients with prostate cancer [125]. The other reported function of 4-PBA is as a chemical chaperone serving to stabilize the folded conformation of a protein [126]. The understanding that 4-PBA is a chemical chaperone partly comes from a study in which 4-PBA stabilized a mutated protein (ΔF508-CFTR) commonly misfolded in cystic fibrosis [127]. Later studies also found that 4-PBA treatment decreased expression of ER stress markers in mice [123]. ER stress is caused by the accumulation of unfolded protein in the ER, thus can be reversed by inducing protein folding [128]. The suggested dual activity of 4-PBA gives it much potential as a therapeutic agent, but may cause different effects in various cell types and conditions.

CHAPTER 2. MATERIALS AND METHODS

2.1 General cell culture and drug treatments

ELT3 cells were a gift from Dr. Cheryl Walker (MD Anderson) and were maintained in DF-8 media as described by Walker and Ginsler [129]. MIA-PACA-2 and PANC1 cells were obtained from Dr. Murray Korc (Indiana University School of Medicine). MIA-PACA-2 and HeLa cells were maintained in Dulbecco's Modified Eagle Medium (DMEM) with 10% fetal bovine serum (FBS) (Atlanta Biologicals) and a penicillin-streptomycin antibiotic mixture. PANC1 cells were maintained in DMEM/5% FBS/penicillin-streptomycin. To facilitate passage of each cell line, the cells were washed once with Phosphate Buffered Saline (PBS) and then treated with trypsin EDTA for 5 minutes. The cells were then resuspended in their respective media to inactivate the trypsin. Cells were frozen slowly in 10% DMSO/20% FBS/DMEM. To starve cells of glucose, media was changed to glucose-free DMEM (Gibco) or glucose/L-glutamine/phenol red free DMEM (Gibco) supplemented with fresh L-glutamine.

In experiments with 4-PBA (Santa Cruz), ELT3 cells were treated with 5 mM 4-PBA for 24 hrs before addition of 20 nM bortezomib (LC laboratories) for an additional 6 hrs. Prereatments with trichostatin A (TSA) (Cell Signaling) were performed in the same way as 4-PBA, except TSA was added at 1 µM. Tubastatin (Cayman) was added to ELT3 cells for 1 hr at 10 µM prior to bortezomib treatment. ELT3 cells were treated with 5 mM 3-MA (Acros Organics) for 24 hrs prior to bortezomib treatment. For experiments using chloroquine (CQ) (Sigma Aldrich), 10 µg/ml CQ was added to PANC1 and MIA-

PACA-2 cells at the same time as the change to glucose free media (24 hrs prior to harvest).

2.2 Lentiviral production

To generate lentivirus, 3 million HEK 293T cells were plated in a 10 cm plate in DMEM/10% FBS/penicillin-streptomycin. The next day, 20 µg of the appropriate lentiviral vector was transfected into the 293T cells using polyethylenimine (PEI) (Sigma Aldrich). For each transfection, 45 µl of 2 mg/ml PEI working solution was added to 1.95 ml Optimem (Gibco). 6 µg of VSV-G Lenti, 5 µg of pRSV-REV, and 10 µg of pMDLg/pRRe (lentiviral packaging vectors) were combined with 20 µg of a lentiviral vector in a total of 1 ml Optimem. The PEI solution was then added dropwise to the DNA solution, while vortexing the DNA solution. Five minutes later, the solution was added dropwise to the plate of 293T cells. The following day, the media was changed to fresh growth media and then 24 hours later, the media was removed from the plate, passed through a 0.45 µm filter, and either immediately used or snap frozen in liquid nitrogen.

2.3 Western blotting and antibodies

For experiments not comparing the detergent-soluble and -insoluble fractions, whole cell lysates were obtained using RIPA buffer solution, composed of 50 nM Tris (pH=7.4), 150 nM NaCl, 2 mM EDTA, 1% Triton X-100, and 1% SDS supplemented with the protease inhibitors aprotinin and PMSF. Cells were washed in cold PBA, treated with RIPA buffer solution, scraped off the plate, collected in microcentrifuge at 10,000 rpm for 10 min at 4°C. The supernatant was transferred to a new tube and, if not immediately used, snapped frozen with liquid nitrogen. Lysates were normalized to protein concentration using a Bradford assay (Bio-Rad) and protein sample solution was added. To analyze RalB and Rgl2, samples were separated by electrophoresis in 10% SDS gels at 120V for about 1 hr. To measure acetylated tubulin and total tubulin, samples were subject to electrophoresis in 12% SDS gels for about 1.5 hrs. To measure the levels of cleaved caspase 3, lamin A/C, LC3, and beta-actin, samples were analyzed using 15% SDS gels for about 2 hrs. Separated proteins were transferred from gels to PVDF-FL membranes (Millipore) at 20V overnight. Membranes were then blocked for one hour in a 5% non-fat dry milk in PBS solution supplemented with 0.02% sodium azide. Membranes were probed with primary and secondary antibodies for one hour each. Between blocking and antibody incubations, membranes were washed in Tris-Buffered Saline solution with 0.1% Tween 20 (TBS-T). Antibodies specific to cleaved caspase 3 (#9661), total tubulin (#2125), acetylated tubulin (#5335), lamin A/C (#4777), and LC3 (#3868) were obtained from Cell Signaling Technologies. Antibodies specific to beta-actin (sc-47778) and ubiquitin (sc-8017) were obtained from Santa Cruz Biotechnology. Antibodies specific to Rgl2 (H00005863-M02) and RalB (04-037) were obtained from Abnova and Millipore, respectively. Dilutions of antibodies are indicated in Table 1. Western blots were visualized by using X-ray film and ECL Western Blotting or

SuperSignal West Femto Maximum Sensitivity substrates (Thermo Scientific). The films were then scanned and quantitated by using ImageJ software.

Table 1. Antibody dilutions

Antibody	**Dilution**
Acetylated-tubulin	1:1000
Cleaved caspase 3	1:1000
Lamin A/C	1:1000
LC3	1:1000
Mouse-HRP	1:30,000
Mouse-Texas-Red	1:1000
Rabbit-HRP	1:30,000
RalB	1:1000
Rgl2	1:2500
Tubulin	1:1000
Ubiquitin	1:200 (Western blot), 1:100 (Immunofluorescence)
B-actin	1:5000

2.4 Immunofluorescence microscopy

To image cells using immunofluorescence, 50,000 ELT3 cells were plated on glass coverslips in 35 mm dishes. The next day, cells were serum starved and treated with 5 mM 4-PBA or vehicle. 24 hrs later, cells were treated with 20 nM bortezomib or control for 8 hrs. Coverslips were then washed three times in cold PBS and incubated in cold methanol for 10 min. Coverslips were again washed three times in cold PBS and stored overnight in 20% in PBS at 4°C. The next day, coverslips were washed three times again in cold PBA and then incubated in 1:100 anti-ubiquitin antibody for one hour. After three more washes in cold PBS, the coverslips were incubated in 1:1000 anti-mouse-Texas-Red (Invitrogen). The coverslips were washed three times again in cold PBS and mounted to a microscope slide using VECTASHIELD Hard Set Mounting Medium with DAPI (Vector Laboratories). The slides were imaged on a Zeiss 468 AxioObserverZ1 microscope.

2.5 Soluble/insoluble fractionation

Insoluble and soluble fractions were collected to determine the levels of aggregated ubiquitinated protein. To obtain these fractions, cells were lysed in RIPA buffer solution as described above. After the supernatant (soluble fraction) was collected, however, the pellet was resuspended in 8 M Urea/5% SDS solution and boiled for 10 min (insoluble fraction). The insoluble fraction samples were normalized to the protein levels of the paired soluble fraction levels measured with a Bradford assay (Bio-Rad). The samples were then analyzed via Western blotting as described above.

2.6 Live imaging

In order to image fluorescent GFP-RFP-LC3 and GFP-RFP-p62, MIA-PACA-2 and PANC1 cells were plated in 35 mm MakTek dishes with glass bottoms. To each plate, 100 µl of the appropriate leniviral media and 3 µl 4mg/ml polybrene was added. The next day, media was changed and puromycin was added at 1-2 µg/ml. After two days of puromycin selection, media was changed to DMEM or glucose-free DMEM. Three hours later, the plates were either imaged on a Zeiss 468 AxioObserverZ1 widefield microscope or a Nikon TE-2000U inverted confocal microscope.

2.7 Colony formation assay

To measure anchorage-dependent colony formation, 500 PANC1 or MIA-PACA-2 cells were plates in 60 mm dishes with 100 µl of the appropriate lentiviral media and 6 µl polybrene. The next day, the media was changed and puromycin was added. The cells were grown and puromycin selected for 8 days, changing the media every other day. On the eighth day, the cells were washed in PBS and fixed to the dish for 10 min in 10% methanol/10% acetic acid. After washing again, the dishes were stained with 0.5% crystal violet (Sigma Aldrich)/10% methanol/10% acetic acid. After staining, the dished were rinsed in water and dried overnight on paper towel. The number of colonies was then counted by eye.

2.8 Trypan blue assay

To measure cell death by trypan blue staining, 100,000 MIA-PACA-2 cells were plated in 35 mm dishes with 500 µl of the appropriate lentiviral media and 3 µl polybrene. The next day, the media was changed and puromycin was added. After two days puromycin selection, the media was changed to DMEM or glucose-free DMEM. Thirteen hours later, the media from each was collected, each dish was washed with 1ml PBS, and the wash was collected. The cells were then released from the dish with 500 µl of trypsin EDTA and pooled with the matched media and wash. Each sample was then centrifuged at 800 rpm at 4°C for 5 min. The supernatant was next aspirated off and the pellet of cells was resuspended in 200 µl cold PBS. After vortexing, 10 µl of the sample was combined with 10 ul PBS:0.4% Trypan blue (Sigma Aldrich). This mixture was then put on a hemocytometer (Reichert) and images were taken with a light microscope. The number of living and dead cells was then counted from these images in ImageJ.

2.9 Statistical Analysis

Western blot quantitation was performed in ImageJ and exported to Microsoft Excel. The background of each blot was subtracted from each sample measurement and each sample was normalized to its corresponding beta-actin measurement (acetylated tubulin was normalized to total tubulin). The Western blot data was then normalized to the control sample of each experiment.

To quantitate GFP-RFP-p62 signal in PANC1 cells, images were first exported to Adobe Photoshop Elements. Individual cells were outlined and the red signal was set at a 50% threshold. Any cell with remaining red signal was considered positive. To quantitate GFP-RFP-LC3 signal in MIA-PACA-2 cells, images were first exported to ImageJ. Individual cells were outlined and the red signal was set to an automatic threshold using the Image>Adjust>Auto Threshold>MaxEntropy function. The number of red vesicles was then determined with the Analyze>Analyze Particles function. Due to variable expression per cell, individual thresholds for green signal were set for each cell. To threshold the green signal, the mean intensity of the cytosol was first measured. The threshold was then set to the mean intensity of the cytosol multiplied by two using the Image>Adjust>Threshold function (the value of the multiplier was determined empirically). The number of green vesicles was then determined using the Analyze>Analyze Particles function. The reported “Percent of Mature Autophagosomes” is the difference of the number of red vesicles and green vesicles divided by the number of red vesicles.

Bar graphs represent data from 2 to 4 experiments with error bars representing the standard deviation from the mean for sets of experiments of 3 or more. Reported p-values were calculated using the Student's T-test function in Microsoft Excel (only for sets of 3 or more experiments).

CHAPTER 3. TREATMENT WITH 4-PBA INHIBITS CELL SURVIVAL AND STRESS INDUCED AGGRESOME FORMATION IN ELT3 CELLS

3.1 Introduction

Newly synthesized proteins must first be properly folded before they can be functional. Misfolded proteins can aggregate and excessive protein aggregation is toxic to the cell [83]. The cell has three mechanisms to deal with misfolded proteins: folding the protein with a chaperone protein, degrading the misfolded protein via the proteasome, or sequestering the protein aggregates at an aggresome to be degraded via autophagy [84]. Cells with excessive mTOR activity have increased protein synthesis and therefore a greater requirement for protein folding [130]. Therefore, these cells are more vulnerable to protein clearance inhibition. We hypothesized that inhibiting both aggresome formation and proteasomes will induce death of TSC2 null cells.

HDAC6 is required to recruit protein aggregates to the aggresome [86]. Therefore, inhibition of HDAC6 should prevent aggresome formation and cause an accumulation of toxic protein aggregates in the cytosol. The small compound 4-PBA has been reported to be both a chemical chaperone and to inhibit HDAC activity. We hypothesized that inhibition of HDAC6 by 4-PBA would overcome its protein folding activity and induces aggregate-induced toxicity. We hoped to exacerbate this effect by blocking protein clearance through the proteasome with the proteasome inhibitor, bortezomib.

We tested the combined effect of 4-PBA and bortezomib in ELT3 cells, a rat TSC2 null model, and found that the combination induces greater cell death compared to either compound alone. 4-PBA also decreases the accumulation of protein aggregates induced by bortezomib treatment. In order to link this reduction in aggregates with HDAC inhibition, we repeated the experiment with the pan-HDAC inhibitor trichostatin A (TSA) and the HDAC6-specific inhibitor tubastatin. Both TSA and tubastatin also decrease the aggregate accumulation induced by bortezomib in ELT3 cells. 4-PBA was not, however, able to increase tubulin acetylation, a target of HDAC6. Because the aggresome is also degraded through autophagy, we hypothesized that 4-PBA could alternatively be inducing autophagy. Experiments with the autophagy inhibitor 3-methyladenine (3-MA), however, did not restore aggregate accumulation. Therefore, 4-PBA induces cell death and decreases aggregate accumulation, but these phenomena appear to be independent of HDAC6 activity or autophagy.

3.2 Results

3.2.1 Treatment with 4-PBA increases cell death

Reports in the literature suggest that 4-PBA can be protective against cellular stress, but this work was done in mice with genetically induced ER stress [123]. Therefore, we wanted to first test how 4-PBA affects cell survival during proteasome inhibition in our TSC model, ELT3 cells. ELT3 cells were pretreated with 5mM 4-PBA or vehicle for 24 hrs and then treated with 20nM bortezomib for 0, 12, 15, or 18 hrs. Cleaved caspase 3 was then measured as a marker of apoptosis. Cells pretreated with 4-PBA exhibited increased levels of apoptosis after 12, 15, and 18 hrs of proteasome inhibition (Figure 3-1). Contrary to previous findings, these results suggest 4-PBA increases the cellular stress induced by proteasome inhibition in this cell type [123].

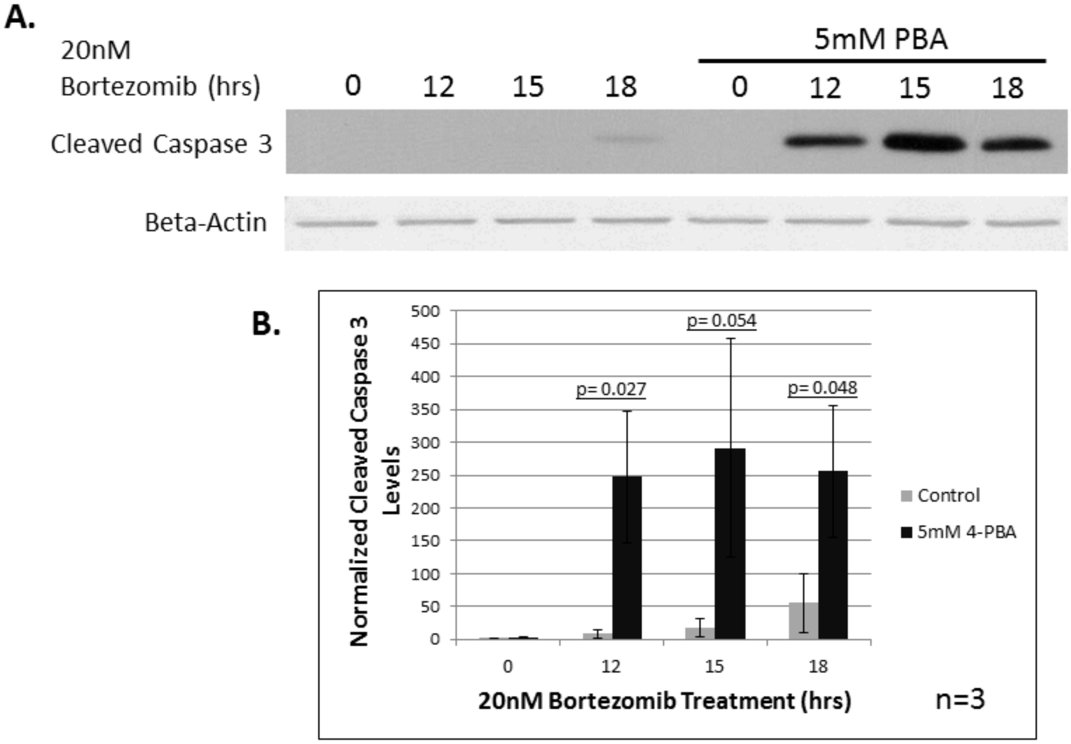

Figure 3-1. Treatment with 4-PBA increases ELT3 cell death

A. ELT3 cells were treated with 5 mM 4-PBA or vehicle for 24 hrs and then with bortezomib or vehicle for 0, 12, 15, or 18 hrs. Cleaved caspase 3 and beta-actin levels were then determined via immunoblot analysis. Blot is representative of three experiments.

B. Quantification of A. All conditions normalized to beta-actin levels. Error bars represent standard deviation of the mean and p-values determined with a Student's T-Test.

3.2.2 Treatment with 4-PBA decreases protein aggregation

The aggresome is typically defined as a perinuclear accumulation of ubiquitinated and aggregated proteins [83]. Therefore, fluorescent imaging of the localization of ubiquitinated proteins and biochemically measuring total ubiquitinated protein aggregates are two of the best ways to measure the aggresome. Because of its HDAC inhibiting activity, we predicted that 4-PBA inhibits HDAC6 to inhibit aggresome formation. To test this, we pretreated ELT3 cells with 5 mM 4-PBA or vehicle for 25 hrs and then with bortezomib for a further 8 hrs (still in presence of 4-PBA). Bortezomib was used to prevent misfolded protein degradation through the proteasome and consequently enhance aggresome formation. Immunofluorescence microscopy analysis was then performed on these cells with an anti-ubiquitin probe (conjugated to Texas Red) and a nuclear marker (DAPI). Bortezomib treatment induced perinuclear accumulation of ubiquitin puncta, but pretreatment with 4-PBA decreased this effect (Figure 3-2a). To measure protein aggregation in an additional way, ELT3 cells were pretreated with 5 mM 4-PBA or vehicle for 24 hrs followed by the addition of 20 nM bortezomib to the medium for 0, 2, 4, or 6 hrs. The cells were then lysed in RIPA buffer solution and separated into soluble and insoluble fractions by centrifugation. Protein aggregates are not soluble in RIPA but the pellet could be subsequently solubilized in 8 M Urea/5% SDS and separated by SDS-PAGE for detection of ubiquitinated proteins by Western blot. Bortezomib treatment induced an accumulation of ubiquitinated protein in the insoluble fraction. While not statistically significant, there was a consistent trend of 4-PBA reducing this accumulation in each of three experiments(Figure 3.2b). Both the immunofluorescence and biochemical experimental results suggest that 4-PBA decreases aggresome formation induced by proteasome inhibition.

A.

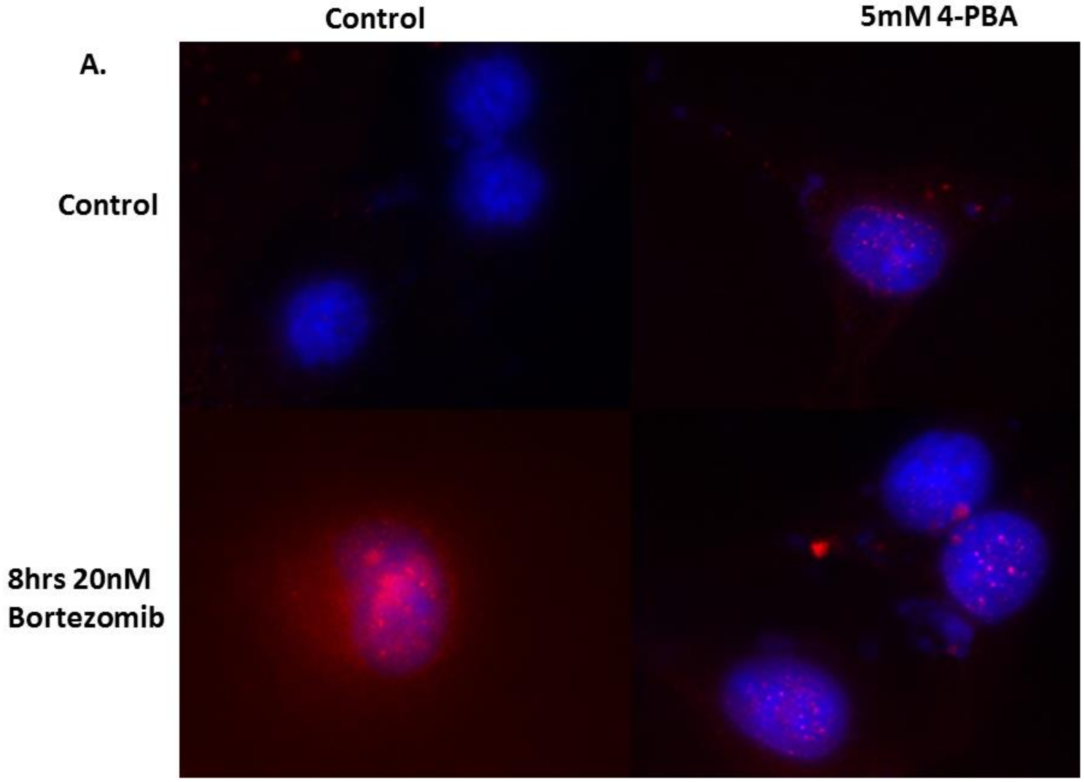
Control
5mM 4-PBA
Control
8hrs 20nM Bortezomib

B.

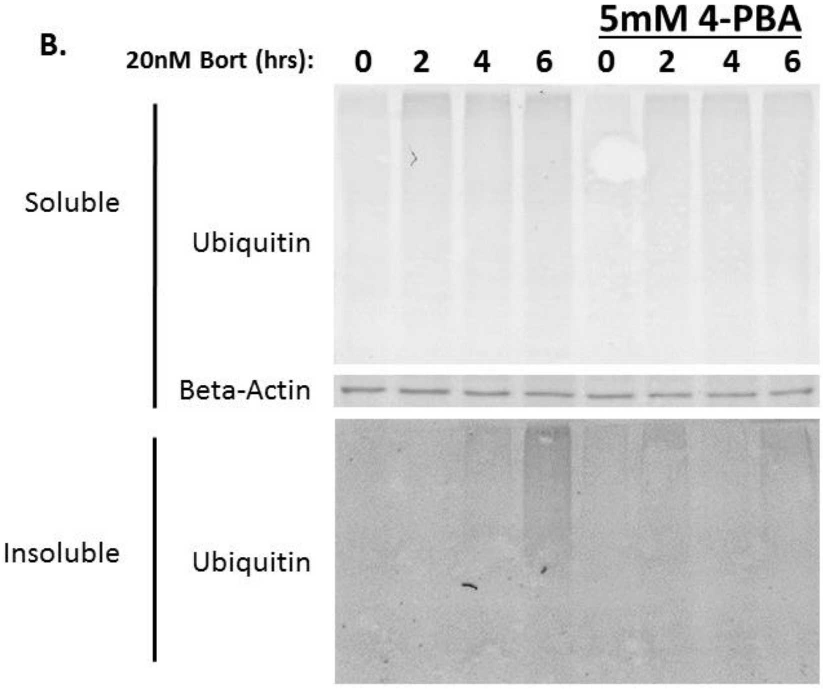
5mM 4-PBA
20nM Bort (hrs):
0
2
4
6
0
2
4
6
Soluble
Ubiquitin
Beta-Actin
Insoluble
Ubiquitin

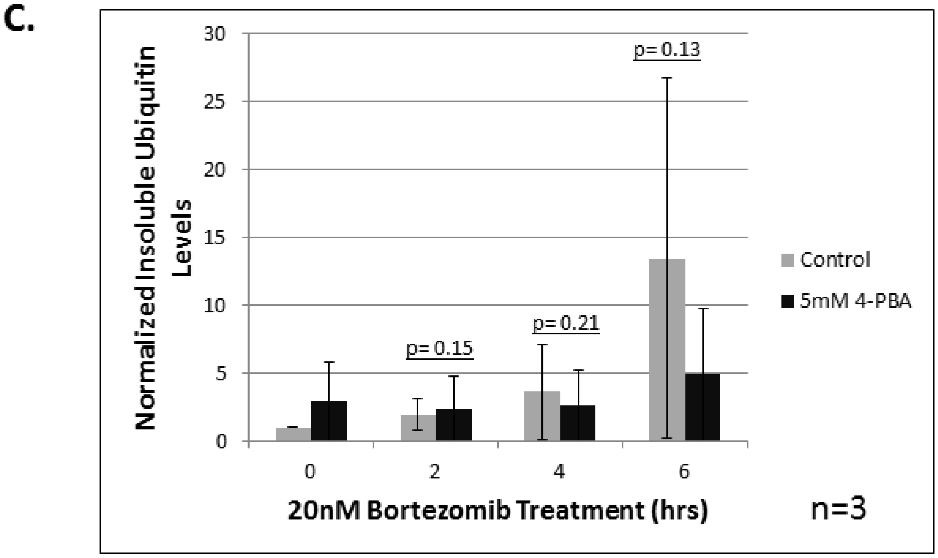

Figure 3-2. Treatment with 4-PBA decreases ubiquitinated protein aggregation

A. ELT3 cells were treated with 5 mM 4-PBA or vehicle for 24 hrs and then with bortezomib or vehicle for 8 hrs. Immufluorescent analysis was then performed with an anti-ubiquitin-Texas-Red antibody and a DAPI stain. Images are representative of three experiments.

B. ELT3 cells were treated with 5 mM 4-PBA or vehicle for 24 hrs and then with bortezomib or vehicle for 0, 2, 4, or 6 hrs. The lysates were then separated into soluble and insoluble fractions. Soluble ubiquitin, soluble beta-actin, and insoluble ubiquitin levels were then determined via immunoblot analysis. Blot is representative of three experiments.

C. Quantification of B. Error bars represent standard deviation of the mean and p-values determined with a Student's T-Test.

3.2.3 Treatment with HDAC inhibitors decreases protein aggregation

We next sought to determine how 4-PBA reduces aggresome accumulation. 4-PBA has been used as a lead compound in the synthesis of HDAC inhibitors and exhibits HDAC-attenuating ability [124]. We hypothesized that 4-PBA inhibits HDAC6, which is required to recruit protein aggregates to the aggresome [86]. Therefore, we attempted to reproduce this effect with other HDAC inhibitors, TSA and tubastatin. ELT3 cells were pretreated with 5 mM 4-PBA or 1 µM TSA for 24 hrs or with 10 µM tubastatin for 1 hr, prior to a 6 hr treatment with 20 nM bortezomib. Time course experiments were performed to determine the ideal treatment time for each HDAC inhibitor, tubastatin only required 1 hr treatment while TSA and 4-PBA required 24 hrs (data not shown). Ubiquitin levels were then analyzed in both the RIPA buffer soluble and insoluble fractions. As before, treatment with bortezomib induced ubiquitinated protein aggregates. In a similar manner to 4-PBA, TSA and tubastatin decreased this accumulation (Figure 3-3). These results supported the notion that 4-PBA reduces protein aggregation via HDAC inhibition.

A.

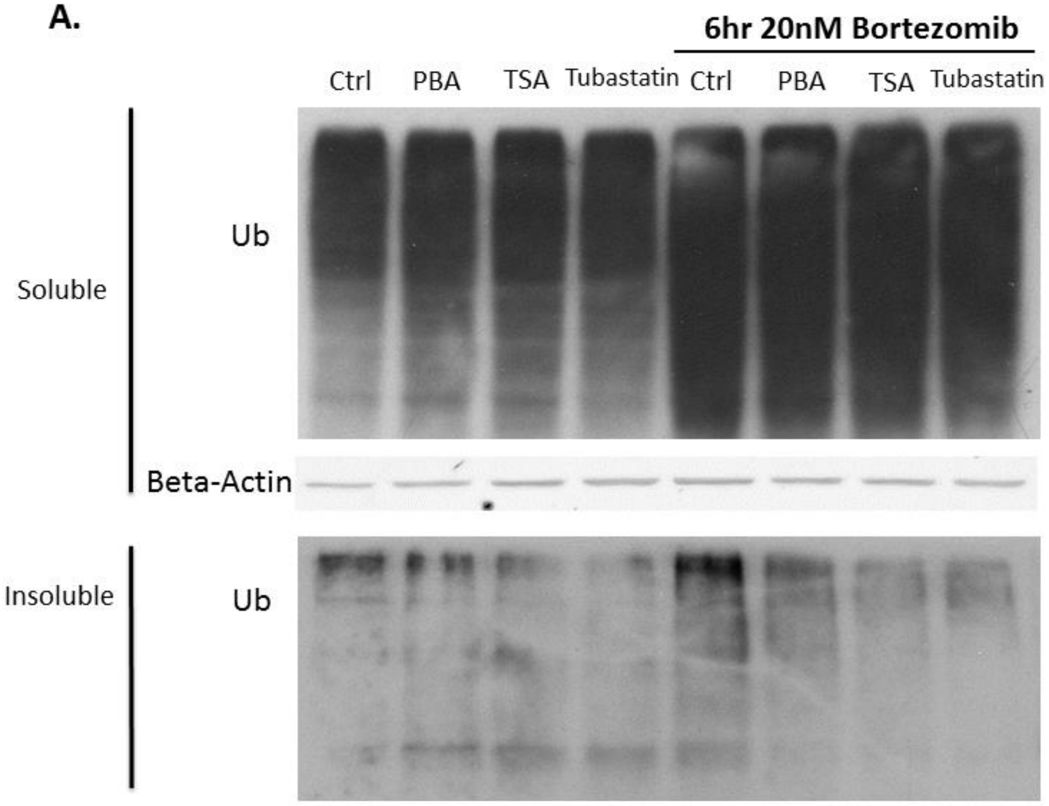
6hr 20nM Bortezomib
Ctrl
PBA
TSA
Tubastatin
Ctrl
PBA
TSA
Tubastatin
Soluble
Ub
Beta-Actin
Insoluble
Ub

B.

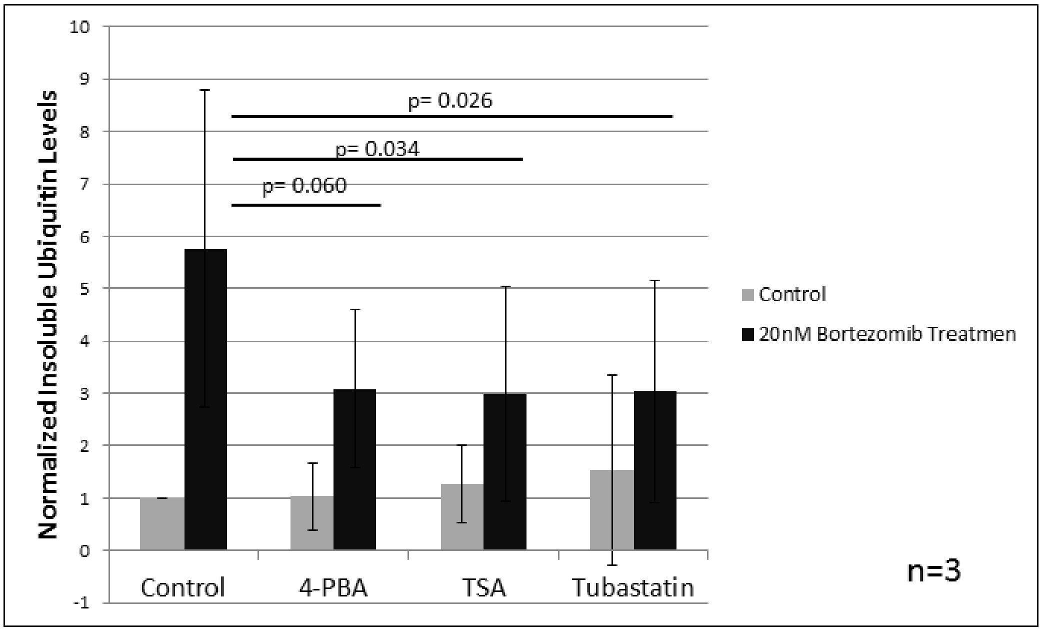
Normalized Insoluble Ubiquitin Levels
10
9
8
7
6
5
4
3
2
1
0
-1
p= 0.026
p= 0.034
p= 0.060
Control
4-PBA
TSA
Tubastatin
Control
20nM Bortezomib Treatmen
n=3

Figure 3-3. Treatment with HDAC inhibitors decreases ubiquitinated protein aggregation

A. ELT3 cells were treated with 5 mM 4-PBA, 1 µM TSA, or vehicle for 24 hrs or 10 µM tubastatin for 1 hr. The cells were then treated with bortezomib or vehicle for 6 hrs. The lysates were then separated into soluble and insoluble fractions. Soluble ubiquitin, soluble beta-actin, and insoluble ubiquitin levels were then determined via immunoblot analysis. Blot is representative of three experiments.

B. Quantification of A. Error bars represent standard deviation of the mean and p-values determined with a Student’s T-Test.

3.2.4 4-PBA treatment does not increase tubulin acetylation

Because of its role in aggresome formation, we next wanted to determine if 4-PBA inhibits HDAC6 activity. One target of HDAC6 is tubulin; therefore, HDAC6 inhibition should increase tubulin acetylation. To test this, ELT3 cells were pretreated with 5 mM 4-PBA or 1 µM TSA for 24 hrs or 10 µM tubastatin for 1 hr, prior to a 6 hr treatment with 20 nM bortezomib. The pretreatment times for the HDAC inhibitors were used in order to stay consistent with the data in Figure 3.2.3. Lysates were then probed for total tubulin and acetylated tubulin using a specific anti-acetyl group antibody. Tubastatin, an HDAC6 specific inhibitor, increased tubulin acetylation but neither 4-PBA nor TSA, a pan-HDAC inhibitor, affected acetylation levels (Figure 3-4). This result suggested that HDAC6 inhibition is not the mechanism by which these compounds decrease protein aggregates.

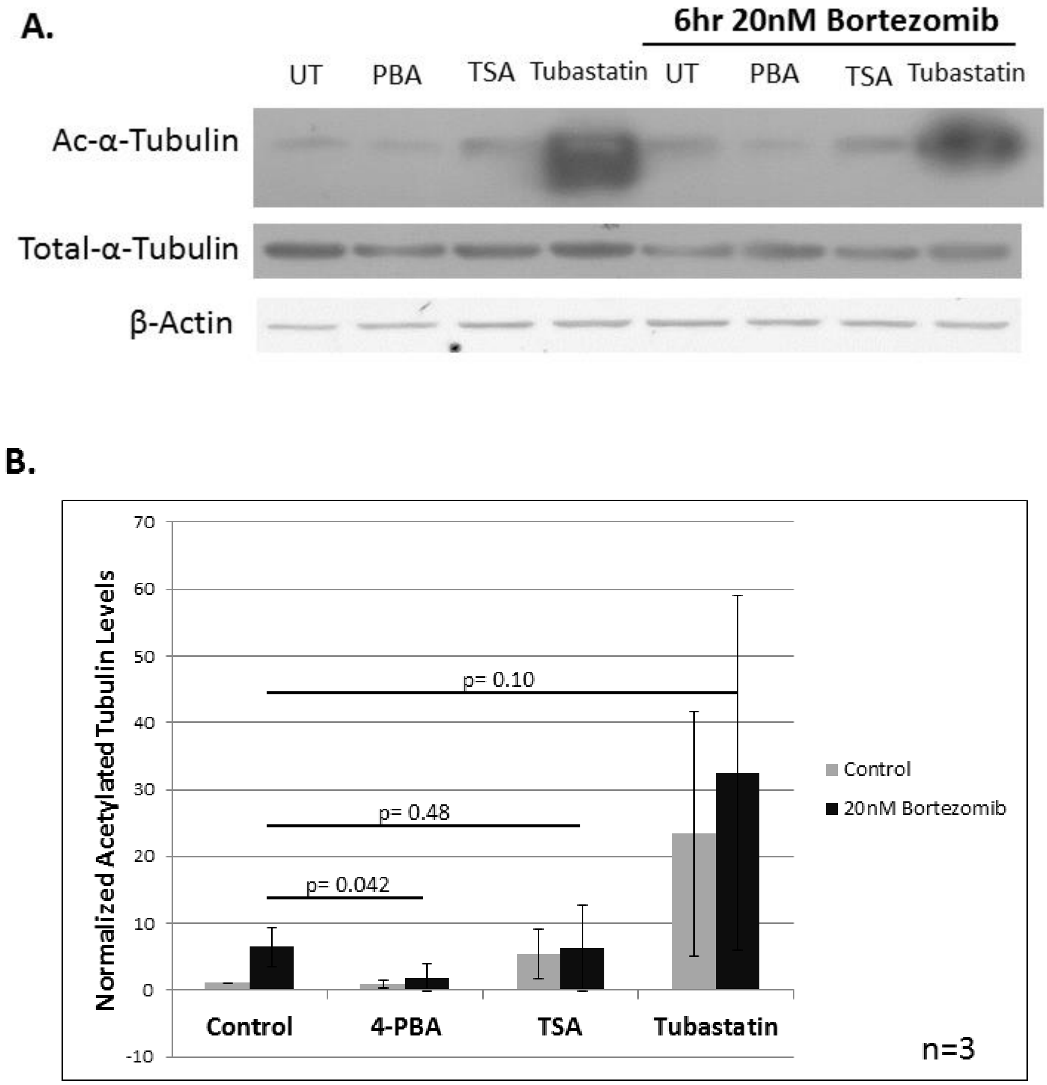

Figure 3-4. 4-PBA treatment does not increase tubulin acetylation

A. ELT3 cells were treated with 5 mM 4-PBA, 1 µM TSA, or vehicle for 24 hrs or 10 µM tubastatin for 1 hr. The cells were then treated with bortezomib or vehicle for 6 hrs. Total tubulin, acetylated tubulin, and beta-actin levels were then determined via immunoblot analysis. Blot is representative of three experiments.

B. Quantification of A. All conditions normalized to total tubulin levels. Error bars represent standard deviation of the mean and p-values determined with a Student's T-Test.

3.2.5 Autophagy inhibition does not restore protein aggregation decreased by 4-PBA

The reduction in aggresomes caused by 4-PBA treatment could either be caused by an inhibition in aggresome formation or an increase in aggresome clearance. The method of clearance for the aggresome is thought to be autophagy. Therefore, 4-PBA may be increasing the rate of autophagy. To test if this is the case, the autophagy inhibitor 3-methyladenine (3-MA) was used. ELT3 cells were pretreated with 5 mM 4-PBA or vehicle and 5 mM 3-MA or vehicle for 24 hrs, and then treated with 20 nM bortezomib for 6 hrs. Ubiquitin levels were then analyzed in both the RIPA buffer soluble and insoluble fractions. LC3 levels were also measured in the soluble control and 3-MA treated samples to ensure autophagy inhibition. 3-MA treatment successfully inhibited LC3-II clearance in the ELT3 cells (Figure 3-5). As before, 4-PBA decreased the bortezomib-induced accumulation of aggregated proteins. Cotreating with 3-MA, however, did not prevent this 4-PBA-induced aggregate reduction (Figure 3-5). Therefore, the reduction in aggresomes caused by 4-PBA is not dependent on autophagy.

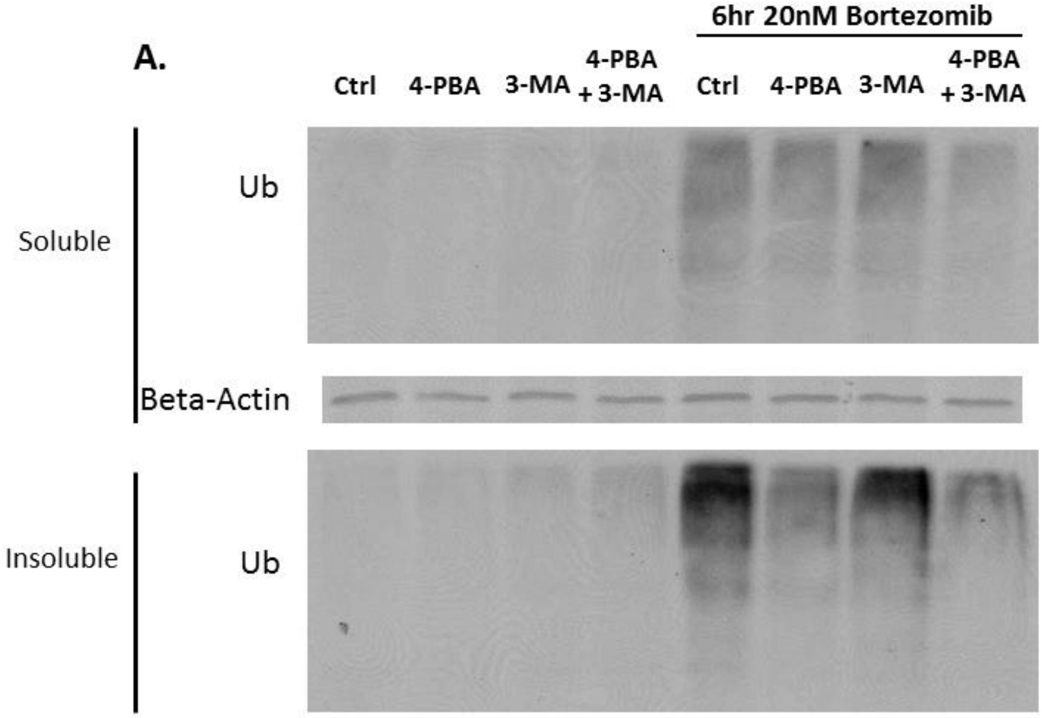
A.
6hr 20nM Bortezomib
Ctrl
4-PBA
3-MA
4-PBA + 3-MA
Ctrl
4-PBA
3-MA
4-PBA + 3-MA
Soluble
Ub
Beta-Actin
Insoluble
Ub

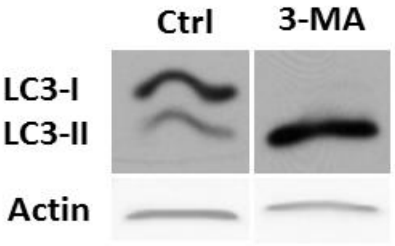
Ctrl
3-MA
LC3-I
LC3-II
Actin

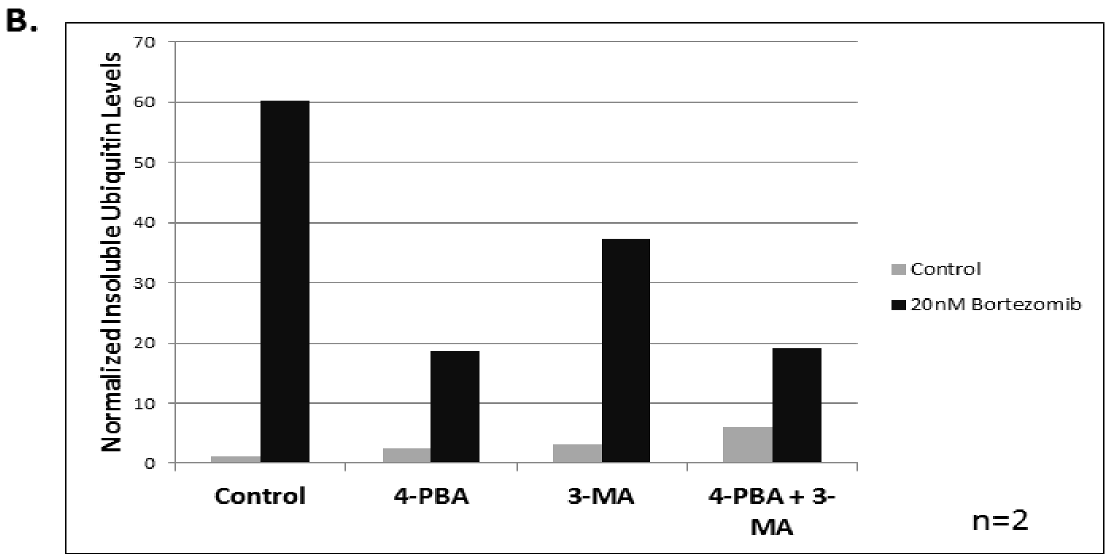

Figure 3-5. 3-MA treatment does not restore protein aggregation decreased by 4-PBA

A. ELT3 cells were pretreated with 5 mM 4-PBA or vehicle and 5 mM 3-MA or vehicle for 24 hrs and then with bortezomib or vehicle for 6 hrs. The lysates were then separated into soluble and insoluble fractions. Soluble ubiquitin, soluble beta-actin, and insoluble ubiquitin levels were then determined via immunoblot analysis. Blot is representative of two experiments. LC3 levels were determined separately as a control in the control and 3-MA treated samples.

B. Quantification of A. Statistics not performed due to only two experiments performed.

3.3 Discussion

3.3.1 4-PBA treatment does not protect against cell death

It was previously reported in the literature that 4-PBA is protective against cellular stress. A large amount of unfolded protein will increase stress, and the ability of 4-PBA to reduce stress was accredited to its activity as a chemical chaperone [123]. Our findings suggest, however, that 4-PBA treatment increases cell death in ELT3 cells (Figure 3-1). Our hypothesis was that the HDAC6 inhibitory activity of 4-PBA was overcoming its ability to fold protein and actually inhibiting aggresome formation. This mechanism of cell death, by inhibiting aggresome formation, has also been reported in the literature. In a study by Zhou et al., proteasome inhibition sensitized TSC2 null cells to cell death due to aggregate accumulation [131]. Our findings, however, demonstrate a novel chemical mechanism of inducing this effect. Other work has also shown that HDAC inhibition can abrogate aggresome formation. Inhibiting both HDACs and the proteasome increased cell death in multiple myeloma cells [132]. We also found that 4-PBA treatment reduces bortezomib-induced aggresome accumulation (Figure 3-2). These findings of the increased cell death and decreased aggresome accumulation caused by 4-PBA treatment support our hypothesis.

3.3.2 The inhibition of aggresome formation by 4-PBA treatment does not correlate with HDAC6 inhibition

To test if the ability of 4-PBA to reduce aggresomes was due to its HDAC inhibitory activity, we repeated the experiment with other HDAC inhibitors. The pan-HDAC inhibitor, TSA, and the HDAC6-specific inhibitor, tubastatin, both reduced bortezomib-induced aggresomes in ELT3 cells (Figure 3-3). These results confirm previous findings and correlate with the effects of 4-PBA treatment [132]. To connect the reduction in aggresomes with HDAC6 inhibition we measured the level of tubulin acetylation after 4-PBA, TSA, and tubastatin treatment. Because tubulin is a target of HDAC6, HDAC6 inhibition will cause an increase in tubulin acetylation. Tubastatin treatment increased tubulin acetylation, but 4-PBA and TSA did not (Figure 3-4). Because tubastatin is specific to HDAC6, tubastatin is expected to have a more intense effect on tubulin acetylation. 4-PBA and TSA, however, did not even have a measurable effect. One explanation for this could be treatment duration of the HDAC inhibitors. 4-PBA and TSA required 24 hr pretreatment to reduce aggresome accumulation, but tubastatin only required one hour. Long exposure to HDAC inhibitors has an effect on a number of cellular pathways, including gene expression and genomic stability [133]. Therefore, treatment with 4-PBA may indirectly alter another cellular mechanism resulting in a reduction of aggresomes. We hypothesized next that instead of 4-PBA inhibiting aggresome formation, it is actually increasing aggresomal degradation. The pathway for aggresomal degradation is thought to be autophagy [84]. Thus, we attempted to use 3-MA to inhibit autophagy and restore aggresome levels. Cotreating cells with 4-PBA and 3-MA did not, however, restore bortezomib-induced aggregate levels (Figure 3-5). Therefore, 4-PBA-mediated reduction in aggregate levels is independent of HDAC6 and autophagy. The fact that TSA and tubastatin also reduced aggregate levels, however, suggests that this effect is due to HDAC inhibition. One possible mechanism could be changes in gene expression, a typical result of HDAC inhibition since chromatin/histones is their major target [133]. A global reduction in gene expression would decrease unfolded protein levels and stress, especially in TSC2 cells. Our findings show that 4-PBA increases ELT3 cell death and decreases aggresome levels, but the relationship between these phenomena remains unclear.

3.4 Future directions

A number of further experiments could be done to determine the exact mechanism in which 4-PBA and the other HDAC inhibitors reduce protein aggregates. Because of the long treatment time required for 4-PBA and TSA to have an effect, we hypothesize that these compounds may have an effect on global gene expression. TSC2 null cells (such as ELT3 cells) have increased gene expression due to constitutive mTOR activity. HDAC inhibition has been to shown to reduce gene expression [133]. Therefore, the reduction in aggresomes caused by 4-PBA treatment may just be due to reduced gene expression and less requirement for protein folding. We could then determine if actinomycin (a transcription inhibitor) or cycloheximide (a translation inhibitor) inhibit bortezomib-dependent protein aggregation. A reduction in aggresomes caused by these compounds would then correlate with our 4-PBA data. Another way to test this hypothesis would be to directly measure how 4-PBA affects gene expression. A radio-labeled amino acid chase experiment with or without 4-PBA would demonstrate how 4-PBA alters protein synthesis. This experiment would be done with a variety of 4-PBA treatment times to determine if any effect is time-dependent. A reduction in global protein synthesis with 4-PBA treatment (specifically at longer treatment times) would suggest there is a correlation between protein synthesis and aggresome formation. To determine if 4-PBA, TSA, and tubastatin increase protein folding, a mutated cystic fibrosis transmembrane conductance regulator construct (ΔF508-CFTR) could be used. ΔF508-CFTR will only fold, and thus be detected via Western blotting, under conditions that promote protein folding (such as in the presence of a chaperone) [134]. ΔF508-CFTR could then be expressed in cells and then we could determine if 4-PBA, TSA, or tubastatin is able to induce folding. There is evidence that 4-PBA does restore ΔF508-CFTR folding, but it is unclear if TSA or tubastatin also do [127]. If all three HDAC inhibitors do restore ΔF508-CFTR folding, then the reduction in aggresomes may be due to a reduction in misfolded protein. Also, our hypothesis was based on the cells being TSC2 null, thus having higher protein synthesis and stress. Further experiments with cells with wild type TSC2 could determine if 4-PBA also induces cell death during proteasome inhibition. These experiments would help explain how 4-PBA and the other HDAC inhibitors reduce aggregated proteins.

CHAPTER 4. RGL2 LOSS INHIBITS CELL SURVIVAL BUT NOT AUTOPHAGY IN MIA-PACA-2 PANCREATIC CANCER CELLS

4.1 Introduction

Over 90% of PDAC tumors have activating mutations in *KRas*, which leads to constitutive KRas signaling [60]. This then causes increased activity of such downstream effectors as PI3K, Raf, and the RalGDS proteins. Because of their increased activity in pancreatic cancer, much research has been done attempting to therapeutically target KRas and its effectors. However, little success has been achieved in this regard [135]. Less research, though, has targeted the Ral pathway relative to the other KRas effectors. Recent work has shown that Rgl2 is overexpressed in PDAC and loss of Rgl2 inhibits PDAC cell survivals [50]. Because of these results, we looked into what are the underlying mechanisms by which Rgl2 can regulate cell survival. The abovementioned study showed that mutationally activated RalA only partially restored survival reduced by loss of Rgl2 and showed that loss of Rgl2 preferentially inhibits RalB activation over RalA [50]. These two findings lead us to hypothesize that Rgl2 stimulates survival via some RalB-dependent mechanism(s). A separate study showed that RalB facilitates the binding of Ulk1 and Vps34 complexes onto the exocyst, initiating autophagosome formation [105]. Although autophagy can be a possible death pathway, there is also much evidence that suggests that autophagy can promote survival in tumor cells, especially in low nutrient environments (such as a PDAC tumor) [136]. Therefore we hypothesized that Rgl2 promotes PDAC cell survival by facilitating autophagy and subsequent reclamation of nutrients.

We first wanted to determine if loss of Rgl2, and not another RalGEF, decreased autophagy in PANC1, a PDAC cell line. We focused on the two RalGEFs that have been shown to have highest expression in PDAC cells, RalGDS and Rgl2 [50]. Our initial experiments with a fluorescent LC3 construct showed that loss of Rgl2 and not RalGDS inhibited autophagosome maturation. To confirm that loss of Rgl2 inhibits PDAC survival, we again used shRNA to decrease Rgl2 levels in PANC1 and MIA-PACA-2 cells, another KRas mutant PDAC cell line. Loss of Rgl2 decreased colony formation in both these cells and increased cell death in MIA-PACA-2 cells. We next developed a quantitative method of measuring p62-positive cells by counting the number of cells with signal above a 50% threshold. Initial quantitation methods demonstrated that loss of Rgl2 decreased total number of autophagosomes. This method of measuring autophagosomes, however, had a number of weaknesses. To address these method deficiencies, another quantitation method was developed to specifically count the number of mature and immature autophagosomes per cell. Alternatively, this more sophisticated method revealed that loss of Rgl2 had no effect on LC3-positive autophagosome number or maturation. To elaborate on the fluorescent autophagy data, we next measured the effects of loss of Rgl2 on endogenous LC3 levels. We first measured how glucose starvation changed LC3 levels in PDAC cells, using HeLa cells as a control cell line. Glucose starvation caused a decrease in LC3-II levels in HeLa cells, but increased LC3-II levels in the two PDAC cell lines. We then measured how the loss of Rgl2 affects LC3 loss in the PDAC cells. Surprisingly loss of Rgl2, or the positive control RalB, did not inhibit starvation-induced increase in the PDAC cell lines. Because LC3 levels are constantly in flux during autophagy, we next used the autophagy inhibitor CQ to measure the accumulation of LC3-II. Loss of Rgl2 and RalB, however, did not inhibit the accumulation of LC3-II. The imaging data together with the endogenous LC3 data revealed that while loss of Rgl2 inhibits survival, it does not significantly inhibit autophagy.

4.2 Results

4.2.1 Rgl2 but not RalGDS loss inhibits autophagosome maturation in PANC1 cells

RalGDS and Rgl2 are both highly expressed in PDAC cell lines [50]. Therefore, we first determined if loss of either RalGEF inhibited autophagosome maturation. To measure autophagosome maturation, we used a doubly- RFP/GFP tagged fluorescent-LC3. Fluorescence from the RFP tag persists in the low pH environment of lysosomes but that of GFP is quenched. Therefore, a mature acidified autophagosome will be red while an immature autophagosome will appear “yellow” (fluorescing both red and green) [98]. PANC1 cells were infected via lentivirus with the LC3 construct and RalGDS, Rgl2, or control shRNA. The cells were then glucose starved for 3 hrs to induce autophagy and imaged live with a widefield microscope. After starvation, the cells infected with the RalGDS shRNA appeared to have more red vesicles than the cells infected with the control shRNA. Loss of Rgl2, however, caused an increase in the amount of immature (yellow) autophagosomes after starvation (Figure 4-1). These results suggested that the loss of Rgl2, but not RalGDS, inhibits autophagosome maturation. Loss of RalGDS, however, was not able to be confirmed due to the lack of a commercially available antibody. Quantitative PCR experiments were attempted to determine efficacy of RalGDS shRNA, but were not successfully optimized. Further attempts to optimize were halted due to lack of focus on RalGDS. Also, the low resolution and high background signal prevented quantitation of the number of vesicles per cell, a problem addressed in Chapters 4.2.4 and 4.2.5. Regardless, these results encouraged further analysis of the relationship between Rgl2 and autophagy.

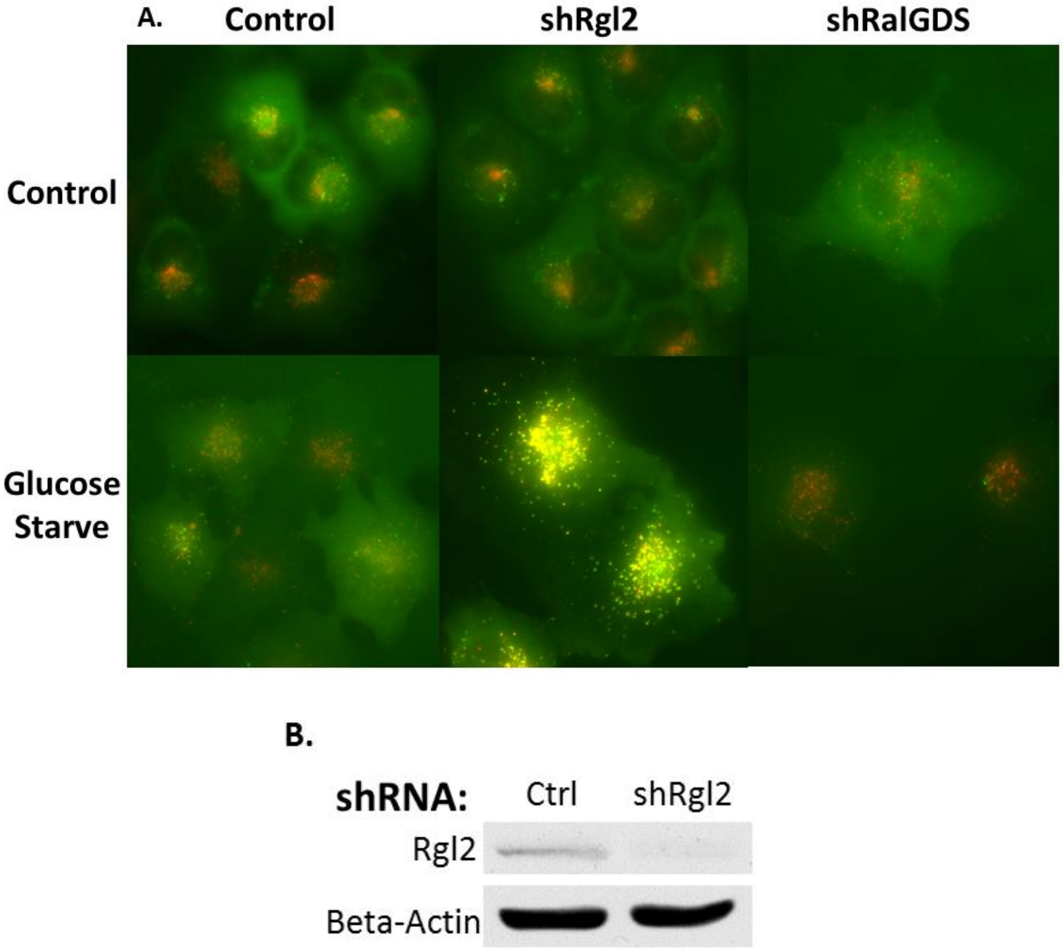
A.
Control
shRgl2
shRalGDS
Control
Glucose Starve
B.
shRNA:
Ctrl
shRgl2
Rgl2
Beta-Actin

Figure 4-1. Rgl2 but not RalGDS loss inhibits autophagosome maturation in PANC1 cells

A. PANC1 cells were infected with control, RalGDS, or Rgl2 shRNA as well as a GFP-RFP-LC3 construct. After three days of puromycin selection, cells were glucose starved for three hours and images were taken with a widefield microscope. Images are representative of two experiments.

B. Rgl2 and beta-actin levels from the control and shRgl2 samples from A. were determined using immunoblot analysis. RalGDS levels were not determined due to lack of a commercially available antibody. Blot is representative of two experiments.

4.2.2 Loss of Rgl2 inhibits anchorage-dependent colony formation in PDAC cells

We next sought to confirm that the loss of Rgl2 inhibits PDAC cell viability. Previous work observed that the loss of Rgl2 inhibited anchorage-independent colony formation [50]. We repeated this experiment, but measured anchorage-dependent colony formation instead. This assay is the gold standard in cancer cell biology [137] for identifying genes necessary for cancer cell growth and will supplement the previous findings. We used shRNA to decrease Rgl2 levels in PANC1 and MIA-PACA-2 cells and then plated the cells at very low confluency. Eight days later the number of colonies was measured. Loss of Rgl2 caused a loss in the number of adherent colonies in both PDAC cell lines (Figure 4-2). These results confirm findings from previous studies and demonstrate that loss of Rgl2 inhibits PDAC cell viability [50].

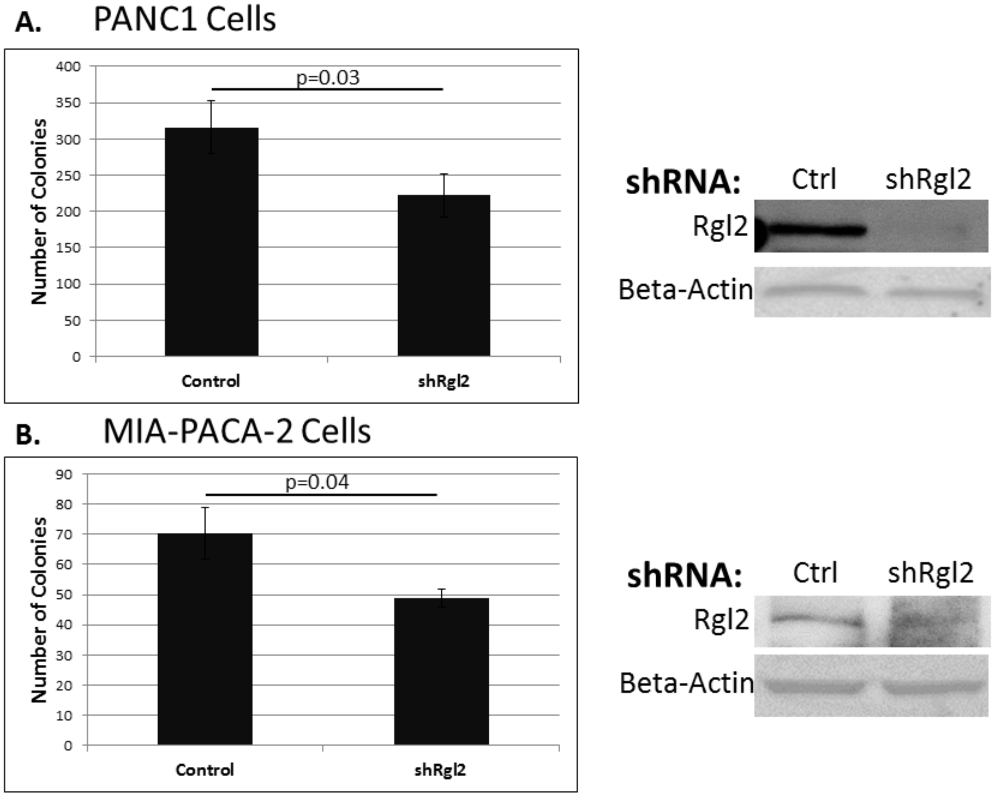

Figure 4-2. Loss of Rgl2 inhibits anchorage-dependent colony formation in PDAC cells

A. A low number of PANC1 cells were infected with control or Rgl2 shRNA and were grown and selected with puromycin for eight days. At that point, colonies were stained with crystal violet and counted. The levels of Rgl2 and beta-actin were also measured using immunoblot analysis in samples plated in parallel. Error bars represent standard deviation of the mean and p-values determined with a Student's T-Test. Data is exemplary of two experiments.

B. The above assay was performed using MIA-PACA-2 cells. Error bars represent standard deviation of the mean and p-values determined with a Student's T-Test. Data is exemplary of two experiments.

4.2.3 Loss of Rgl2 increases cell death in MIA-PACA-2 cells

To further support the data from chapter 4.2.2 and demonstrate how Rgl2 promotes cell viability, we next addressed the mechanism by which loss of Rgl2 affects PDAC cell survival. To do so, Rgl2 was knocked down using shRNA in MIA-PACA-2 cells. Cells were also glucose starved, to measure cell death in autophagic conditions. Cell death was then measured in two ways. First, the dead cells were stained with trypan blue and counted. Loss of Rgl2 caused a significantly higher number of dead MIA-PACA-2 cells. Also, cleaved lamin A/C fragment levels were measured as a marker of apoptosis. While not significant, there was a trend in three different experiments that loss of Rgl2 increased lamin A/C fragment levels both with and without glucose starvation. Loss of Rgl2 did not, however, induce cell death in PANC1 cells (data not shown). These results demonstrate that loss of Rgl2 inhibits cell survival in addition to colony formation in MIA-PACA-2 cells.

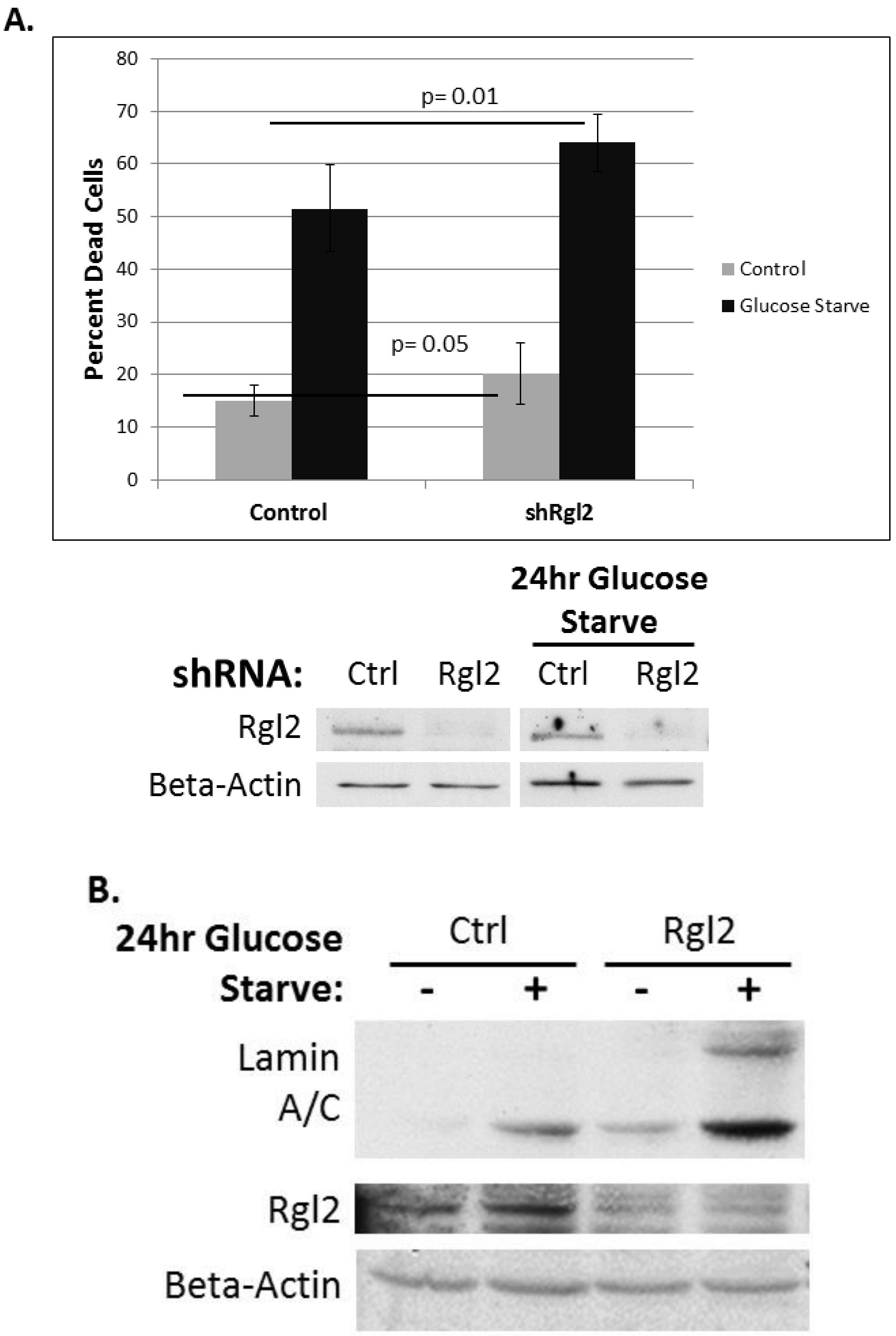
A.
80
70
60
50
40
30
20
10
0
Percent Dead Cells
p= 0.01
p= 0.05
Control
shRgl2
Control
Glucose Starve
24hr Glucose Starve
shRNA:
Ctrl
Rgl2
Ctrl
Rgl2
Rgl2
Beta-Actin
B.
24hr Glucose Starve:
Ctrl
Rgl2
-
+
-
+
Lamin A/C
Rgl2
Beta-Actin

C.

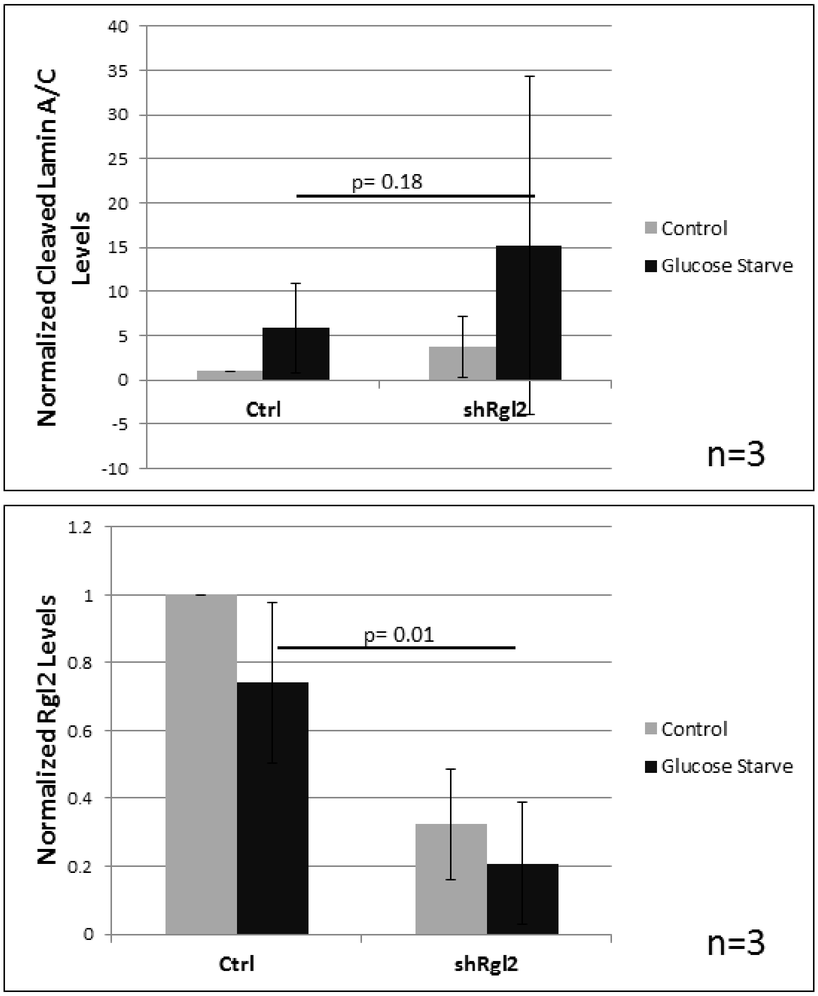
Normalized Cleaved Lamin A/C Levels
40
35
30
25
20
15
10
5
0
-5
-10
p= 0.18
Ctrl
shRgl2
■ Control
■ Glucose Starve
n=3
Normalized Rgl2 Levels
1.2
1
0.8
0.6
0.4
0.2
0
p= 0.01
Ctrl
shRgl2
■ Control
■ Glucose Starve
n=3

Figure 4-3. Loss of Rgl2 increases MIA-PACA-2 cell death

A. MIA-PACA-2 cells were infected with control or Rgl2 shRNA and conditions were plated in triplicate. After three days of selection, cells were glucose starved for 24 hrs. At that point, the media and cells were harvested and the number of dead cells was identified using trypan blue. The levels of Rgl2 and beta-actin were also measured using immunoblot analysis in samples plated in parallel. Data is representative of the combined data of two experiments. Error bars represent standard deviation of the mean and p-values determined with a Student's T-Test.

B. MIA-PACA-2 cells were infected with control or Rgl2 shRNA and selected with puromycin for three days. At that point, cells were glucose starved for 24 hrs and lysates were harvested. Lamin A/C, Rgl2, and beta-actin levels were then determined using immunoblot analysis. Blot is representative of three experiments.

C. Quantification of B. All conditions normalized to beta-actin levels. Error bars represent standard deviation of the mean and p-values determined with a Student's T-Test.

4.2.4 Loss of Rgl2 decreases total p62-positive puncta in PANC1 cells during glucose starvation

Due to low resolution and high background, we were unable to quantitate the previous autophagy microscopy data (Figure 4-1). To generate quantifiable data, we used a p62 fluorescent construct instead of the LC3 construct. We observed that p62 only localized to puncta when autophagy was induced, as opposed to LC3 which forms puncta without stimulation. This observation led us to generate a quantitation method with the p62 construct. PANC1 cells were infected with the doubly tagged p62 construct and Rgl2 or control shRNA. PANC1 cells were used to be consistent with Figure 4-1. The cells were then glucose starved for 3 hrs to induce autophagy and imaged live with a widefield microscope. The images were exported to Adobe Photoshop, individual cells were outlined, and the red signal was set at a threshold of 50%. Any cell still containing red signal after thresholding was then considered positive. Glucose starving the control cells caused an increase in the number of positive cells. The samples without Rgl2 did not exhibit this starvation-induced increase in number of positive cells, and starved samples without Rgl2 had significantly less positive cells than starved control cells (Figure 4-4). This method of quantitating autophagy supports the idea that loss of Rgl2 inhibits autophagy. This method of quantitation, however, has a number of potential shortcomings. The number of puncta per cell and the maturity of the vesicle (color) are two pieces of information that are lost by measuring this way. Because of these flaws, we next sought a better method of quantitating autophagy.

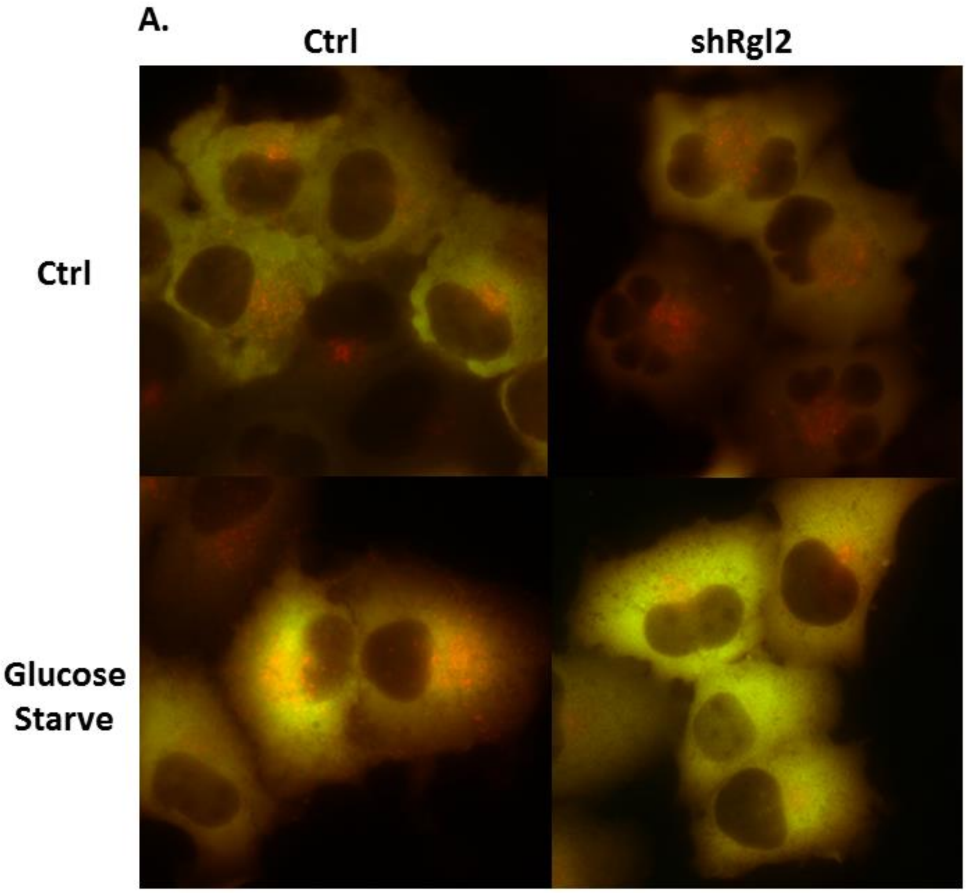
A.
Ctrl
shRgl2
Ctrl
Glucose Starve

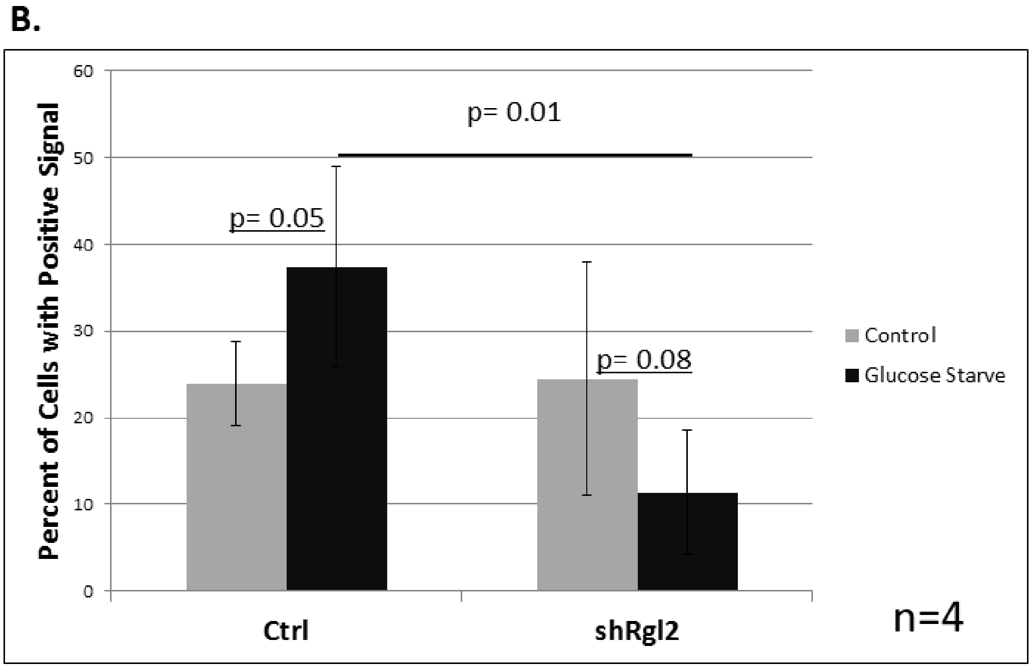
B.
Percent of Cells with Positive Signal
60
50
40
30
20
10
0
p= 0.01
p= 0.05
p= 0.08
Ctrl
shRgl2
▨ Control
■ Glucose Starve
n=4

Figure 4-4. Loss of Rgl2 decreases total p62-positive puncta in PANC1 cells during glucose starvation

A. PANC1 cells were infected with control or Rgl2 shRNA as well as a GFP-RFP-p62 construct. After three days of puromycin selection, cells were glucose starved for three hours and images were taken with a widefield microscope. Images are representative of four experiments.

B. Quantitation of images from A. To quantitate, images were exported to Adobe Photoshop, individual cells were identified, and the red signal was set at a 50% threshold. Any cell still containing red signal after the threshold was considered positive. Data is representative of four experiments. Error bars represent standard deviation of the mean and p-values determined with a Student's T-Test.

4.2.5 Loss of Rgl2 has no effect on autophagosome maturation in MIA-PACA-2 cells

A few measures were then taken to develop a more improved method of quantitating autophagy. First, to improve the resolution and facilitate measuring individual puncta, a confocal microscope was used instead of a widefield microscope. Also, the doubly-tagged fluorescent LC3 construct was used instead of the p62 construct. The LC3 construct allows for measuring changes in acidity more readily than the p62 construct (determined empirically and reflected in the data). Lastly, the number of puncta per cell was measured versus the total number of cells with thresholded signal. To gather images, MIA-PACA-2 cells were infected with the doubly tagged LC3 construct and Rgl2, RalB, or control shRNA. MIA-PACA-2 cells were used for these imaging experiments in order to stay consistent with the survival data (Figure 4-3). The cells were then glucose starved for 3 hrs to induce autophagy and imaged live with a confocal microscope by the contributor Seth Winfree. The images were exported to ImageJ, cells were outlined, and red and green signals were separately thresholded. The number of puncta was determined automatically with the ImageJ software. Supporting published data, loss of RalB inhibited the starvation-induced accumulation of mature autophagosomes and decrease in immature autophagosomes (Figure 4-5). Nonstarved cells without RalB had similar levels of immature and mature autophagosomes compared with starved control cells. These results suggest that loss of RalB may increase autophagy levels even in cells not subject to starvation, an idea further pursued in

Chapter 4.2.8. The level of autophagosomes in all conditions was not significantly different in cells without Rgl2 compared to control cells. The method of quantitation described in this section maintains much of the information lost with the previous quantitation method (Figure 4-4). Therefore, these results suggest that loss of Rgl2 has no effect on autophagy.

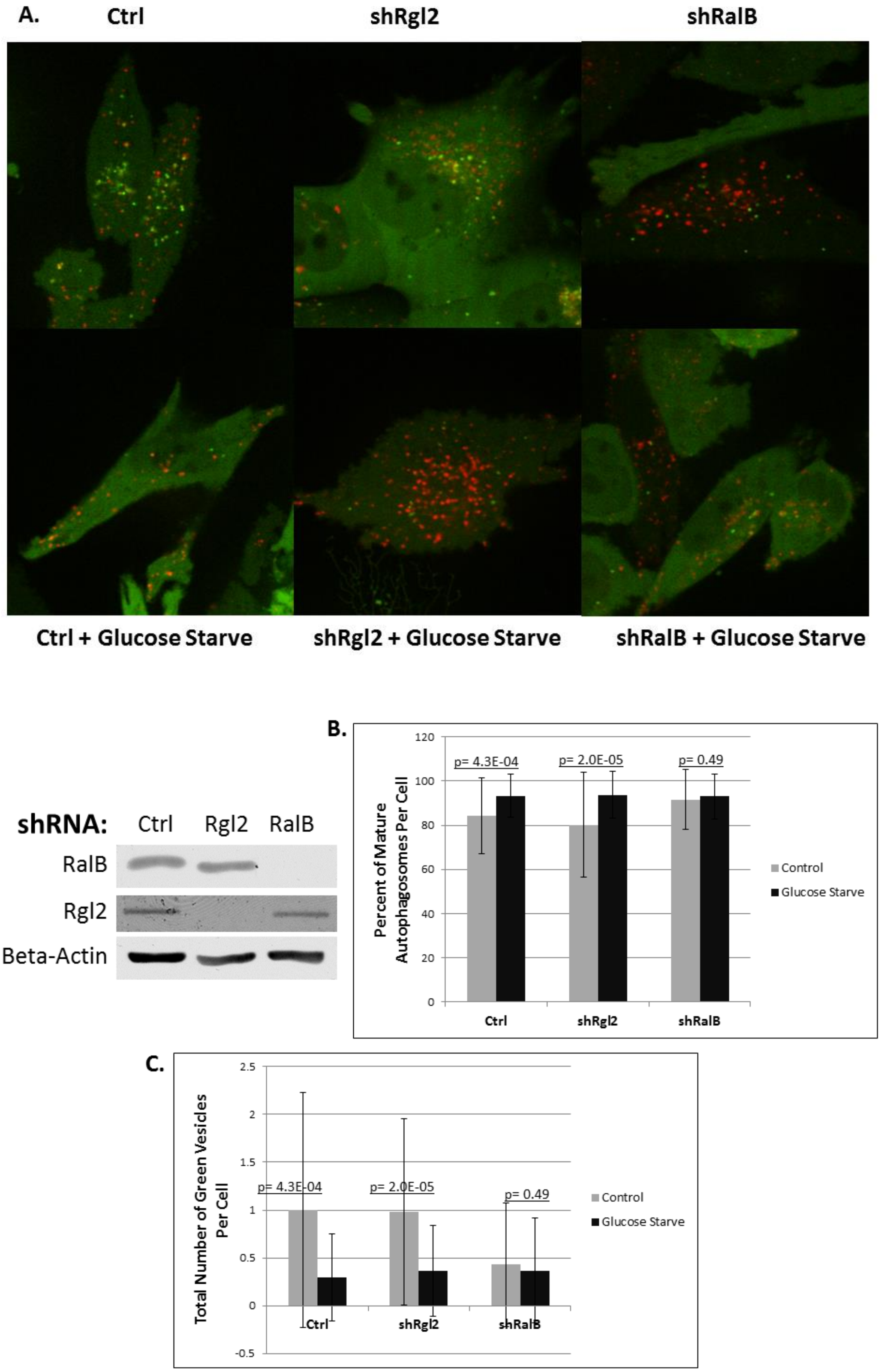
A.
Ctrl
shRgl2
shRalB
Ctrl + Glucose Starve
shRgl2 + Glucose Starve
shRalB + Glucose Starve
shRNA:
Ctrl
Rgl2
RalB
RalB
Rgl2
Beta-Actin
B.
Percent of Mature Autophagosomes Per Cell
0
20
40
60
80
100
120
p= 4.3E-04
p= 2.0E-05
p= 0.49
Ctrl
shRgl2
shRalB
Control
Glucose Starve
C.
Total Number of Green Vesicles Per Cell
-0.5
0
0.5
1
1.5
2
2.5
p= 4.3E-04
p= 2.0E-05
p= 0.49
Ctrl
shRgl2
shRalB
Control
Glucose Starve

Figure 4-5. Loss of Rgl2 has no effect on autophagosome maturation in MIA-PACA-2 cells

A. MIA-PACA-2 cells were infected with control, Rgl2, or RalB shRNA as well as a GFP-RFP-LC3 construct. After three days of puromycin selection, cells were glucose starved for three hours and images were taken with a confocal microscope by Seth Winfree. The levels of Rgl2 and beta-actin were also measured using immunoblot analysis in samples plated in parallel. Images are representative of two experiments.

B. Quantitation of the percent of mature autophagosomes per cell. The number of red and green vesicles was determined by exporting the images to ImageJ, individually selecting cells, setting a threshold for each channel, and using the software to determine the number of vesicles. A mature autophagosome was considered a vesicle that had red signal but no green signal. Data is representative of the combined data of two experiments. Error bars represent standard deviation of the mean and p-values determined with a Student's T-Test.

C. Quantitation of the number of green vesicles. The number of green vesicles was determined using the same method described in B. Data is representative of the combined data of two experiments. Error bars represent standard deviation of the mean and p-values determined with a Student's T-Test.

4.2.6 PDAC cells accumulate LC3-II during glucose starvation

We next measured endogenous LC3 as another method of determining if loss of Rgl2 has an effect on autophagy in PDAC cells. Because of the different levels of basal autophagy in different cell lines, however, we first just measured how glucose starvation affects LC3 levels in PDAC cells. During autophagy, LC3-I is lipid modified to generate LC3-II, then LC3-II is degraded with the contents of the autophagosome [96]. Therefore, by measuring LC3-II levels over the course of time one can track autophagy progression. To do this, we used HeLa cells as a technical control (since they had been used in [105]) in addition to the PDAC cell lines PANC1 and MIA-PACA-2. Each cell line was glucose starved for 0, 0.5, 3, 6, or 24 hrs and LC3 levels were measured using immunoblotting. After 24 hrs glucose starvation, LC3-II levels decreased in HeLa cells but increased in both the PDAC cell lines (Figure 4-6). These results are consistent with previously published data [138, 139]. Therefore, these results show that accumulation of LC3-II is a good marker of glucose starvation-induced autophagy in PDAC cells.

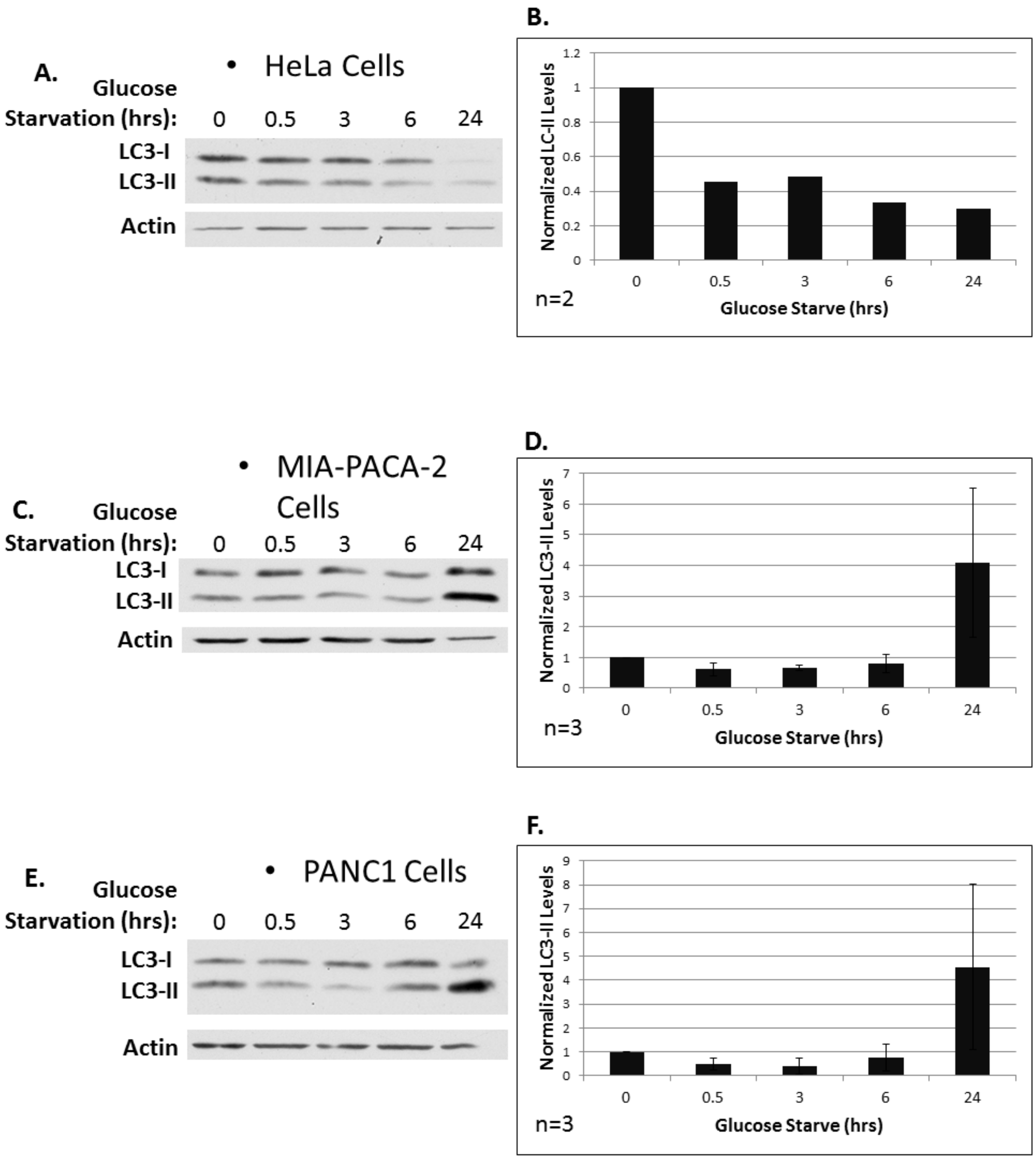
A.
• HeLa Cells
Glucose
Starvation (hrs):
0
0.5
3
6
24
LC3-I
LC3-II
Actin
B.
Normalized LC-II Levels
0
0.2
0.4
0.6
0.8
1
1.2
0
0.5
3
6
24
Glucose Starve (hrs)
n=2
C.
• MIA-PACA-2 Cells
Glucose
Starvation (hrs):
0
0.5
3
6
24
LC3-I
LC3-II
Actin
D.
Normalized LC3-II Levels
0
1
2
3
4
5
6
7
0
0.5
3
6
24
Glucose Starve (hrs)
n=3
E.
• PANC1 Cells
Glucose
Starvation (hrs):
0
0.5
3
6
24
LC3-I
LC3-II
Actin
F.
Normalized LC3-II Levels
0
1
2
3
4
5
6
7
8
9
0
0.5
3
6
24
Glucose Starve (hrs)
n=3

Figure 4-6. PDAC cells accumulate LC3-II during glucose starvation

A. HeLa cells were starved for 0, 0.5, 3, 6, or 24 hrs. Lysates were harvested and LC3 and beta-actin levels were determined with immunoblot analysis. Blot is representative of two experiments.

B. Quantification of A. All conditions normalized to beta-actin levels.

C. The same assay from A. was performed using MIA-PACA-2 cells. Blot is representative of three experiments.

D. Quantification of C. All conditions normalized to beta-actin levels. Error bars represent standard deviation of the mean.

E. The same assay from A. was performed using PANC1 cells. Blot is representative of three experiments.

F. Quantification of E. All conditions normalized to beta-actin levels. Error bars represent standard deviation of the mean.

4.2.7 Loss of Rgl2 and RalB do not significantly inhibit LC3-II accumulation during glucose starvation in PDAC cells

We next measured how loss of Rgl2 affects endogenous LC3-II levels. Previous published data reported that loss of RalB inhibits autophagy, so RalB shRNA was used as a positive control [105]. Another positive control used was Atg5 shRNA, a protein that mediates the elongation of the phagophore [95]. Our previous results showed that loss of Rgl2 has no effect on autophagy (Figure 4-5); however, that experiment was performed with highly expressed, exogenous, fluorescent LC3 which may have skewed the results. To look at endogenous LC3 levels, HeLa cells (to confirm results from previous studies) and the PDAC cells PANC1 and MIA-PACA-2 were infected with control, Rgl2, RalB, and Atg5 shRNAs [105]. The cells were then glucose starved for 24 hrs and LC3 levels were measured using immunoblotting. Loss of ATG5 decreased LC3-II loss in HeLa cells and slightly decreased LC3-II accumulation in the PDAC cell lines (Figure 4-7). An antibody against Atg5 was not available to ensure knockdown but the biological effect on LC3-II levels suggests it does work. Loss of Rgl2 and RalB surprisingly had no effect on LC3-II accumulation in the PDAC cell lines. These results further support the data presented in Chapter 4.2.5 to suggest loss of Rgl2 has no effect on autophagy in PDAC cells.

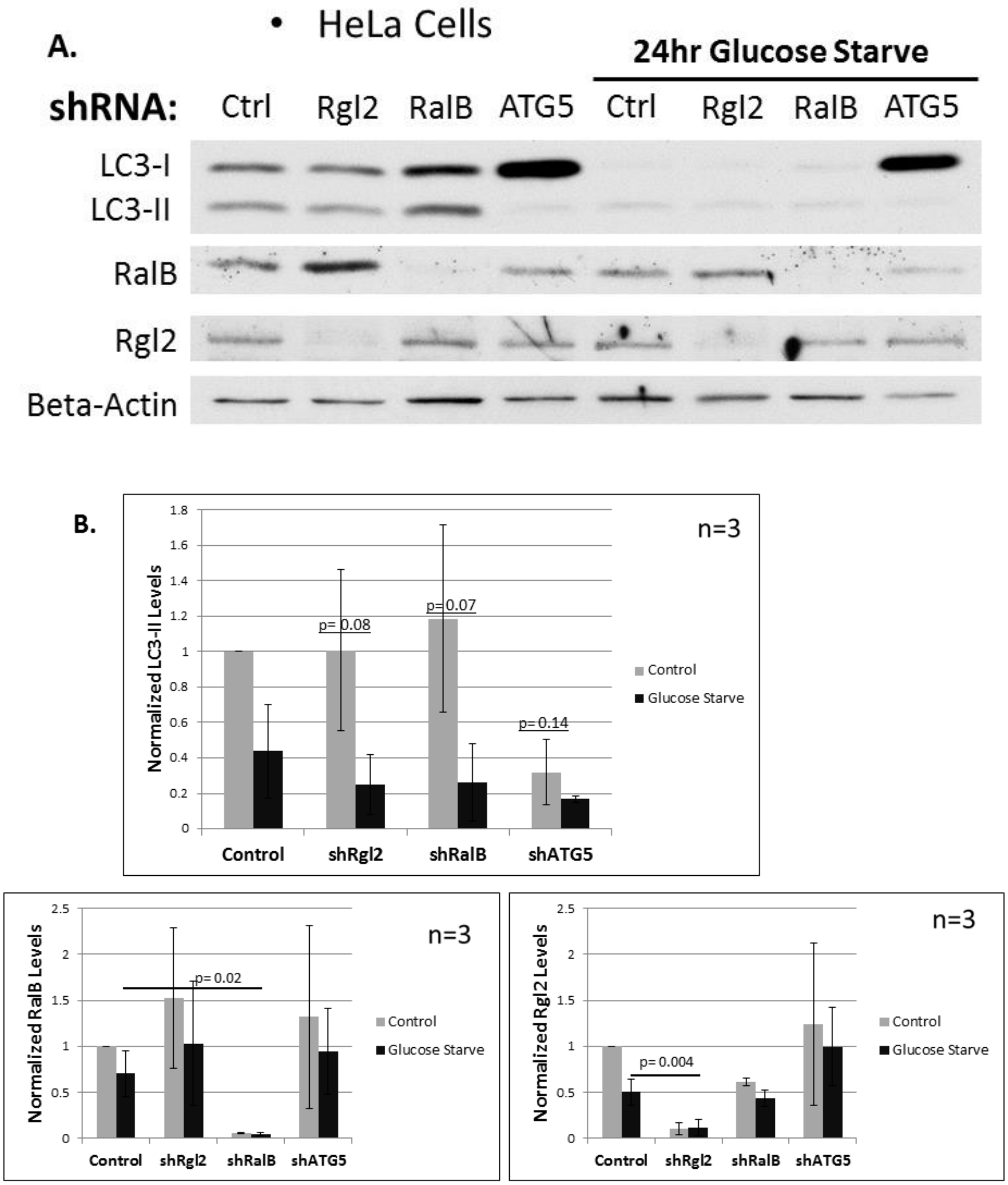
A.
• HeLa Cells
24hr Glucose Starve
shRNA:
Ctrl
Rgl2
RalB
ATG5
Ctrl
Rgl2
RalB
ATG5
LC3-I
LC3-II
RalB
Rgl2
Beta-Actin
B.
n=3
Normalized LC3-II Levels
1.8
1.6
1.4
1.2
1
0.8
0.6
0.4
0.2
0
p= 0.08
p= 0.07
p= 0.14
Control
shRgl2
shRalB
shATG5
Control
Glucose Starve
n=3
Normalized RalB Levels
2.5
2
1.5
1
0.5
0
p= 0.02
Control
shRgl2
shRalB
shATG5
Control
Glucose Starve
n=3
Normalized Rgl2 Levels
2.5
2
1.5
1
0.5
0
p= 0.004
Control
shRgl2
shRalB
shATG5
Control
Glucose Starve

C.

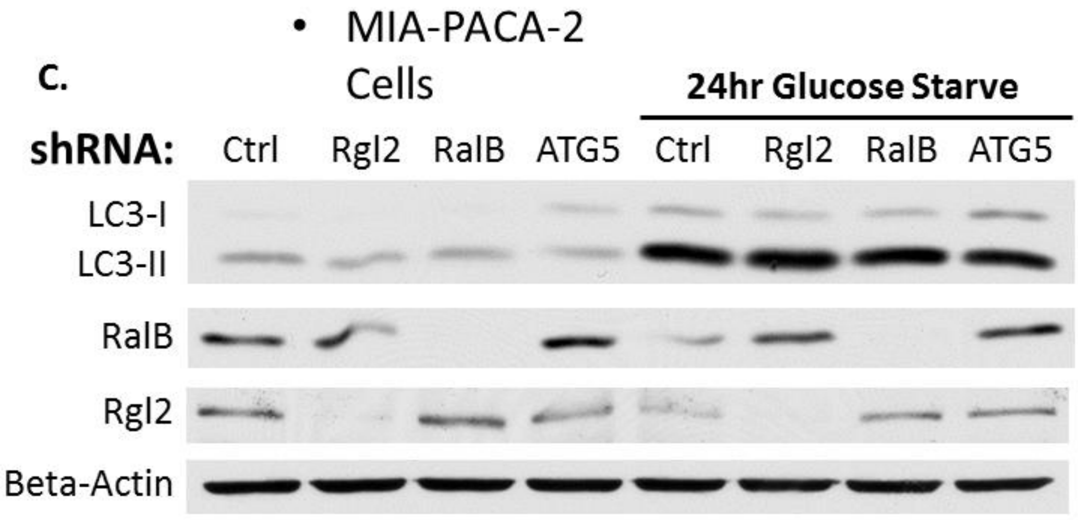

• MIA-PACA-2 Cells
24hr Glucose Starve
shRNA:
Ctrl
Rgl2
RalB
ATG5
Ctrl
Rgl2
RalB
ATG5
LC3-I
LC3-II
RalB
Rgl2
Beta-Actin

D.

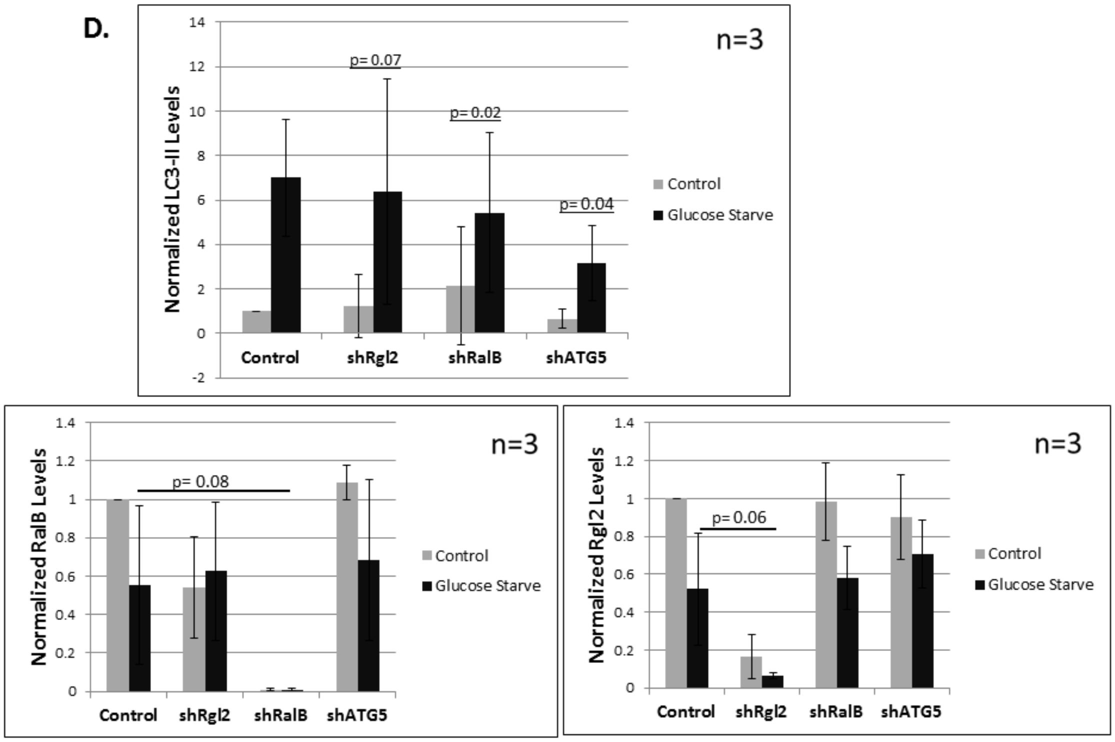

n=3
Normalized LC3-II Levels
14
12
10
8
6
4
2
0
-2
p= 0.07
p= 0.02
p= 0.04
Control
shRgl2
shRalB
shATG5
Control
Glucose Starve
n=3
Normalized RalB Levels
1.4
1.2
1
0.8
0.6
0.4
0.2
0
p= 0.08
Control
shRgl2
shRalB
shATG5
Control
Glucose Starve
n=3
Normalized Rgl2 Levels
1.4
1.2
1
0.8
0.6
0.4
0.2
0
p= 0.06
Control
shRgl2
shRalB
shATG5
Control
Glucose Starve

E.

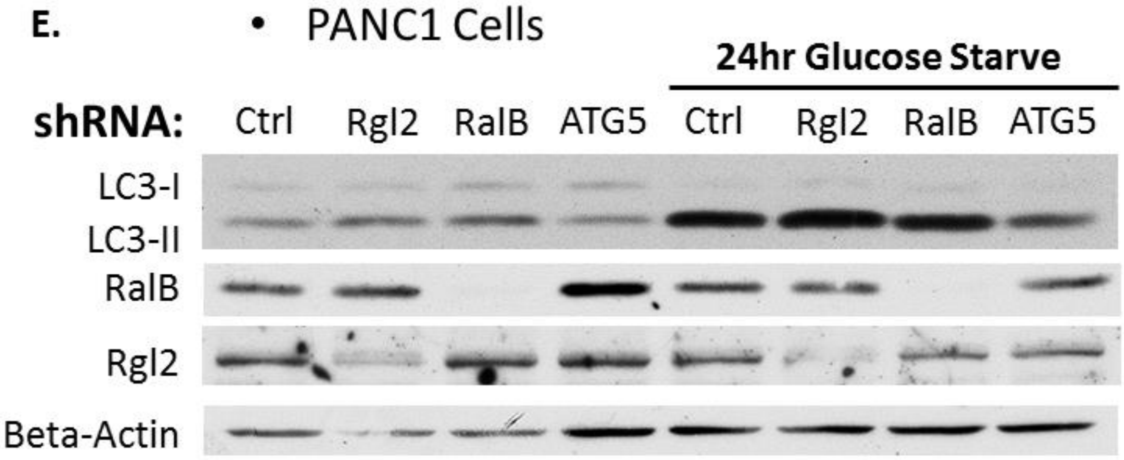
• PANC1 Cells
24hr Glucose Starve
shRNA:
Ctrl
Rgl2
RalB
ATG5
Ctrl
Rgl2
RalB
ATG5
LC3-I
LC3-II
RalB
Rgl2
Beta-Actin

F.

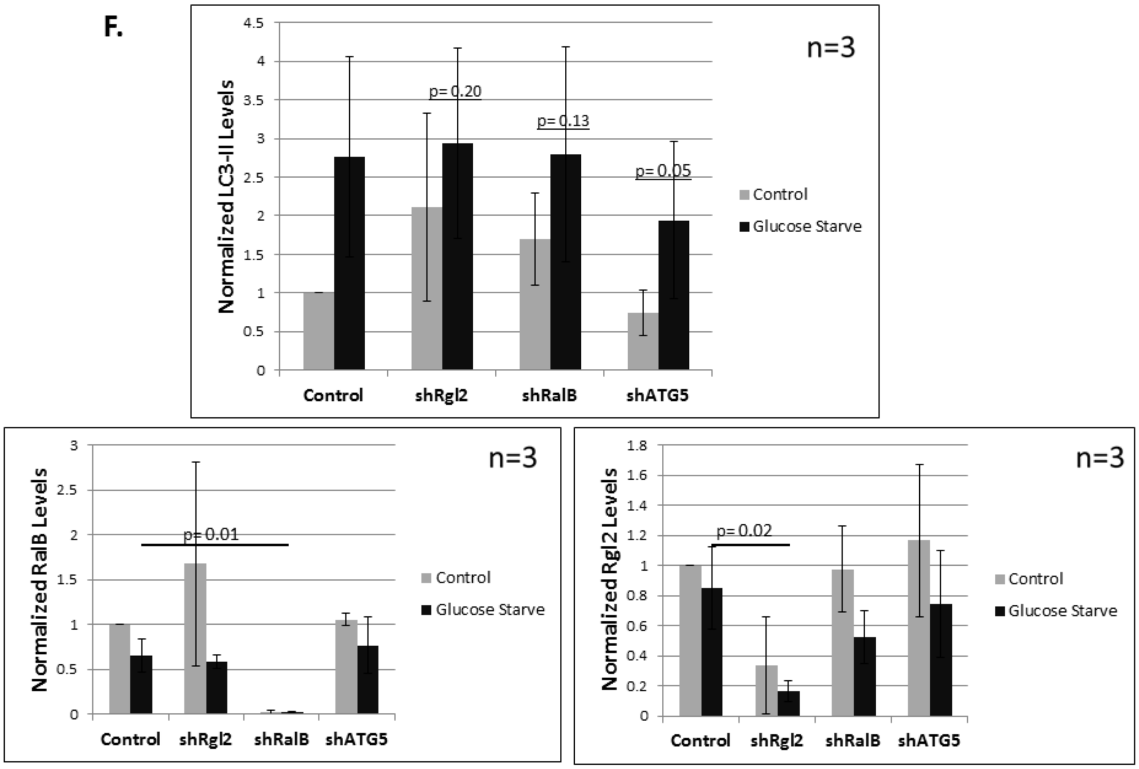
n=3
Normalized LC3-II Levels
4.5
4
3.5
3
2.5
2
1.5
1
0.5
0
p= 0.20
p= 0.13
p= 0.05
Control
shRgl2
shRalB
shATG5
Control
Glucose Starve
n=3
Normalized RalB Levels
3
2.5
2
1.5
1
0.5
0
p= 0.01
Control
shRgl2
shRalB
shATG5
Control
Glucose Starve
n=3
Normalized Rgl2 Levels
1.8
1.6
1.4
1.2
1
0.8
0.6
0.4
0.2
0
p= 0.02
Control
shRgl2
shRalB
shATG5
Control
Glucose Starve

Figure 4-7. Loss of Rgl2 and RalB do not significantly inhibit LC3-II accumulation during glucose starvation in PDAC cells

A. HeLa cells were infected with control, Rgl2, RalB, or Atg5 shRNA. After three days of puromycin selection, cells were glucose starved for three hours and lysates were harvested. The levels of LC3, RalB, Rgl2, and beta-actin were then measured using immunoblot analysis. Blots are representative of three experiments.

B. Quantification of A. All conditions normalized to beta-actin levels. Error bars represent standard deviation of the mean and p-values determined with a Student's T-Test.

C. The same assay from A. was performed using MIA-PACA-2 cells. Blot is representative of three experiments.

D. Quantification of C. All conditions normalized to beta-actin levels. Error bars represent standard deviation of the mean.

E. The same assay from A. was performed using PANC1 cells. Blot is representative of three experiments.

F. Quantification of E. All conditions normalized to beta-actin levels. Error bars represent standard deviation of the mean.

4.2.8 Loss of Rgl2 and RalB do not significantly impact LC3 flux during glucose starvation in PDAC cells

As discussed before, LC3-II is both generated and degraded over the course of autophagy [96]. Because of this flux, it is a common practice to also measure the total accumulation of LC3-II when studying autophagy [140]. If an inhibitor is used to prevent LC3-II degradation, one can measure the rate of LC3-I to LC3-II conversion. We next used this method to determine how loss of Rgl2 may affect LC3-II accumulation. Also the results in Chapter 4.2.5 suggested that loss of RalB may be increasing rates of autophagy, and measuring LC3-II accumulation could confirm this. To test this, MIA-PACA-2 and PANC1 cells were infected with control, Rgl2, or RalB shRNAs. The cells were then treated with CQ, an autophagy inhibitor, or vehicle and two control plates were starved for 24 hrs. As expected, CQ caused LC3-II to accumulate in both cell lines but loss of Rgl2 and RalB had no effect on this accumulation (Figure 4-8). Glucose starvation was used as a positive control to increase accumulation of LC3-II, and this was seen to a small degree in PANC1 cells. The combination of CQ and glucose starvation, however, was toxic to the MIA-PACA-2 cells, making LC3-II measurement difficult. These unexpected results may be due to the 24 hr CQ treatment time, which might have been excessively long. These results do suggest, however, that loss of Rgl2 and RalB have no significant effect on LC3 flux.

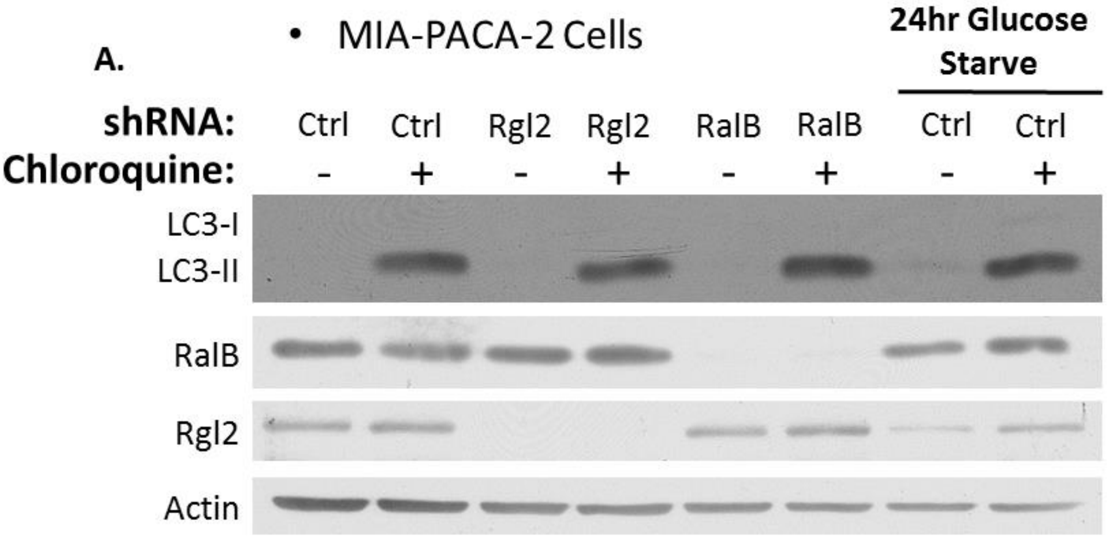
A.
• MIA-PACA-2 Cells
24hr Glucose Starve
shRNA: Ctrl Ctrl Rgl2 Rgl2 RalB RalB Ctrl Ctrl
Chloroquine: - + - + - + - +
LC3-I
LC3-II
RalB
Rgl2
Actin

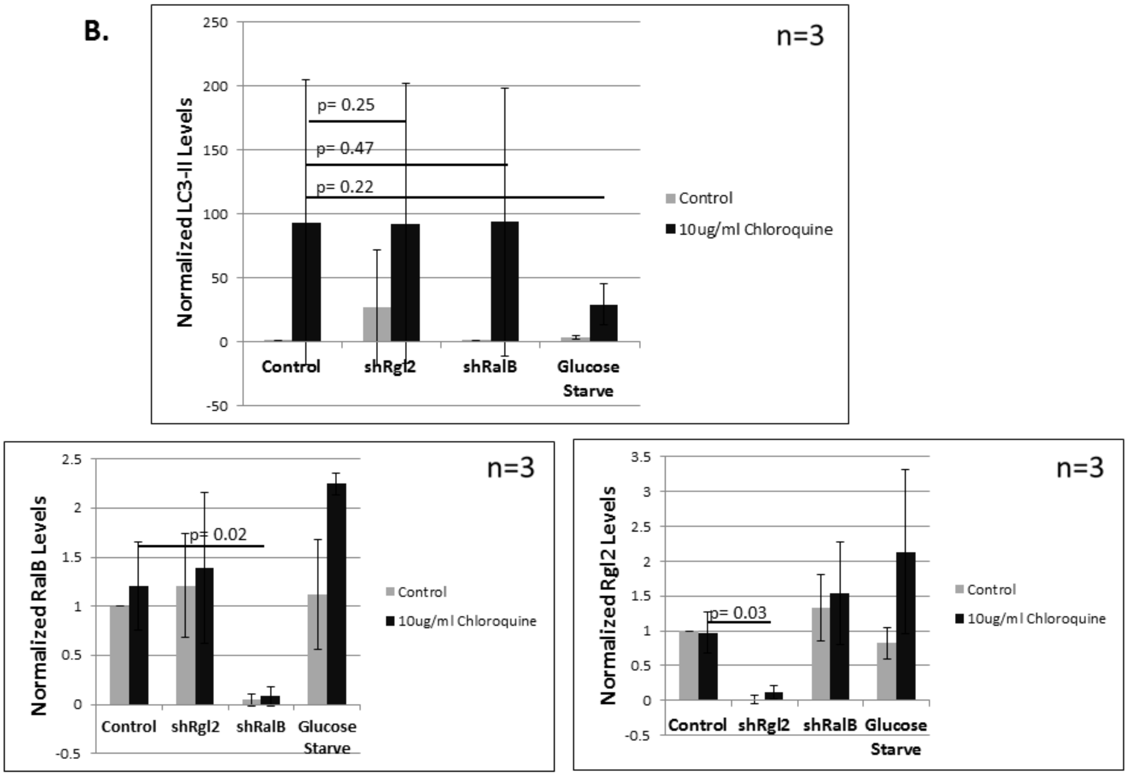
B.
n=3
Normalized LC3-II Levels
250
200
150
100
50
0
-50
p= 0.25
p= 0.47
p= 0.22
Control
shRgl2
shRalB
Glucose Starve
▪ Control
▪ 10ug/ml Chloroquine
n=3
Normalized RalB Levels
2.5
2
1.5
1
0.5
0
-0.5
p= 0.02
Control
shRgl2
shRalB
Glucose Starve
▪ Control
▪ 10ug/ml Chloroquine
n=3
Normalized Rgl2 Levels
3.5
3
2.5
2
1.5
1
0.5
0
-0.5
p= 0.03
Control
shRgl2
shRalB
Glucose Starve
▪ Control
▪ 10ug/ml Chloroquine

C.

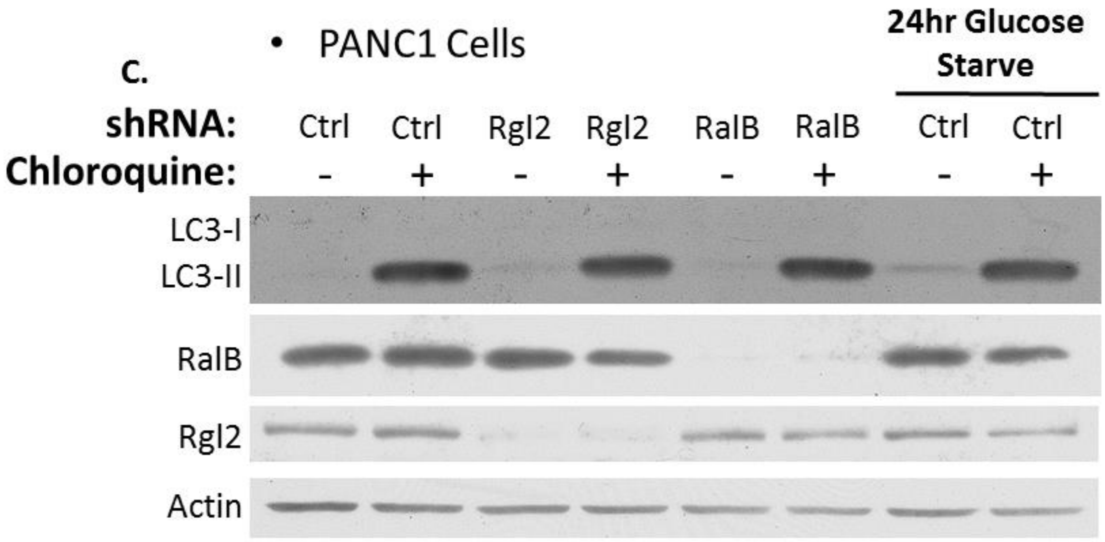
• PANC1 Cells
24hr Glucose Starve
shRNA:
Ctrl
Ctrl
Rgl2
Rgl2
RalB
RalB
Ctrl
Ctrl
Chloroquine:
-
+
-
+
-
+
-
+
LC3-I
LC3-II
RalB
Rgl2
Actin

D.

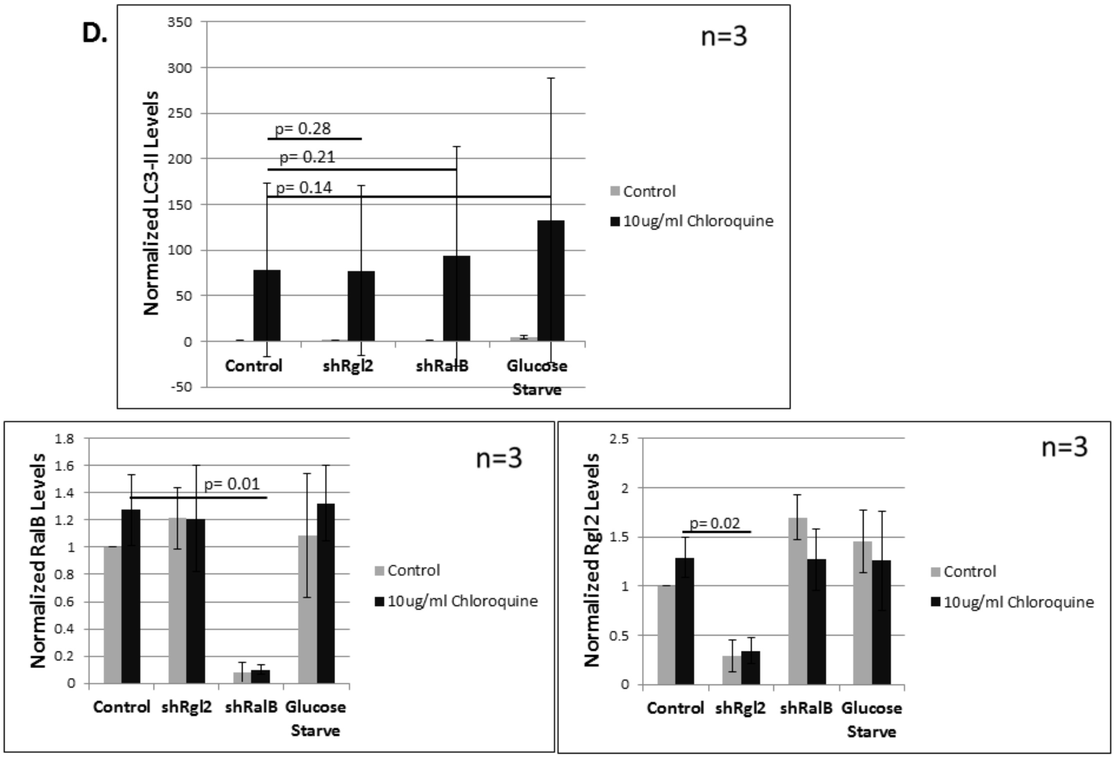
n=3
Normalized LC3-II Levels
350
300
250
200
150
100
50
0
-50
p= 0.28
p= 0.21
p= 0.14
Control
shRgl2
shRalB
Glucose Starve
■ Control
■ 10ug/ml Chloroquine
n=3
Normalized RalB Levels
1.8
1.6
1.4
1.2
1
0.8
0.6
0.4
0.2
0
p= 0.01
Control
shRgl2
shRalB
Glucose Starve
■ Control
■ 10ug/ml Chloroquine
n=3
Normalized Rgl2 Levels
2.5
2
1.5
1
0.5
0
p= 0.02
Control
shRgl2
shRalB
Glucose Starve
■ Control
■ 10ug/ml Chloroquine

Figure 4-8. Loss of Rgl2 and RalB do not significantly impact LC3 flux during glucose starvation in PDAC cells

A. MIA-PACA-2 cells were infected with control, Rgl2, or RalB shRNA. After three days of puromycin selection, cells were glucose starved and treated with chloroquine (CQ) for 24 hours and lysates were harvested. The levels of LC3, RalB, Rgl2, and beta-actin were then measured using immunoblot analysis. Blots are representative of three experiments.

B. Quantification of A. All conditions normalized to beta-actin levels. Error bars represent standard deviation of the mean and p-values determined with a Student's T-Test.

C. The same assay from A. was performed using PANC1 cells. Blot is representative of three experiments.

D. Quantification of C. All conditions normalized to beta-actin levels. Error bars represent standard deviation of the mean.

4.3 Discussion

It was previously reported that loss of RalB inhibits autophagy by preventing autophagosome formation [105]. These findings led us to hypothesize that loss of Rgl2 would inhibit RalB activation and autophagy in PDAC cells, thereby increasing PDAC cell death. Loss of Rgl2 did in fact inhibit PDAC cell viability and increase cell death (Figures 4-2 and 4-3). However, when we measured the effect of Rgl2 loss on number of dead cells during glucose starvation (Figure 4-3), glucose starvation did not have a synergistic effect with Rgl2 loss. This result suggests that the mechanism by which Rgl2 regulates cell death is independent of autophagy. Our microscopy experiments, furthermore, revealed that loss of Rgl2 does not significantly inhibit autophagosome number or maturation (Figure 4-5). Loss of Rgl2 also had no effect on endogenous LC3-II processing (Figures 4-7 and 4-8). These results suggest that loss of Rgl2 has no significant effect on autophagy in PDAC cells. The inability of loss of Rgl2 to inhibit autophagy could be because of several reasons. One could be that another RalGEF, besides Rgl2, is regulating autophagy. Recently published work found that RalGDS regulates RalB-dependent autophagy in cardiomyocytes [141]. This work also showed that loss of RalGDS inhibits cardiomyocyte growth [141]. Our initial microscopy data suggested that loss of RalGDS has no effect on autophagy in PDAC cells, but this was a preliminary assay and may require further investigation. Loss of RalA has been shown to inhibit PDAC cell survival, therefore the loss of Rgl2-mediated inhibition of cell survival may be entirely be due to RalA inhibition [50]. Therefore, RalB-dependent autophagy and cell growth may be regulated by another RalGEF in PDAC cells.

As expected, loss of RalB did inhibit starvation-induced autophagosome reduction and maturation (Figure 4-5). These results from the microscopy data suggest that RalB does regulate autophagy in PDAC cells. RalB and Atg5 shRNAs were also used as positive controls while measuring endogenous LC3-II levels (Figure 4-7). As expected, loss of Atg5 inhibited LC3-II processing. Loss of RalB, on the other hand, did not affect LC3-II processing. These results are not consistent with the literature or even our own microscopy data. There are a few explanations that could account for this inconsistency. First of all, in the microscopy data we were measuring exogenously expressed LC3 while in the blotting data we were measuring endogenous LC3. Endogenous levels of LC3 are always in flux, are variable between tissues, and do not always correlate with autophagy activity, therefore LC3-II levels can be an inconsistent measure of autophagy [140]. Also, deletion of some autophagy proteins (such as Beclin1) will not necessarily inhibit LC3-II formation [142]. Because of the dynamic expression of LC3, exogenously expressed LC3 is a more reliable marker of autophagic flux [140]. Another possibility for the inconsistent results may be due to how the PDAC cells were starved. The previous published data showed that loss of RalB inhibited autophagy induced by combined glucose and amino acid starvation [105]. To describe a more specific autophagy pathway, we starved the cells of only glucose. Recently published data, however, suggests that glucose starvation does not induce prosurvival autophagy [143]. Even more surprisingly, this paper suggests that glucose starvation does not actually increase autophagic flux. Even though this work is somewhat controversial, it does suggest that there is a distinction between autophagy induced by glucose compared to that induced by amino acid starvation. Therefore, RalB and Rgl2 may regulate autophagy induced by amino acid starvation but not glucose starvation. In conclusion, while loss of Rgl2 does increase PDAC cell death, it does not significantly inhibit autophagy.

4.4 Future directions

Our findings, that loss of Rgl2 inhibits PDAC cell survival but has no significant effect on autophagy, can be expanded upon with a number of further experiments. Firstly, as discussed in a recent paper, glucose starvation is a controversial method of inducing autophagy [143]. Therefore, it would be important to compare how starving PDAC cells of glucose and amino acids differently induce autophagy. All that would be required for these experiments would be media depleted of amino acids and media without glucose. This comparison could be done in the survival assays as well as the LC3 microscopy and endogenous LC3 assays. These experiments would show if Rgl2 and RalB differently regulate amino acid- or glucose-dependent autophagy pathways. Another possible experiment would be to compare how loss of the different RalGEFs affects autophagy. Even though it has been shown that Rgl2 and RalGDS are the most highly expressed RalGEFs in PDAC cells, the other RalGEFs may have increased activity in spite of low expression [50]. Further experiments could also address whether loss of the RalGEFs inhibit cell survival proportionally with autophagy inhibition. For example, loss of RalGDS may inhibit autophagy and cell survival while loss of Rgl2 only inhibits cell survival. These experiments would help reveal if there is a link between RalB-mediated autophagy and survival. A link between these phenomena and the Ral proteins could also be drawn using constitutively active RalA and RalB. For instance, the increase in cell death caused by loss of Rgl2 may be restored with a constitutively active RalA but not RalB. Using these constructs could further elucidate the signaling pathways that link the loss of a RalGEF and the biological response. Also, our hypothesis was dependent on the constitutive activity of KRas and RalB-dependent autophagy. Further experiments with cells with wild type KRas could help us determine if Rgl2 is indeed crucial for cell survival under these conditions. Experiments such as these would help to further describe the relationship between the different RalGEFs and Rals and potentially draw a connection between RalB-dependent autophagy and survival.

APPENDIX – NUCLEOTIDE SEQUENCES

shRNA	**Sequence**
Control	CCTAAGGTTAAGTCGCCCTCG
Atg5	CCGGCCTGAACAGAATCATCCTTAACTCGAGTTAAGGATGATTCTGTTCAGGTTTTTTG
RalB	CCGGCGTGATGAGTTAAAGTTGTATCTCGAGATACAACTTTAACTCATCACGTTTTTG
RalGDS	CCGGTCTACTGCCAACTATGACTTTCTCGAGAAAGTCATAGTTGGCAGTAGATTTTTG
Rgl2	GCAGTGTCTATAAGAGCATTT

REFERENCES

1. Macara, I.G., *Oncogenes, ions, and phospholipids.* Am J Physiol, 1985. **248**(1 Pt 1): p. C3-11.
2. Sibley, D.R., et al., *Regulation of transmembrane signaling by receptor phosphorylation.* Cell, 1987. **48**(6): p. 913-22.
3. Busse, R. and I. Fleming, *Pulsatile stretch and shear stress: physical stimuli determining the production of endothelium-derived relaxing factors.* J Vasc Res, 1998. **35**(2): p. 73-84.
4. Waterfield, M.D., *Growth factor receptors.* Br Med Bull, 1989. **45**(2): p. 541-53.
5. Roberts, A.B., et al., *Transforming growth factor-beta: possible roles in carcinogenesis.* Br J Cancer, 1988. **57**(6): p. 594-600.
6. Yuspa, S.H., et al., *Signal transduction for proliferation and differentiation in keratinocytes.* Ann N Y Acad Sci, 1988. **548**: p. 191-6.
7. McConkey, D.J. and S. Orrenius, *Signal transduction pathways to apoptosis.* Trends Cell Biol, 1994. **4**(10): p. 370-5.
8. Weinstein, I.B., *The origins of human cancer: molecular mechanisms of carcinogenesis and their implications for cancer prevention and treatment--twenty-seventh G.H.A. Clowes memorial award lecture.* Cancer Res, 1988. **48**(15): p. 4135-43.
9. Weijzen, S., M.P. Velders, and W.M. Kast, *Modulation of the immune response and tumor growth by activated Ras.* Leukemia, 1999. **13**(4): p. 502-13.

10. Krymskaya, V.P., *Tumour suppressors hamartin and tuberin: intracellular signalling.* Cell Signal, 2003. **15**(8): p. 729-39.
11. Wennerberg, K., K.L. Rossman, and C.J. Der, *The Ras superfamily at a glance.* J Cell Sci, 2005. **118**(Pt 5): p. 843-6.
12. Chong, H., H.G. Vikis, and K.L. Guan, *Mechanisms of regulating the Raf kinase family.* Cell Signal, 2003. **15**(5): p. 463-9.
13. Bernards, A. and J. Settleman, *GAP control: regulating the regulators of small GTPases.* Trends Cell Biol, 2004. **14**(7): p. 377-85.
14. Weiss, B., G. Bollag, and K. Shannon, *Hyperactive Ras as a therapeutic target in neurofibromatosis type 1.* Am J Med Genet, 1999. **89**(1): p. 14-22.
15. Schmidt, A. and A. Hall, *Guanine nucleotide exchange factors for Rho GTPases: turning on the switch.* Genes Dev, 2002. **16**(13): p. 1587-609.
16. Nimnual, A. and D. Bar-Sagi, *The two hats of SOS.* Sci STKE, 2002. **2002**(145): p. pe36.
17. Downward, J., *Targeting RAS signalling pathways in cancer therapy.* Nat Rev Cancer, 2003. **3**(1): p. 11-22.
18. Kirsten, W.H. and L.A. Mayer, *Malignant lymphomas of extrathymic origin induced in rats by murine erythroblastosis virus.* J Natl Cancer Inst, 1969. **43**(3): p. 735-46.
19. Colicelli, J., *Human RAS superfamily proteins and related GTPases.* Sci STKE, 2004. **2004**(250): p. RE13.

20. Pizon, V., et al., *Human cDNAs rap1 and rap2 homologous to the Drosophila gene Dras3 encode proteins closely related to ras in the 'effector' region.* Oncogene, 1988. **3**(2): p. 201-4.

21. Kitayama, H., et al., *A ras-related gene with transformation suppressor activity.* Cell, 1989. **56**(1): p. 77-84.

22. Hamad, N.M., et al., *Distinct requirements for Ras oncogenesis in human versus mouse cells.* Genes Dev, 2002. **16**(16): p. 2045-57.

23. Kolch, W., *Meaningful relationships: the regulation of the Ras/Raf/MEK/ERK pathway by protein interactions.* Biochem J, 2000. **351 Pt 2**: p. 289-305.

24. Morrison, D.K., et al., *Signal transduction from membrane to cytoplasm: growth factors and membrane-bound oncogene products increase Raf-1 phosphorylation and associated protein kinase activity.* Proc Natl Acad Sci U S A, 1988. **85**(23): p. 8855-9.

25. Baccarini, M., *Second nature: biological functions of the Raf-1 "kinase".* FEBS Lett, 2005. **579**(15): p. 3271-7.

26. Chen, Z., et al., *MAP kinases.* Chem Rev, 2001. **101**(8): p. 2449-76.

27. Arlt, A., S.S. Muerkoster, and H. Schafer, *Targeting apoptosis pathways in pancreatic cancer.* Cancer Lett, 2013. **332**(2): p. 346-58.

28. Rodriguez-Viciana, P., et al., *Activation of phosphoinositide 3-kinase by interaction with Ras and by point mutation.* EMBO J, 1996. **15**(10): p. 2442-51.

29. Yuan, T.L. and L.C. Cantley, *PI3K pathway alterations in cancer: variations on a theme.* Oncogene, 2008. **27**(41): p. 5497-510.

30. Cantley, L.C., *The phosphoinositide 3-kinase pathway.* Science, 2002. **296**(5573): p. 1655-7.

31. Ching, C.B. and D.E. Hansel, *Expanding therapeutic targets in bladder cancer: the PI3K/Akt/mTOR pathway.* Lab Invest, 2010. **90**(10): p. 1406-14.

32. Lim, K.H. and C.M. Counter, *Reduction in the requirement of oncogenic Ras signaling to activation of PI3K/AKT pathway during tumor maintenance.* Cancer Cell, 2005. **8**(5): p. 381-92.

33. Ruggeri, B.A., et al., *Amplification and overexpression of the AKT2 oncogene in a subset of human pancreatic ductal adenocarcinomas.* Mol Carcinog, 1998. **21**(2): p. 81-6.

34. Normanno, N., et al., *Implications for KRAS status and EGFR-targeted therapies in metastatic CRC.* Nat Rev Clin Oncol, 2009. **6**(9): p. 519-27.

35. Ferro, E. and L. Trabalzini, *RalGDS family members couple Ras to Ral signalling and that's not all.* Cell Signal, 2010. **22**(12): p. 1804-10.

36. Rebhun, J.F., H. Chen, and L.A. Quilliam, *Identification and characterization of a new family of guanine nucleotide exchange factors for the ras-related GTPase Ral.* J Biol Chem, 2000. **275**(18): p. 13406-10.

37. Jullien-Flores, V., et al., *Bridging Ral GTPase to Rho pathways. RLIP76, a Ral effector with CDC42/Rac GTPase-activating protein activity.* J Biol Chem, 1995. **270**(38): p. 22473-7.

38. Nakashima, S., et al., *Small G protein Ral and its downstream molecules regulate endocytosis of EGF and insulin receptors.* EMBO J, 1999. **18**(13): p. 3629-42.

39. Moskalenko, S., et al., *The exocyst is a Ral effector complex.* Nat Cell Biol, 2002. **4**(1): p. 66-72.

40. Moskalenko, S., et al., *Ral GTPases regulate exocyst assembly through dual subunit interactions.* J Biol Chem, 2003. **278**(51): p. 51743-8.

41. Hsu, S.C., et al., *Targeting vesicles to specific sites on the plasma membrane: the role of the sec6/8 complex.* Trends Cell Biol, 1999. **9**(4): p. 150-3.

42. Shirakawa, R., et al., *Tuberous sclerosis tumor suppressor complex-like complexes act as GTPase-activating proteins for Ral GTPases.* J Biol Chem, 2009. **284**(32): p. 21580-8.

43. Chardin, P. and A. Tavitian, *Coding sequences of human ralA and ralB cDNAs.* Nucleic Acids Res, 1989. **17**(11): p. 4380.

44. Lim, K.H., et al., *Divergent roles for RalA and RalB in malignant growth of human pancreatic carcinoma cells.* Curr Biol, 2006. **16**(24): p. 2385-94.

45. Martin, T.D. and C.J. Der, *Differential involvement of RalA and RalB in colorectal cancer.* Small GTPases, 2012. **3**(2): p. 126-30.

46. Cascone, I., et al., *Distinct roles of RalA and RalB in the progression of cytokinesis are supported by distinct RalGEFs.* EMBO J, 2008. **27**(18): p. 2375-87.

47. Shipitsin, M. and L.A. Feig, *RalA but not RalB enhances polarized delivery of membrane proteins to the basolateral surface of epithelial cells.* Mol Cell Biol, 2004. **24**(13): p. 5746-56.

48. Kashatus, D.F., *Ral GTPases in tumorigenesis: emerging from the shadows.* Exp Cell Res, 2013. **319**(15): p. 2337-42.

49. Ferro, E., et al., *G-protein binding features and regulation of the RalGDS family member, RGL2.* Biochem J, 2008. **415**(1): p. 145-54.

50. Vigil, D., et al., *Aberrant overexpression of the Rgl2 Ral small GTPase-specific guanine nucleotide exchange factor promotes pancreatic cancer growth through Ral-dependent and Ral-independent mechanisms.* J Biol Chem, 2010. **285**(45): p. 34729-40.

51. Vezina, C., A. Kudelski, and S.N. Sehgal, *Rapamycin (AY-22,989), a new antifungal antibiotic. I. Taxonomy of the producing streptomycete and isolation of the active principle.* J Antibiot (Tokyo), 1975. **28**(10): p. 721-6.

52. Gomez-Pinillos, A. and A.C. Ferrari, *mTOR signaling pathway and mTOR inhibitors in cancer therapy.* Hematol Oncol Clin North Am, 2012. **26**(3): p. 483-505, vii.

53. Foster, K.G., et al., *Regulation of mTOR complex 1 (mTORC1) by raptor Ser863 and multisite phosphorylation.* J Biol Chem, 2010. **285**(1): p. 80-94.

54. Raught, B., A.C. Gingras, and N. Sonenberg, *The target of rapamycin (TOR) proteins.* Proc Natl Acad Sci U S A, 2001. **98**(13): p. 7037-44.

55. Gingras, A.C., B. Raught, and N. Sonenberg, *Regulation of translation initiation by FRAP/mTOR.* Genes Dev, 2001. **15**(7): p. 807-26.

56. Groenewoud, M.J. and F.J. Zwartkruis, *Rheb and Rags come together at the lysosome to activate mTORC1.* Biochem Soc Trans, 2013. **41**(4): p. 951-5.

57. Inoki, K., et al., *Rheb GTPase is a direct target of TSC2 GAP activity and regulates mTOR signaling.* Genes Dev, 2003. **17**(15): p. 1829-34.

58. Inoki, K., et al., *TSC2 integrates Wnt and energy signals via a coordinated phosphorylation by AMPK and GSK3 to regulate cell growth.* Cell, 2006. **126**(5): p. 955-68.

59. Wullschleger, S., R. Loewith, and M.N. Hall, *TOR signaling in growth and metabolism.* Cell, 2006. **124**(3): p. 471-84.

60. Muniraj, T., P.A. Jamidar, and H.R. Aslanian, *Pancreatic cancer: A comprehensive review and update.* Dis Mon, 2013. **59**(11): p. 368-402.

61. Siegel, R., D. Naishadham, and A. Jemal, *Cancer statistics, 2013.* CA Cancer J Clin, 2013. **63**(1): p. 11-30.

62. Hezel, A.F., et al., *Genetics and biology of pancreatic ductal adenocarcinoma.* Genes Dev, 2006. **20**(10): p. 1218-49.

63. Moore, M.J., et al., *Erlotinib plus gemcitabine compared with gemcitabine alone in patients with advanced pancreatic cancer: a phase III trial of the National Cancer Institute of Canada Clinical Trials Group.* J Clin Oncol, 2007. **25**(15): p. 1960-6.

64. Means, A.L., et al., *Pancreatic epithelial plasticity mediated by acinar cell transdifferentiation and generation of nestin-positive intermediates.* Development, 2005. **132**(16): p. 3767-76.

65. Tuveson, D.A. and J.P. Neoptolemos, *Understanding metastasis in pancreatic cancer: a call for new clinical approaches.* Cell, 2012. **148**(1-2): p. 21-3.

66. Malkoski, S.P. and X.J. Wang, *Two sides of the story? Smad4 loss in pancreatic cancer versus head-and-neck cancer.* FEBS Lett, 2012. **586**(14): p. 1984-92.

67. Orlova, K.A. and P.B. Crino, *The tuberous sclerosis complex.* Ann N Y Acad Sci, 2010. **1184**: p. 87-105.

68. Goncharova, E.A. and V.P. Krymskaya, *Pulmonary lymphangioleiomyomatosis (LAM): progress and current challenges.* J Cell Biochem, 2008. **103**(2): p. 369-82.

69. Bissler, J.J., et al., *Sirolimus for angiomyolipoma in tuberous sclerosis complex or lymphangioleiomyomatosis.* N Engl J Med, 2008. **358**(2): p. 140-51.

70. Van Cutsem, E., et al., *Phase III trial of gemcitabine plus tipifarnib compared with gemcitabine plus placebo in advanced pancreatic cancer.* J Clin Oncol, 2004. **22**(8): p. 1430-8.

71. Martin, N.E., et al., *A phase I trial of the dual farnesyltransferase and geranylgeranyltransferase inhibitor L-778,123 and radiotherapy for locally advanced pancreatic cancer.* Clin Cancer Res, 2004. **10**(16): p. 5447-54.

72. Rejiba, S., et al., *K-ras oncogene silencing strategy reduces tumor growth and enhances gemcitabine chemotherapy efficacy for pancreatic cancer treatment.* Cancer Sci, 2007. **98**(7): p. 1128-36.

73. Rinehart, J., et al., *Multicenter phase II study of the oral MEK inhibitor, CI-1040, in patients with advanced non-small-cell lung, breast, colon, and pancreatic cancer.* J Clin Oncol, 2004. **22**(22): p. 4456-62.

74. Ito, D., et al., *In vivo antitumor effect of the mTOR inhibitor CCI-779 and gemcitabine in xenograft models of human pancreatic cancer.* Int J Cancer, 2006. **118**(9): p. 2337-43.

75. Neel, N.F., et al., *The RalGEF-Ral Effector Signaling Network: The Road Less Traveled for Anti-Ras Drug Discovery.* Genes Cancer, 2011. **2**(3): p. 275-87.

76. Yang, Z. and D.J. Klionsky, *Eaten alive: a history of macroautophagy.* Nat Cell Biol, 2010. **12**(9): p. 814-22.

77. Kroemer, G., G. Marino, and B. Levine, *Autophagy and the integrated stress response.* Mol Cell, 2010. **40**(2): p. 280-93.

78. Boya, P., F. Reggiori, and P. Codogno, *Emerging regulation and functions of autophagy.* Nat Cell Biol, 2013. **15**(7): p. 713-20.

79. Reggiori, F., et al., *Autophagy: more than a nonselective pathway.* Int J Cell Biol, 2012. **2012**: p. 219625.

80. Shi, C.S., et al., *Activation of autophagy by inflammatory signals limits IL-1beta production by targeting ubiquitinated inflammasomes for destruction.* Nat Immunol, 2012. **13**(3): p. 255-63.

81. Taylor, J.P., et al., *Aggresomes protect cells by enhancing the degradation of toxic polyglutamine-containing protein.* Hum Mol Genet, 2003. **12**(7): p. 749-57.

82. Johansen, T. and T. Lamark, *Selective autophagy mediated by autophagic adapter proteins.* Autophagy, 2011. **7**(3): p. 279-96.

83. Garcia-Mata, R., Y.S. Gao, and E. Sztul, *Hassles with taking out the garbage: aggravating aggresomes.* Traffic, 2002. **3**(6): p. 388-96.

84. Wickner, S., M.R. Maurizi, and S. Gottesman, *Posttranslational quality control: folding, refolding, and degrading proteins.* Science, 1999. **286**(5446): p. 1888-93.

85. Garcia-Mata, R., et al., *Characterization and dynamics of aggresome formation by a cytosolic GFP-chimera.* J Cell Biol, 1999. **146**(6): p. 1239-54.

86. Kawaguchi, Y., et al., *The deacetylase HDAC6 regulates aggresome formation and cell viability in response to misfolded protein stress.* Cell, 2003. **115**(6): p. 727-38.

87. Hubbert, C., et al., *HDAC6 is a microtubule-associated deacetylase.* Nature, 2002. **417**(6887): p. 455-8.

88. Pankiv, S., et al., *p62/SQSTM1 binds directly to Atg8/LC3 to facilitate degradation of ubiquitinated protein aggregates by autophagy.* J Biol Chem, 2007. **282**(33): p. 24131-45.

89. Rodriguez-Gonzalez, A., et al., *Role of the aggresome pathway in cancer: targeting histone deacetylase 6-dependent protein degradation.* Cancer Res, 2008. **68**(8): p. 2557-60.

90. Chin, L.S., J.A. Olzmann, and L. Li, *Parkin-mediated ubiquitin signalling in aggresome formation and autophagy.* Biochem Soc Trans, 2010. **38**(Pt 1): p. 144-9.

91. Hamasaki, M., S.T. Shibutani, and T. Yoshimori, *Up-to-date membrane biogenesis in the autophagosome formation.* Curr Opin Cell Biol, 2013. **25**(4): p. 455-60.

92. Suzuki, K. and Y. Ohsumi, *Molecular machinery of autophagosome formation in yeast, Saccharomyces cerevisiae.* FEBS Lett, 2007. **581**(11): p. 2156-61.

93. Suzuki, K., et al., *The pre-autophagosomal structure organized by concerted functions of APG genes is essential for autophagosome formation.* EMBO J, 2001. **20**(21): p. 5971-81.

94. Weidberg, H., E. Shvets, and Z. Elazar, *Biogenesis and cargo selectivity of autophagosomes.* Annu Rev Biochem, 2011. **80**: p. 125-56.

95. Geng, J. and D.J. Klionsky, *The Atg8 and Atg12 ubiquitin-like conjugation systems in macroautophagy. 'Protein modifications: beyond the usual suspects' review series.* EMBO Rep, 2008. **9**(9): p. 859-64.

96. Rubinsztein, D.C., T. Shpilka, and Z. Elazar, *Mechanisms of autophagosome biogenesis.* Curr Biol, 2012. **22**(1): p. R29-34.

97. Jager, S., et al., *Role for Rab7 in maturation of late autophagic vacuoles.* J Cell Sci, 2004. **117**(Pt 20): p. 4837-48.

98. Kimura, S., T. Noda, and T. Yoshimori, *Dissection of the autophagosome maturation process by a novel reporter protein, tandem fluorescent-tagged LC3.* Autophagy, 2007. **3**(5): p. 452-60.

99. Zhong, Y., et al., *Distinct regulation of autophagic activity by Atg14L and Rubicon associated with Beclin 1-phosphatidylinositol-3-kinase complex.* Nat Cell Biol, 2009. **11**(4): p. 468-76.

100. Renna, M., et al., *Autophagic substrate clearance requires activity of the syntaxin-5 SNARE complex.* J Cell Sci, 2011. **124**(Pt 3): p. 469-82.

101. Kamada, Y., et al., *Tor directly controls the Atg1 kinase complex to regulate autophagy.* Mol Cell Biol, 2010. **30**(4): p. 1049-58.

102. Settembre, C., et al., *A lysosome-to-nucleus signalling mechanism senses and regulates the lysosome via mTOR and TFEB.* EMBO J, 2012. **31**(5): p. 1095-108.

103. Jung, C.H., et al., *mTOR regulation of autophagy.* FEBS Lett, 2010. **584**(7): p. 1287-95.

104. Wei, Y., et al., *JNK1-mediated phosphorylation of Bcl-2 regulates starvation-induced autophagy.* Mol Cell, 2008. **30**(6): p. 678-88.

105. Bodemann, B.O., et al., *RalB and the exocyst mediate the cellular starvation response by direct activation of autophagosome assembly.* Cell, 2011. **144**(2): p. 253-67.

106. Mizushima, N. and M. Komatsu, *Autophagy: renovation of cells and tissues.* Cell, 2011. **147**(4): p. 728-41.

107. Liang, X.H., et al., *Induction of autophagy and inhibition of tumorigenesis by beclin 1.* Nature, 1999. **402**(6762): p. 672-6.

108. Yang, Z.J., et al., *The role of autophagy in cancer: therapeutic implications.* Mol Cancer Ther, 2011. **10**(9): p. 1533-41.

109. Aita, V.M., et al., *Cloning and genomic organization of beclin 1, a candidate tumor suppressor gene on chromosome 17q21.* Genomics, 1999. **59**(1): p. 59-65.

110. Qu, X., et al., *Promotion of tumorigenesis by heterozygous disruption of the beclin 1 autophagy gene.* J Clin Invest, 2003. **112**(12): p. 1809-20.

111. Maddodi, N., et al., *Induction of autophagy and inhibition of melanoma growth in vitro and in vivo by hyperactivation of oncogenic BRAF.* J Invest Dermatol, 2010. **130**(6): p. 1657-67.

112. Guo, J.Y., et al., *Activated Ras requires autophagy to maintain oxidative metabolism and tumorigenesis.* Genes Dev, 2011. **25**(5): p. 460-70.

113. Elgendy, M., et al., *Oncogenic Ras-induced expression of Noxa and Beclin-1 promotes autophagic cell death and limits clonogenic survival.* Mol Cell, 2011. **42**(1): p. 23-35.

114. Kim, J.H., et al., *Involvement of mitophagy in oncogenic K-Ras-induced transformation: overcoming a cellular energy deficit from glucose deficiency.* Autophagy, 2011. **7**(10): p. 1187-98.

115. Ko, Y.H., et al., *Prognostic significance of autophagy-related protein expression in resected pancreatic ductal adenocarcinoma.* Pancreas, 2013. **42**(5): p. 829-35.

116. Wu, Z., et al., *Autophagy Blockade Sensitizes Prostate Cancer Cells towards Src Family Kinase Inhibitors.* Genes Cancer, 2010. **1**(1): p. 40-9.

117. Petiot, A., et al., *Distinct classes of phosphatidylinositol 3'-kinases are involved in signaling pathways that control macroautophagy in HT-29 cells.* J Biol Chem, 2000. **275**(2): p. 992-8.

118. Li, J., et al., *Inhibition of autophagy augments 5-fluorouracil chemotherapy in human colon cancer in vitro and in vivo model.* Eur J Cancer, 2010. **46**(10): p. 1900-9.

119. Brusilow, S.W. and N.E. Maestri, *Urea cycle disorders: diagnosis, pathophysiology, and therapy.* Adv Pediatr, 1996. **43**: p. 127-70.

120. Collins, A.F., et al., *Oral sodium phenylbutyrate therapy in homozygous beta thalassemia: a clinical trial.* Blood, 1995. **85**(1): p. 43-9.

121. Ricobaraza, A., et al., *Phenylbutyrate ameliorates cognitive deficit and reduces tau pathology in an Alzheimer's disease mouse model.* Neuropsychopharmacology, 2009. **34**(7): p. 1721-32.

122. Inden, M., et al., *Neurodegeneration of mouse nigrostriatal dopaminergic system induced by repeated oral administration of rotenone is prevented by 4-phenylbutyrate, a chemical chaperone.* J Neurochem, 2007. **101**(6): p. 1491-1504.

123. Ozcan, U., et al., *Chemical chaperones reduce ER stress and restore glucose homeostasis in a mouse model of type 2 diabetes.* Science, 2006. **313**(5790): p. 1137-40.

124. Shack, S., et al., *Vulnerability of multidrug-resistant tumor cells to the aromatic fatty acids phenylacetate and phenylbutyrate.* Clin Cancer Res, 1996. **2**(5): p. 865-72.

125. Carducci, M.A., et al., *A Phase I clinical and pharmacological evaluation of sodium phenylbutyrate on an 120-h infusion schedule.* Clin Cancer Res, 2001. **7**(10): p. 3047-55.

126. Welch, W.J. and C.R. Brown, *Influence of molecular and chemical chaperones on protein folding.* Cell Stress Chaperones, 1996. **1**(2): p. 109-15.

127. Rubenstein, R.C., M.E. Egan, and P.L. Zeitlin, *In vitro pharmacologic restoration of CFTR-mediated chloride transport with sodium 4-phenylbutyrate in cystic fibrosis epithelial cells containing delta F508-CFTR.* J Clin Invest, 1997. **100**(10): p. 2457-65.

128. Cyr, D.M. and D.N. Hebert, *Protein quality control--linking the unfolded protein response to disease. Conference on 'From Unfolded Proteins in the Endoplasmic Reticulum to Disease'.* EMBO Rep, 2009. **10**(11): p. 1206-10.

129. Walker, C. and J. Ginsler, *Development of a quantitative in vitro transformation assay for kidney epithelial cells.* Carcinogenesis, 1992. **13**(1): p. 25-32.

130. Wyttenbach, A., et al., *Amelioration of protein misfolding disease by rapamycin: translation or autophagy?* Autophagy, 2008. **4**(4): p. 542-5.

131. Zhou, X., et al., *Rheb controls misfolded protein metabolism by inhibiting aggresome formation and autophagy.* Proc Natl Acad Sci U S A, 2009. **106**(22): p. 8923-8.

132. Catley, L., et al., *Aggresome induction by proteasome inhibitor bortezomib and alpha-tubulin hyperacetylation by tubulin deacetylase (TDAC) inhibitor LBH589 are synergistic in myeloma cells.* Blood, 2006. **108**(10): p. 3441-9.

133. Eot-Houllier, G., et al., *Histone deacetylase inhibitors and genomic instability.* Cancer Lett, 2009. **274**(2): p. 169-76.

134. Loffing-Cueni, D., et al., *Trafficking of GFP-tagged DeltaF508-CFTR to the plasma membrane in a polarized epithelial cell line.* Am J Physiol Cell Physiol, 2001. **281**(6): p. C1889-97.

135. Baines, A.T., D. Xu, and C.J. Der, *Inhibition of Ras for cancer treatment: the search continues.* Future Med Chem, 2011. **3**(14): p. 1787-808.

136. Donohue, E., et al., *The autophagy inhibitor verteporfin moderately enhances the antitumor activity of gemcitabine in a pancreatic ductal adenocarcinoma model.* J Cancer, 2013. **4**(7): p. 585-96.

137. Rafehi, H., et al., *Clonogenic assay: adherent cells.* J Vis Exp, 2011(49).

138. Lock, R., et al., *Autophagy facilitates glycolysis during Ras-mediated oncogenic transformation.* Mol Biol Cell, 2011. **22**(2): p. 165-78.

139. Wang, R.C., et al., *Akt-mediated regulation of autophagy and tumorigenesis through Beclin 1 phosphorylation.* Science, 2012. **338**(6109): p. 956-9.

140. Klionsky, D.J., et al., *Guidelines for the use and interpretation of assays for monitoring autophagy.* Autophagy, 2012. **8**(4): p. 445-544.

141. Rifki, O.F., et al., *RalGDS-dependent cardiomyocyte autophagy is required for load-induced ventricular hypertrophy.* J Mol Cell Cardiol, 2013. **59**: p. 128-38.

142. Matsui, Y., et al., *Distinct roles of autophagy in the heart during ischemia and reperfusion: roles of AMP-activated protein kinase and Beclin 1 in mediating autophagy.* Circ Res, 2007. **100**(6): p. 914-22.

143. Ramirez-Peinado, S., et al., *Glucose-starved cells do not engage in prosurvival autophagy.* J Biol Chem, 2013. **288**(42): p. 30387-98.

CURRICULUM VITAE

Jeremiah William Hendricks

EDUCATION

Bachelor of Science in Applied Physics
Purdue University, West Lafayette, Indiana Graduated May 2009
Master of Science in Biochemistry and Molecular Biology
Indiana University, Indianapolis, Indiana Graduated April 2014

RESEARCH EXPERIENCE

Independent Research, Dr. Marc Caffee, Purdue University 2006

- I created programs in Excel and MATLAB to be used as tools for accelerator mass spectrometry in the PRIME lab.

Summer Research, Dr. Bryan Schneider, Indiana University Summers 2007, 2008

- I researched how genetic polymorphisms affect efficacy of angiogenesis targeted cancer drugs and which microRNAs regulate the protein VEGF.

Independent Research, Dr. David Riese, Purdue University 2008-2009

- I researched the mechanism of alcohol's effect on the invasiveness of breast cancer cells.

Graduate Research, Dr. Lawrence Quilliam, Indiana University 2011-2014

- I researched inhibiting protein clearance to treat tuberous sclerosis and pancreatic cancer.

HONORS AND AWARDS

Ascarelli Fellowship / Research Assistantship, Purdue University	2005
Purdue Academic Success Award, Purdue University	2005
Dean's List and Semester Honor's, Purdue University	2005-2009

PUBLICATIONS

Mammalian target of rapamycin complex 1 (mTORC1) enhances bortezomib-induced death in tuberous sclerosis complex (TSC)-null cells by a c-MYC-dependent induction of the unfolded protein response. Babcock JT, Nguyen HB, He Y, **Hendricks JW**, Wek RC, Quilliam LA. J Biol Chem. 2013 May 31;288(22):15687-98.

PLATFORM PRESENTATIONS AND POSTERS

"Targeting nucleotide excision repair: Chemical synthetic lethality and biology-based combination therapy." John J. Turchi, Jiyoon Lee, **Jeremiah Hendricks**, Tracy M. Neher, Richard W. Fitch. AACR Annual Meeting, April 3, 2012.

"Rgl2 regulates autophagy and cell survival in pancreatic cancer cells." **Jeremiah W. Hendricks**, and Lawrence A. Quilliam. IU Simon Cancer Center Cancer Research Day, May 22 2013.

LABORATORY TECHNIQUES AND COMPUTER SKILLS

- Managing cell cultures
- cDNA cloning
- PCR and qPCR
- SDS-PAGE, Western blotting, and immunoprecipitation
- Protein expression
- DNA preps
- Bacterial transformation and cell culture transfection
- Lentiviral production
- Electromobility shift assays (EMSA)
- ELISA
- Wound healing assays
- Anchorange-dependent and –independent colony formation assays
- Luciferase assays
- Assisting in immunohistochemical staining and FISH
- Immunofluorescent and fluorescent live cell imaging
- Some experience handling animals
- Microsoft Word, PowerPoint, Excel, ImageJ

WORK AND EXTRA CURRICULUM ACTIVITY

- Delivery driver, AutoValue, 2006-2007 (Paid)
- Science ambassador, Purdue University, 2007-2009 (Volunteer)
- Grounds manager, Milo Properties Inc, 2007-2010 (Paid)
- Purdue Stadium Rescue Squad, 2007-2008 (Volunteer)
- Serenity Hospice, 2007-2009 (Volunteer)
- Cook, Jake's Roadhouse, 2009-2010 (Paid)